

**Analysis of Sterol Regulatory Element Binding Protein (SREBP) dependent
regulation of gaseous signaling and cell biology during fungal biofilm development
in *Aspergillus nidulans***

Dissertation

Presented in Partial Fulfillment of the Requirements for the Degree Doctor of Philosophy
in the Graduate School of The Ohio State University

By

Shobhana Rajasenan

Graduate Program in Molecular Genetics

The Ohio State University

2021

Dissertation Committee

Dr. Stephen Osmani, Advisor

Dr. Anna Dobritsa, Committee Member

Dr. Amanda Bird, Committee Member

Dr. Anita Hopper, Committee Member

Dr. Jian-Qiu Wu, Committee Member

Copyrighted by
Shobhana Rajasenan
2021

Abstract

Fungal biofilm founder cells experience self-generated hypoxia leading to dramatic changes in their cell biology. For example, during *Aspergillus nidulans* biofilm formation microtubule (MT) disassembly is triggered causing dispersal of EB1 (a MT ‘+’ end binding protein) from MT tips. This process is dependent on SrbA, a sterol regulatory element binding transcription factor required for adaptation to hypoxia. We find that SrbA, an ER resident protein prior to activation, is proteolytically activated during early stages of biofilm formation and that its activating proteases are required for normal biofilm cell regulation. In addition to SrbA, the AtrR transcription factor is also found to be required to modulate cellular responses to gaseous signaling during biofilm development. Using co-cultures, we show that cells lacking *srbA* or *atrR* are capable of responding to biofilm generated hypoxia and are actually more sensitive to this signal than wild type cells. SrbA is a regulator of ergosterol biosynthetic genes and we find that the levels of seven GFP-tagged Erg proteins differentially accumulate during biofilm formation. This uncovers a complex pattern of regulation with biofilm accumulation of only some Erg proteins being dependent on SrbA with others accumulating to higher levels in its absence. Because different membrane sterols are known to influence cell permeability to gaseous molecules, including oxygen, we propose that differential regulation of ergosterol biosynthetic proteins by SrbA may calibrate the cell’s

responsiveness to gaseous signaling which in turn modifies the cell biology of developing biofilm cells.

Dedication

I dedicate this thesis, the product of my cumulative study and passion in genetics and science in general, to the following people.

My parents and family for providing an upbringing that placed a high value on education, knowledge and science. To my grandfather (Dadada) who set an example for disciplined, single minded pursuit of academic knowledge as a professor of mathematics, for all the textbooks he insisted on buying me and the persistent lectures on the beauty of math I had to endure as a child. To my grandmother (Ammama) for bringing spiritual balance to my upbringing with exposure to the Vedanta, Ramayana and Mahabharata and for developing my memory powers by insisting on Bhagavad Geeta chanting.

I thank my parents for prioritizing my education over a comfortable and easy family life. To my father for making the sacrifice of working long distance to facilitate my pivotal education and upbringing in India. To my mother for her perspective in recognizing the value of Indian education and her never-ending energy and determination to ensure that I got it, for pushing me to greater challenges and never doubting my capabilities.

Finally, I dedicate this work to my school, Chinmaya Vidyalaya, and its teachers for the rigorous education in science and math balanced with a wide variety of extra-curricular activities that laid the foundation for who I am today.

Acknowledgments

I am deeply grateful to Dr. Stephen Osmani for taking me on as a graduate student and being my advisor when I was a student without a lab. I appreciate the complete freedom he gave me not only in organizing my work life but also in developing my ideas and never saying “no” to an experiment. I am thankful to Aysha Osmani for all the technical lab training she provided and keeping the lab running smoothly, making it a treat to work in. Dr. Nandini Shukla was invaluable in helping me pick up the ropes of microscopy and image analysis. Her previous work in microtubule disassembly served as a springboard for this thesis. This thesis owes a lot to Matthew Johns, who did a tremendous amount of work crossing and saving strains, making media and so on that freed me up to focus on core experiments. I am grateful to all members of the Osmani Lab for their support through this journey.

My advisory committee, Dr. Amanda Bird, Dr. Anna Dobritsa, Dr. Anita Hopper and Dr. Jian-Qiu Wu provided the scientific engagement, critique and encouragement that was vital for this project. Last and by no means least, I would like to thank Dr. Robin Wharton and Dr. Susan Cole for seeing me through a difficult time of life and helping me turn this PhD journey around.

Vita

2009-2013	B.Tech Genetic Engineering, SRM University
2013- present	Graduate Teaching and Research Associate, Department of Molecular Genetics, The Ohio State University

Fields of Study

Major Field: Molecular Genetics

Table of Contents

Abstract.....	ii
Dedication.....	iv
Acknowledgments.....	v
Vita.....	vi
List of Tables	ix
List of Figures	x
Chapter 1 Introduction	1
Chapter 2. Materials and Methods.....	13
2.1 General Techniques	13
2.2 Strain Generation	13
2.2.1 Design of the DNA Transformation Cassette	14
2.2.2 Transformation of <i>Aspergillus nidulans</i>	16
2.3 Cell culture for microscopy	16
2.4 Microscopy	18
2.5 Image processing and analysis.....	18
Chapter 3. The proteolytic activation and nuclear translocation of the SrbA protein in response to gaseous signaling in <i>Aspergillus nidulans</i>	27
3.1 Introduction.....	27
3.2 Results.....	32
3.2.1 The Sterol Regulatory Element Binding Protein (SREBP) SrbA undergoes proteolytic activation and nuclear accumulation in basal biofilm cells.....	32
3.2.2 SrbA activation is reversible in basal biofilm cells	34
3.2.3 SrbA nuclear accumulation is transiently activated by exogenously supplied nitric oxide	35
3.3 Discussion.....	38

Chapter 4. The role of sterol-regulatory transcription factors in biofilm MT disassembly	48
4.1 Introduction	48
4.2 Results	53
4.2.1 Complete proteolytic processing of SrbA protein is required to trigger MT disassembly in basal biofilm cells	53
4.2.2 An additional hypoxic transcription factor, AtrR, is required for MT disassembly in basal biofilm cells	55
4.2.3 WT cells can create the gaseous microenvironment that triggers MT dispersal in Δ <i>srbA</i> and Δ <i>atrR</i> cells	56
4.2.4 Δ <i>srbA</i> cells respond to a lower threshold of the MT dispersal signal	58
4.2.5 Δ <i>srbA</i> and Δ <i>atrR</i> can independently trigger MT disassembly in shaken cultures	59
4.3 Discussion	61
Chapter 5. Protein expression analysis of ergosterol biosynthetic genes that are targets SrbA and AtrR transcriptional regulation	72
5.1 Introduction	72
5.2 Results	76
5.3 Discussion	82
Chapter 6. Conclusion	98
Bibliography	105

List of Tables

Table 1 List of Strains.....	22
Table 2 List of Primers	24

List of Figures

Figure 1. 1 Phases of <i>Aspergillus</i> biofilm development.....	12
Figure 2. 1 Schematic representation of homologous recombination with fusion PCR constructs..	21
Figure 3. 1 <i>SrbA</i> protein structure and regulation.	42
Figure 3. 2 Schematic of experimental setup to track hypoxic biofilm cell biology.	43
Figure 3. 3 <i>SrbA</i> protein undergoes activation and nuclear translocation in basal cells during the early stages of biofilm development.....	44
Figure 3. 4 Examination of the <i>SrbA</i> activation process within the same basal biofilm cells.	45
Figure 3. 5 <i>SrbA</i> activation in basal biofilm cells is reversible in response to air exchange.	46
Figure 3. 6 Proteolytic activation of <i>SrbA</i> is triggered by NOC-18 treatment.	47
Figure 4. 1 Model of <i>SrbA</i> protein proteolytic activation and Ebl protein tracking.	65
Figure 4. 2 Fully processed <i>SrbA</i> transcription factor is required for MT dispersal in basal biofilm cells.	66
Figure 4. 3 <i>srbA</i> and <i>atrR</i> are required for progression of biofilm cells to MT disassembly stage.....	67
Figure 4. 4 WT cells can create the gaseous microenvironment that triggers MT dispersal in Δ <i>srbA</i> and Δ <i>atrR</i> cells.....	68
Figure 4. 5 Δ <i>srbA</i> cells are more sensitive to the MT dispersal signal relative to WT cells.	69
Figure 4. 6 Reversal of MT dynamics by lid removal and replacement.....	70

Figure 4. 7 Δ <i>srbA</i> and Δ <i>atrR</i> cells can disperse MTs after shaking treatment.....	71
Figure 5. 1 Aspergillus ergosterol biosynthetic pathway.	87
Figure 5. 2 Ergosterol proteins of 3 oxygen dependent catalytic steps investigated during biofilm development.	88
Figure 5. 3 Real-time expression of GFP-tagged Erg24 protein in living <i>A. nidulans</i> cells.	89
Figure 5. 4 Real-time expression of GFP-tagged Erg11A protein in living <i>A. nidulans</i> cells.	90
Figure 5. 5 Real-time expression of GFP-tagged Erg11B protein in living <i>A. nidulans</i> cells.	91
Figure 5. 6 Real-time expression of GFP-tagged Erg25A protein in living <i>A. nidulans</i> cells.	92
Figure 5. 7 Real-time expression of GFP-tagged Erg25B protein in living <i>A. nidulans</i> cells.	93
Figure 5. 8 Real-time expression of GFP-tagged Erg3A protein in living <i>A. nidulans</i> cells.	94
Figure 5. 9 Real-time expression of GFP-tagged Erg3B protein in living <i>A. nidulans</i> cells.	95
Figure 5. 10 Comparative expression levels of all 7 Erg proteins in the presence or absence of <i>srbA</i> during biofilm development.	96
Figure 5. 11 Model of <i>SrbA</i> regulation of ergosterol pathway enzymes during biofilm development.	97
Figure 6. 1 Relative timing of different cell biological changes triggered by gaseous signaling in different stages of biofilm development.	104

Chapter 1 Introduction

A biofilm is a complex community of microbial cells, usually enclosed by an extracellular matrix, that typically adheres to a biotic or abiotic surface (Fig 1.1). Biofilms are the predominant mode of growth for bacteria, yeast and fungi in nature. The theory of biofilms being the predominant mode of growth in natural ecosystems was proposed in 1978¹ and was based on exhaustive data collected from natural aquatic ecosystems -“...the majority of bacteria grow in matrix-enclosed biofilms adherent to surfaces in all nutrient-sufficient aquatic ecosystems and that these sessile bacterial cells differ profoundly from their planktonic (floating) counterparts.”². In natural environments where nutrients are limiting and microbial cells are subject to inter-species competition, there are distinct advantages to be gained by the formation of a biofilm. The development of a biofilm in close proximity to a nutrient source allows easy access to resources for all cells within the biofilm compared to free-living (planktonic) forms of the same species. The encapsulated biofilm structure also provides superior resistance to antimicrobial agents, whether biological or chemical. Naturally occurring biofilms may also be composed of a variety of microbial species coexisting within the same community that confers adaptive fitness and various mutual benefits to the species involved. All these features of the biofilm mode of growth naturally provide selective advantages for species

survival. It is therefore not surprising that biofilms are the preferred mode of growth for the vast majority of microbes in natural ecosystems.

Why Study Microbial Biofilms?

The cells of a given microbial species within a biofilm display features and behavior distinct from those of independently growing cells. Most microbiological experiments to date have been carried out on free-living unattached (planktonic) cells. While there is great experimental utility in using planktonic cells, it is possible that results obtained from such experiments do not carry over to biofilm grown cells of the same species. Given that the biofilm mode of growth is the most natural lifestyle for the vast majority of bacterial and fungal species, investigating biofilm cell biology is both important and urgent.

Cells within a biofilm show significant heterogeneity in architecture and gene expression³⁻⁷. Cells at the periphery of the biofilm have more access to nutrients and resources like oxygen compared to cells at the biofilm core. On the other hand, cells at the core are buffered from fluctuating environmental conditions outside the biofilm, that peripheral cells are exposed to. Such variations in the microenvironment of the biofilm cells produce differential effects on their respective cell biologies. This results in heterogenous subpopulations with specialized functions similar to cell differentiation and specialization in multi-cellular eukaryotic organisms.

There are numerous examples of specific differences between biofilm and planktonic cells. For instance, biofilms are typically encapsulated by an extracellular

polysaccharide matrix, unlike planktonic cells. The extracellular matrix, composed of carbohydrate, protein, lipids and extracellular DNA⁸⁻¹⁰, is secreted by the biofilm cells within 24 hours of attachment and growth^{3,4}. In the fungal biofilm of *Candida albicans*, cells contain more lipid rafts in their plasma membrane than planktonic cells¹¹. Lipidomic analysis via mass spectrometry has revealed that phospholipids are significantly higher in *C. albicans* biofilms compared to planktonic cells¹¹. Sterol levels are also significantly altered within planktonic, early, intermediate and mature phase biofilms¹².

A classic example of alternate cell behavior between planktonic and biofilm cells is the difference in resistance to antimicrobial drugs. Bacterial or fungal cells of a particular species in the planktonic form can have radically different levels of resistance to antimicrobial drugs compared to biofilm grown cells of the same species. Biofilm cells can have 10X-1000X greater tolerance to antimicrobial drugs relative to planktonic forms^{3,13,14}. A study testing the efficacies of multiple antifungal drugs at different stages of biofilm development in *Aspergillus fumigatus* demonstrated that resistance to the drugs increased as the biofilm advanced to more mature stages of development¹⁵. Similar results were also obtained in a study regarding drug resistance at different stages of *Candida albicans* biofilm development⁴. Thus, laboratory developed antimicrobial drugs tested on planktonic forms of the microbe in question, have turned out to have significantly reduced efficacy when prescribed in the clinical setting because these microbes grow as biofilms during their pathogenesis.

The Role of Microbial Biofilms in Infectious Disease

One of the most well studied sources of human infection involving the biofilm mode of growth occurs on abiotic surfaces of implanted medical devices: orthopedic prostheses, catheters, mechanical heart valves, coronary stents, cochlear implants, fracture-fixation devices to name a few¹⁶. The *Candida* genus of fungi is the biggest culprit when it comes to device-associated biofilm infections. It is found on catheters, cardiac devices, endotracheal tubes, joint prostheses and breast implants whereas *Aspergillus* is mainly associated with dialysis catheters¹⁷. Widely used contact lenses, of both the hard or soft gel type, readily allow for microbial attachment and biofilm formation^{18,19}. Poor contact lens hygiene can lead to keratitis of the eye caused by these contact-lens associated biofilms. Biofilms that develop on these devices are not only resistant to clinically used anti-microbial drugs but also the host's own immune system and therefore become a source of recurrent infection. A fragment of the biofilm may also break away, under the shear forces of blood flow or other body fluids, resulting in the transport of infection to other parts of the body.

Generally speaking, most microbes adhere poorly to tissue surfaces in a healthy adult human body. Despite this, certain diseases have been identified in the past decade or two that involve a biofilm mode of growth of opportunistic pathogens^{2,17}. Periodontal disease is probably one of the most commonly encountered human infections brought about by microbial biofilms in the oral cavity²⁰. Various gram-positive bacteria that are part of the normal flora of the oral cavity bind to and colonize a proteinaceous film that develops on the tooth enamel. Within days these develop the polysaccharide matrix to form a biofilm (otherwise known as plaque in the field of dentistry). Other diseases

involving microbial biofilms include Native Valve Endocarditis (NVE), Chronic Bacterial Prostatitis, Cystic Fibrosis,²¹ chronic middle-ear infections²² and urinary tract infections²³. In NVE, damaged cardiac endothelial tissue develops a thrombus (an aggregate of platelets, fibrin and red blood cells) at the site of injury². Bacteria that bind to the fibrin and manage to evade white blood cells can initiate the formation of a biofilm containing a variety of microorganisms including *Candida* and *Aspergillus* fungi. *Aspergillus* and *Candida* species can cause infections in humans under specific circumstances i.e., they are not true human pathogens but opportunistic pathogens. For instance, invasive pulmonary aspergillosis is a lethal disease that typically affects immunocompromised patients such as those taking immune-suppressive drugs or the HIV-infected. Nevertheless, diseases like Aspergillosis and Candidiasis pose a significant clinical problem due to their increased biofilm derived tolerance to antifungal drugs.

Fungi, Hypoxia and Biofilms

Oxygen is one of the most fundamental, life-giving molecules on earth. The vast majority of eukaryotic cells including most filamentous fungi are aerobes, requiring O₂ as an electron acceptor for energy production during mitochondrial respiration as well as for the biosynthesis of critical molecules for cell function, including sterols. However, for filamentous fungi, there can be great variations in their exposure to oxygen depending on the specific ecological niche in which they grow which can change over time. Natural environments at a certain depth within soil or compost are hypoxic. Many fungal aquatic ecosystems may also have relatively low oxygen due to significantly lower rate of O₂

dissolution and diffusion in water compared to air²⁴. Importantly, many fungal infection sites within a host are loci of low oxygen concentration. For example, lesions in lung tissue caused by invasive aspergillosis are hypoxic due to the host's immune response diverting oxygen away from the site. Yet the growth of *A. fumigatus*, the dominant *Aspergillus* species causing human disease, is unperturbed by the hypoxic microenvironment during infection. *A. fumigatus* can maintain filamentous growth at low oxygen levels of ~0.1%²⁵. In fact, this hypoxic adaptation of growth in *Aspergillus* appears to be critical for its virulence. Loss of hypoxia-adaptive transcription factors like SrbA and AtrR results in the loss of growth and ability to invade murine lung tissue²⁶⁻²⁹. It is important to note that while *Aspergillus* species of filamentous fungi are able to adapt to hypoxic environments as low as 0.2% oxygen they cannot grow in the complete absence of oxygen i.e., they are not capable of anaerobic growth²⁵.

Biofilms are known to contain hypoxic and even anoxic microenvironments within them. More specifically, an oxygen gradient develops within the biofilm. Cells at the periphery of the biofilm have easy access to ambient oxygen. Biofilm cells are continuously consuming oxygen and are also usually encapsulated in a polysaccharide matrix. Oxygen from the periphery has to penetrate the dense filamentous biomass and the matrix to reach the inner cell layers. Thus, the available oxygen concentration gets progressively lower as distance from the periphery increases, thereby generating an oxygen gradient. Cells located at the central core of the biofilm experience the lowest oxygen concentration and may even become anoxic at some point. If biofilms are the

predominant mode of growth for filamentous fungi in nature, it is only natural that these cells are well adapted to maintaining growth under hypoxia.

Experiments with *Candida albicans* fungal biofilm co-cultured with 5 different bacterial species demonstrated that the biofilm was able to generate a hypoxic microenvironment such that it allowed the growth of two obligate anaerobic bacterial species³⁰. Biofilm oxygen concentration was also measured at different depths using an oxygen sensor. This demonstrated the gradual drop in oxygen from the top (~22% or 300 μ M O₂) to the bottom (~4% or 50 μ M O₂) of the biofilm³⁰. Similarly, in more recent experiments with *Aspergillus fumigatus* biofilms O₂ concentrations were measured using an ampero-metric oxygen sensor at different depths in the biofilm³¹. This demonstrated not only the presence of an oxygen gradient from top to bottom but also that the gradient developed over time, accompanying the accumulation of fungal biomass forming the biofilm. Even in Solid-State Fermentation (SSF, growth on a solid matrix and near complete absence of water) of *Rhizopus oligosporus*, micro-electrode measurements at different depths of the fungal mat revealed a dramatic oxygen gradient from the aerial surface, decreasing to near anaerobic levels³². In *Aspergillus oryzae* SSF the aerial hyphae alone accounted for 75% of the total oxygen uptake³³.

The deletion of the transcription factor *srbA*, known to be required for hypoxic growth, resulted in the inability of cells to develop into a mature biofilm³¹. In this study, the fundamental filamentous structure of the biofilm was altered when the ambient oxygen concentration was lowered using a hypoxic growth chamber. Thus, oxygen levels influence architecture of cells within the biofilm and the inability of the cells to adapt to

hypoxia (in the absence of *srbA*) retards biofilm growth. Resistance of the biofilm to antifungal drugs (voriconazole, amphotericin B, menadione) was found to be dependent on the hypoxic microenvironment within the biofilm³¹. This was investigated with the clever use of oxygen-permeable coverslips at the base of the biofilm. The biofilm grown on the permeable coverslip lost its resistance to the antifungals whereas a biofilm at the same stage of growth grown on a normal coverslip was resistant.

Published experiments in *Aspergillus nidulans* biofilms have also demonstrated dynamic cell biological changes in response changing gaseous microenvironments³⁴. In this study, actively polymerizing microtubules (MT) in basal cells of the biofilm were observed to undergo complete disassembly at a certain stage during biofilm development. This MT disassembly process was shown to be highly sensitive to the gaseous environment based on the fact that when the lid of the culture dish was removed, allowing air exchange, MTs reassembled. This implies that gaseous components must be involved in triggering MT disassembly in the biofilm cells. Interestingly, once MTs were dispersed and the biofilm was allowed to mature further, lid removal no longer triggered MT reassembly. At this stage, only physically scraping off a part of the biofilm could induce MT reassembly. This indicates that passive diffusion of gaseous molecules through the biofilm becomes more restricted as the biofilm matures, possibly due to the increased density of the biomass and extracellular matrix. The exact nature of the gaseous signaling involved in regulating biofilm MT disassembly was not determined. Hypoxia that is known to develop within growing biofilms, is a likely candidate. In addition, the deletion of the hypoxia-adaptive *srbA* gene abolished the MT disassembly process,

retaining actively polymerizing MTs throughout the experiment. However, MT disassembly was also induced by treating cells with a hydrogen sulfide donor and then reversed by washing out the donor molecule. This showed that gaseous molecules other than oxygen may also be involved in the signaling. Studies in animal systems show that hydrogen sulfide is one of the gases produced by cells experiencing hypoxia suggesting that H₂S may act as the functional signaling molecule of hypoxia.

A more recent study investigated the biofilm-associated changes in multiple cell structures using live-cell imaging of organelle-specific markers in basal biofilm cells³⁵. The results showed modifications in ER exit sites, Golgi and endocytic actin patches, while the ER structure itself remained unchanged. These biofilm-driven modifications required the presence of *srbA* and could be reproduced by treating cells with nitric oxide. This data reinforces the importance of gaseous signaling in biofilm development and the wide-ranging effects it has in modifying cell biology.

All these experiments demonstrate the dramatic cell biological changes within fungal biofilm cells. They also indicate the critical role played by gaseous signaling (oxygen and/or hydrogen sulfide, nitric oxide) in regulating fungal cell biology.

SrbA and Hypoxia

SREBPs (Sterol Regulatory Element Binding Protein) are highly conserved (from fungi to mammals) eukaryotic transcription factors that have been well studied for their regulation of oxygen-dependent sterol biosynthesis³⁶. In fungi, SREBP is required for adaptation and growth under hypoxia. Deletion of the *srbA* (*Aspergillus* SREBP) gene in

a strain abolishes the ability of hypoxic (~0.5-2% O₂) growth while maintaining normal growth under normoxic (ambient oxygen levels, ~20% O₂) conditions. The absence of *srbA* also leads to the loss in virulence of fungal species. This is consistent with the fact that hypoxic growth of fungal cells is important for their pathogenesis, as discussed above. The ER-tethered SrbA protein is specifically cleaved through regulated proteolysis under hypoxia to release the transcription factor domain^{27,37,38}. The SrbA transcription factor binds to promoters of hundreds of genes, thereby regulating numerous downstream processes necessary for hypoxic adaptation of the cell³⁹. Some of the noteworthy genes regulated by SrbA are those involved in the biosynthesis of sterol and heme^{28,37}; this is significant because these pathways are heavily dependent on oxygen. Ergosterol is an important component of the fungal cell membrane and its synthesis is necessary to maintain cell growth.

Project Goal

Self-generated hypoxia is a significant characteristic of fungal biofilms. The SrbA transcription factor is clearly important in hypoxic adaptation of fungal cells. Experiments specifically studying biofilm MT disassembly triggered by gaseous signaling as well as biofilm driven modifications to cell structures and organelles showed that the presence of the *srbA* gene is necessary for these cell biological changes^{34,35}. The overarching goal of this project is to investigate the role of SrbA in regulating fungal cell biology in response to the hypoxic microenvironment generated naturally within a

developing *Aspergillus nidulans* biofilm. This project comprises a three-pronged approach:

- I) Investigation of the behavior and expression pattern of the SrbA protein during biofilm development and in response to gaseous signaling.
- II) Dissecting the role of *srbA* in biofilm-driven cellular modifications that are responsive to gaseous signaling.
- III) Real-time analysis of transcriptional regulatory targets of SrbA at the protein level during biofilm development.

This study aims to throw light on the role of this hypoxia-adaptive transcription factor in inducing cellular modifications during biofilm maturation in response to gaseous signaling.

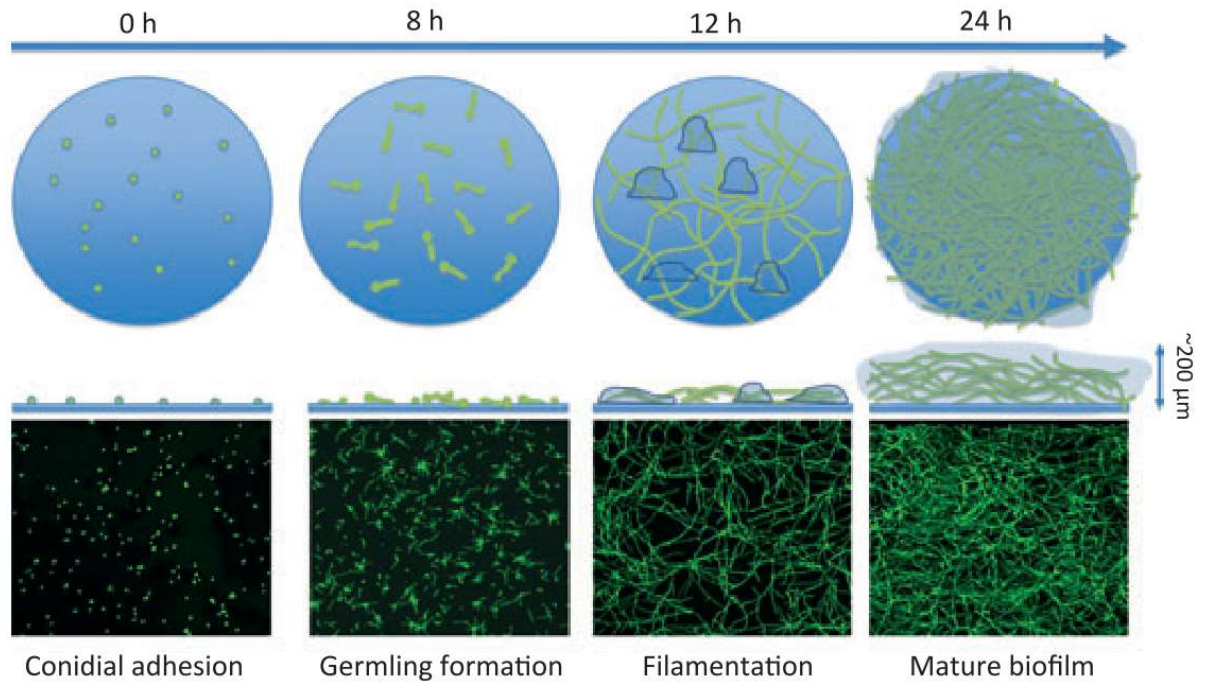


Figure 1. 1 Phases of *Aspergillus* biofilm development.

Adapted from Ramage et al. 2011. “The different phases of biofilm development are represented schematically, from initial adhesion of conidia, germling formation (8 h), a monolayer of intertwined hyphae (12 h) and mature 3D filamentous biomass (c. 200 μm) encased within EPS (24 h). These are also illustrated in the adjacent confocal laser scanning micrographs stained using FUN1 (Molecular Probes)”⁴⁰

Chapter 2. Materials and Methods

2.1 General Techniques

Classical genetic techniques for *Aspergillus nidulans* were carried out as described previously⁴¹. Strains generated in this study are listed in Table 1. Primers used in this project are listed in Table 2.

2.2 Strain Generation

Aspergillus nidulans strains were created through the homologous recombination (at a specific genomic locus) of a linear DNA construct transformed into prepared protoplasts. Alternatively, specific strains were crossed by inducing sexual reproduction to generate new strains with specific combinations of modified genes.

The 4X YFP-SrbA (CSK1647) strain was a kind gift from the Chae Lab³⁷ and a PH^{OSBP}-mRFP strain, generously donated by the Penalva Lab⁴², was crossed with existing lab strains to generate new strains used in this study.

Genes were endogenously tagged or deleted using constructs generated by fusion PCR⁴³ and transformed into *Aspergillus nidulans*^{44,45} as previously described. Gene deletion was carried out at the endogenous locus using fusion PCR generated constructs designed to replace the gene's CDS with a selectable marker. Homologous integration was verified using diagnostic PCR with primers flanking the targeting construct on DNA prepared from the transformants.

2.2.1 Design of the DNA Transformation Cassette

A linear DNA cassette was synthesized using fusion PCR^{45,46}, bypassing the need for plasmid constructs. This DNA cassette would then be transformed into *A. nidulans* protoplasts and would integrate into the genome at a specific target site through homologous recombination. This site-specific integration is possible because the transgene is flanked homologous genomic sequences of the target site, allowing integration at this specific locus (Fig 2.1). The complete linear DNA cassette was comprised of the following in order:

- 5' upstream flanking region (~1kb)
- Transgene
- 3' downstream flanking region (~1kb)

Each of these DNA fragments were first amplified using primers containing specific overhang sequences (~20-25bp). The reverse primer for amplifying the 5' upstream region had an overhang sequence complementary to the first 20-25 bp of the transgene amplicon. Similarly, the forward primer to amplify the 3' downstream region had an overhang complementary to last 20-25bp of the transgene amplicon. Then, after purification, the 5' amplicon, transgene amplicon and the 3' amplicon are combined and fusion PCR carried out using the forward primer for the 5' upstream region and reverse primer for the 3' downstream region. The 5' upstream amplicon has its 3' end complementary to the 5' end of the transgene amplicon and the 3' downstream amplicon has its 5' end complementary to the 3' end of the transgene. This PCR results in the

fusion of the three amplicons in this specific order, producing the desired transformation DNA cassette. The amplified DNA was gel purified for transformation.

To carry out the deletion of a gene, the deletion construct consisted of a selectable nutritional marker flanked by 1kb 5' and 3' of the target gene CDS. Homologous recombination of this construct at the endogenous locus of the target gene results in the replacement of the target gene CDS with the selectable marker gene, thereby deleting the target gene.

To produce C-terminal GFP-tagged proteins, the transgene used consisted of the GFP coding sequence (without the start codon and with the stop codon as well as a short linker sequence on the 5' end) followed by a selectable marker gene. The 5' upstream flanking sequence consisted of ~1kb DNA sequence exactly upstream of the gene's stop codon and the 3' downstream flanking region consisted of ~1kb DNA sequence immediately downstream of the stop codon. Homologous recombination of this cassette at the endogenous locus resulted in the loss of the target gene stop codon and fusion of the GFP coding sequence in frame with that of the target gene.

The selectable markers used in this study are *pyrG*, *pyroA* and *ptrA*. *pyrG* codes for an enzyme in the pyrimidine biosynthetic pathway and loss of this gene function (*pyrG89* mutant) results in cells unable to synthesize uracil. *pyroA* codes for an enzyme in the pyridoxine biosynthetic pathway and loss of this gene function (*pyroA4* mutant) results in inability to synthesize pyridoxine. The *pyrG* and *pyroA* gene sequences from *Aspergillus fumigatus* were used to complement *A. nidulans* mutant strains *pyrG89* or *pyroA4*. This ensured that there was no spurious recombination between the transgene

cassette and the endogenous *pyrG* or *pyroA* loci. The *ptrA* gene sequence was from *Aspergillus oryzae*. This is a thiamine biosynthetic enzyme that has no homolog in *A. nidulans* but confers resistance to pyrithiamine. The *ptrA* selectable marker can be used for transformation without complementation with a mutant strain.

2.2.2 Transformation of *Aspergillus nidulans*

All transformations were carried out in a $\Delta nkuA$ strain as previously described⁴⁷. *nkuA* is the *Aspergillus nidulans* homolog of animal ku70 gene that is involved in the Non-Homologous End-Joining pathway; deletion of this gene reduces the chances of non-homologous recombination thereby increasing the probability of homologous recombination and the percentage of correctly modified transformed strains.

A. nidulans transformation was conducted as described⁴⁸, but 10 mg/ml Vinoflow FCE (Novozymes A/S, Bagsvaerd, Denmark) was used as the cell wall lytic mix. Freshly grown conidia (spores) were harvested from pour-plates to ensure relative uniformity in age. Quantified conidia were inoculated (2×10^7 /ml in 50ml YG) and monitored while they swelled and were starting to form a germ tube. Lytic mix was then added to digest the outer cell wall, allowing for the release of protoplasts. The protoplasts were then washed and allowed to recover. The purified linear DNA cassette was transformed into the protoplasts through PEG-based heat-shock transformation and then plated on the appropriate selective media.

2.3 Cell culture for microscopy

Agar overlay was used to generate *Aspergillus nidulans* spores after incubation for 36–40 h at 32°C. Harvested spores were washed twice in 0.2% Tween-80 and stored

in spore stock solution (0.02% Tween-80 plus 0.85% NaCl). For all imaging experiments, spores were inoculated in 35 mm glass-bottomed dishes (MatTek, Ashland, MA) containing 3 ml minimal medium at a concentration of 2.5×10^5 spores per ml for biofilm experiments or 1×10^5 spores per ml for general imaging. The medium for microscopy contained glucose (10 g/l), trace elements, urea (10 mM), MgSO_4 (2 mM), KCl (7 mM), and phosphate buffer (6 mM KH_2PO_4 and 6 mM $\text{K}_2\text{HPO}_4 \cdot 3\text{H}_2\text{O}$). The medium was supplemented with uridine (1.2 g/l) and uracil (1.12 g/l), arginine (6.4 g/l) as needed. Imaging dishes were incubated at room temperature (21–25°C) overnight or at 37°C for 7hrs followed by room temperature for the duration of the experiment. These temperatures were used only to facilitate the timing of growth with the same results obtained irrespective of initial growth temperatures.

Shaking culture growth conditions

Spores were inoculated at biofilm-level concentration 2.5×10^5 spores/ml in the imaging culture dish. The dishes were incubated at 37°C for 6 hours followed by room temperature (RT ~20-25°C) growth overnight, approximately 12-18hrs. Incubation at different temperatures was purely to speed up growth during initial germination stages. After overnight RT growth culture dishes were transferred to an orbital shaker set at 100 rpm for the next 10-12 hours. The shaker was set up immediately adjacent to the confocal laser microscope, ensuring continuity in ambient temperature before and during microscopy.

2.4 Microscopy

Microscopy was carried out using a spinning-disc laser confocal microscope. EB1-GFP signal was captured with a 60X objective using exposure at 488 nm for 200 ms and a 0.8 μm z-spacing. Erg-GFP signal was captured with a 100X objective using exposure at 488 nm for 800 ms and a 0.4 μm z-spacing. YFP-SrbA signal was captured using exposure at 514 nm for 500 ms and a 0.8 μm z-spacing. Each image was captured with 9-13 z-slices and all images presented are maximum intensity projections.

2.5 Image processing and analysis

Image analyses were performed using the software Ultraview and ImageJ^{49,50}. Raw microscopy image files were extracted in the 16-bit TIFF format using the Ultraview software and converted into the original 12-bit TIFF files using ImageJ.

General Processing for Viewing

Subtraction of background noise was carried out for general processing of all images. Background noise was calculated by measuring the average of 8 different background pixel intensities. These 8 points were selected from all four corners of the image where no cells were present; the average value of their intensities is a reasonable measure of background signal. This average background noise value was then subtracted from every individual pixel across the entire image. Background signal can come from many different sources- light signal reflected or refracted through the culture medium etc. The remaining signal intensities in each pixel have a higher probability of corresponding to real signal i.e., fluorescence from the tagged protein within the cell.

After background subtraction, images may be cropped to focus on specific cells of interest. Brightness and contrast of signal was adjusted appropriately to view the tagged protein of interest clearly. In a given experiment observing the changes in expression of a specific tagged protein, the same brightness and contrast settings were applied across all images to ensure unbiased representation of protein expression. Gray-scale was used to present images from experiments involving a single tagged protein for better clarity. Color filters were applied to images from experiments involving the capture of signal from multiple tagged proteins in the same cell or in co-cultures.

Analysis of EB1 comet number

To quantify the number of EB1-GFP comets in an image, a threshold was set (using ImageJ) at which only signal specific to the comets was detected. The ‘analyze particles’ function in ImageJ was used to count the number of such particles. A different threshold was then used to measure the total area occupied by all cells within the image. The number of comets was then normalized to the total cell area in the field to produce comet/unit cell area value for the image. For each timepoint, the comets/unit cell area was calculated for three different image fields. The average and standard deviation of these values from the 3 fields was used to plot the graph representing changes in comet number over time during biofilm development.

Quantification of cells with dispersed or active MTs

15-20 different image fields captured at a particular stage of biofilm development were analyzed to quantify the relative state of MTs in WT and *srbA* co-cultured cells. Each cell was classified as either dispersed or not dispersed by visual inspection. A cell was

classified as dispersed if at least 75% of the cell area contained no comets. The total number of dispersed and undispersed cells for each strain were added up from all image fields and plotted on a graph.

Quantification of Erg protein levels

To quantify Erg-GFP signal, first background subtraction was carried out. *Aspergillus nidulans* being a filamentous fungus, three representative filaments were selected in a given image field. Each filament was outlined manually using ImageJ to create a 'Region of Interest' (ROI). The fluorescence signal in an ROI was determined by measuring the total pixel intensity within the ROI. The average and standard deviation of at least 3 ROIs was used as a measure of protein expression at a given timepoint.

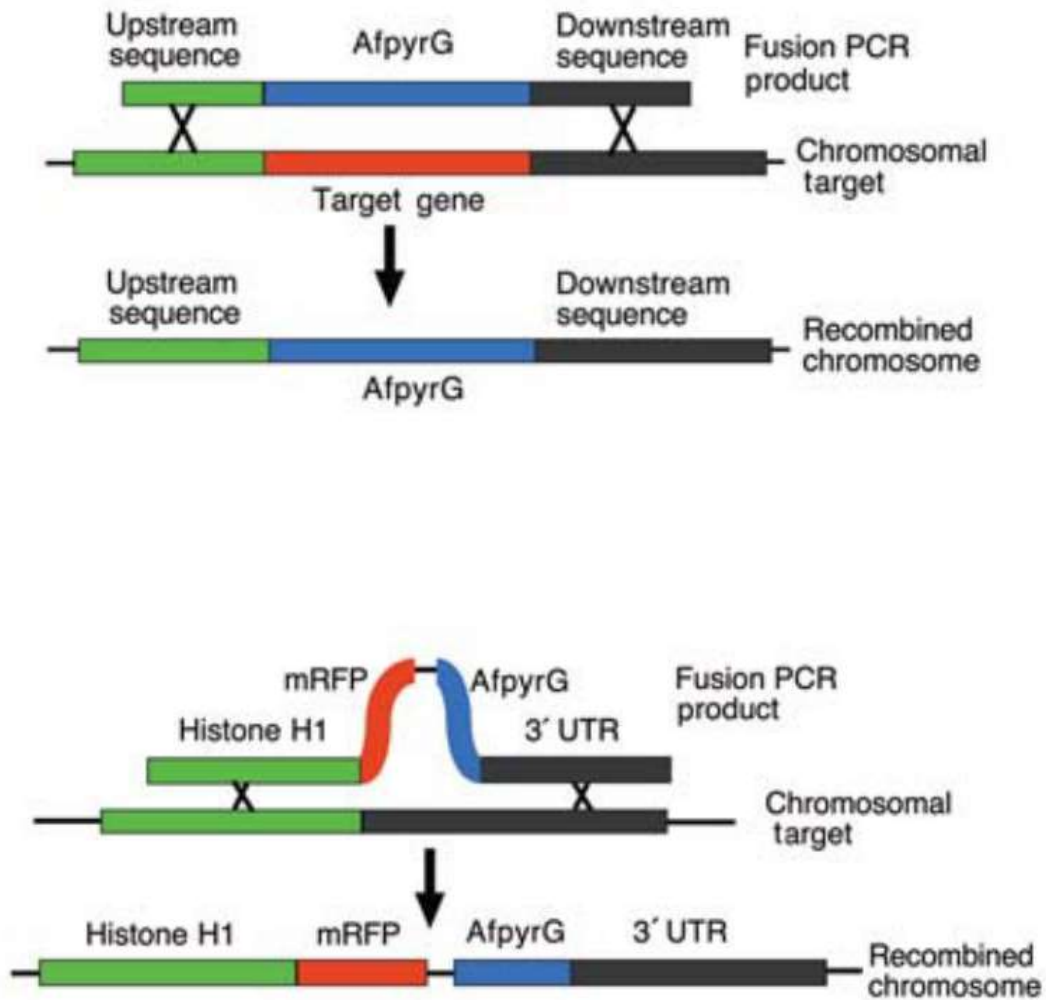


Figure 2. 1 Schematic representation of homologous recombination with fusion PCR constructs. Adapted from Szewczyk et al. 2007⁴⁵ **A.** Gene deletion using an *AfpyrG* construct (*Aspergillus fumigatus pyrG* selectable marker). **B.** C-terminal tagging of Histone H1 gene with mRFP-AfpyrG construct.

Table 1. List of Strains

Strain	Genotype	Source
SR6	Δ sppA::ptrA; EB1-GFP::pyroA; pyroA4; NoDel::pyrGAf; pyrG89; argB2; fwA1; wA3	This study
SR9	Δ dscA::ptrA; EB1-GFP::pyroA; pyroA4; No Del::pyrGAf; pyrG89; argB2; fwA1	This study
SR14	Δ rbdA::ptrA; EB1-GFP::pyroA; pyroA4; No Del::pyrGAf; pyrG89; argB2;fwA1	This study
SO1563	EB1-GFP::pyro(pyroA4); pyrGaf(pyrG89); wA3	Shukla et al 2017
SO1568	EB1-GFP::pyro(pyroA4); Δ AN7661::pyrGaf(pyrG89); wA3	Shukla et al 2017
SO1736	Δ AN4558::pyrGAF (pyrG89); EB1-GFP::pyro (pyroA); pabaA1; Δ nKuA70::argB(argB2) sE15; nirA14; wA3.	This study
SR82	Δ atrR::ptrA; Δ srbA::pyrG ^{Af} ; pyrG89;EB1-GFP::pyroA ^{Af} ; pyroA4; pabaA1; Δ nkuA::argB; argB2; wA3	This study
SO1821	Δ srbA::pyrGaf; EB1GFP::pyroAaf; pyroA4(pyroA*-gpdAmini::mrfp::PHosbp); wA3/wA4.	Lingo et al 2021
SR107	AN1901-GFP::pyrG ^{Af} ; pyrG89; pyroA4; Δ nkuA::argB; argB2; fwA1; chaA1; wA3	This study
SR109	Δ srbA::ptrA; AN1901-GFP::pyrG ^{Af} ; pyrG89; pyroA4; pabaA1; Δ nkuA::argB; argB2; wA3; yA2?	This study
SR111	AN8283-GFP::pyrG ^{Af} ; pyrG89; pyroA4; Δ nkuA::argB; argB2; fwA1; chaA1; wA3	This study
SR113	Δ srbA::ptrA; AN8283-GFP::pyrG ^{Af} ; pyrG89; pyroA4; pabaA1; Δ nkuA::argB; argB2; wA3; yA2?	This study
SR115	AN6973-GFP::pyrG ^{Af} ; pyrG89; pyroA4; Δ nkuA::argB; argB2; fwA1; chaA1; wA3	This study
SR117	Δ srbA::ptrA; AN6973-GFP::pyrG ^{Af} ; pyrG89; pyroA4; pabaA1; Δ nkuA::argB; argB2; wA3; yA2?	This study
SR119	AN8907-GFP::pyrG ^{Af} ; pyrG89; pyroA4; Δ nkuA::argB; argB2; fwA1; chaA1; wA3	This study
SR121	Δ srbA::ptrA; AN8907-GFP::pyrG ^{Af} ; pyrG89; pyroA4; pabaA1; Δ nkuA::argB; argB2; wA3; yA2?	This study
SR123	AN6506-GFP::pyrG ^{Af} ;pyrG89;pyroA4; Δ nkuA::argB;argB2;fwA1;chaA1;wA3	This study

SR125	Δ srbA::ptrA; AN6506-GFP::pyrG ^{Af} ; pyrG89; pyroA4; pabaA1; Δ nkuA::argB; argB2; wA3; yA2?	This study
SR127	AN3638-GFP::pyrG ^{Af} ; pyrG89; pyroA4; Δ nkuA::argB; argB2; fwA1; chaA1; wA3	This study
SR129	Δ srbA::ptrA; AN3638-GFP::pyrG ^{Af} ; pyrG89; pyroA4; pabaA1; Δ nkuA::argB; argB2; wA3; yA2?	This study
SR139	AN4094-GFP::pyrG ^{Af} ; pyrG89; pyroA4; Δ nkuA::argB; argB2; fwA1; chaA1; wA3	This study
SR141	Δ srbA::ptrA; AN4094-GFP::pyrG ^{Af} ; pyrG89; pyroA4; pabaA1; Δ nkuA::argB; argB2; wA3; yA2?	This study
CSK1647	srbA(p):4XYFP-srbA::pyroA; pyroA4; Δ srbA::argB; argB2; alcA(p):RFP:H2A::pabaA; pabaA1; chaA1	Bat-Ochir et al 2016

Table 2 List of Primers

Primer name	Primer Sequence
SR009	GAAGTACAAGGAGTCGTGCCAGTTG
SR010	GAAGAGCATTGTTTGAGGCGGCGATAAAAGGCGACAGACAGC
SR011	GCATCAGTGCCTCCTCTCAGACAGGGAGTTTCAGGCTCGCAGATAATGG
SR012	TTGGCGCAGTCTCTATCACATCAG
SR013	GCCTGTGCTTGTTTCTTCCGGTTG
SR014	CGACGGAAAGTGACAAATCCAACC
SR015	CAAAATTGCCCAGCACGTCTACCAC
SR016	GAAGAGCATTGTTTGAGGCGCGTCCGATGATTCAAGCCACCTTAC
SR017	GCATCAGTGCCTCCTCTCAGACAGGCCTGTCTTGAGAGCTGGATGAAG
SR018	TGCTCTGATCGTCCCTGCTACTTG
SR019	GTTGTGGGAGATGAGGTCCAATCC
SR020	AAACTGTCTTTGCCACGGGATTG
SR021	ACGATGTTGATGGATGTGGGTCTG
SR022	GAAGAGCATTGTTTGAGGCGAATTCGGAGTGAAAACCGCGACAC
SR023	GCATCAGTGCCTCCTCTCAGACAGCGTTCGGACACCCTATCTTGTG
SR024	GATAGTCTTCCAAGCTGCGACAAG
SR025	TGGTGGCCTTATTCCAGCTCCTTG
SR026	AATTACCTCGCTTGGGGTACTCACG
SO642	CTACTTGGAAGTGGCGACTG
SO643	CGCCGCTCTTGAATTGATAC
SO644	GAAGAGCATTGTTTGAGGCGATTATCCAGAGGCACAGTGC
SO645	ATCAGTGCCTCCTCTCAGACAGTAGTATTTACGATGAAACGAAAC
SO646	CTCTCCTCTCAGGTTTCGGG
SO647	GATAAACTGCCGTGTCTCCG
HP065	CGTTCGGCGATCTCGTCTGGGTTC
HP066	GTAAACACCTGGGATAATACGGCTG
HP067	TAGTCGGTGACAACGGTTGGATTG
HP068	TGGAGAGGGATAACTAGCGATACC
HP069	GTTTCGCAGCCGATTATCCCAGGTGTTTACGGAGCTGGTGCAGGCGCTGGAGCC

HP070	AGAACTCAATCCAACCGTTGTCACCGACTACTGTCTGAGAGGA GGCACTGATGCGTG
HP072	GGCTTTCTATGTTCTGGACGGACTC
HP073	ATAATCAATGGCGTACGTCAAGGGC
SR96	CTACAAGGGAAGGAGGTTTCGCAAG
SR97	GGCTCCAGCGCCTGCACCAGCTCCTGAACGTGCGGGAAAGCG TC
SR98	GCATCAGTGCCTCCTCTCAGACAGGTTCTGTAGACAAATTCAA T
SR99	GTACGAAACCGTCAGCGTCTGTTC
SR100	TCTCCTCGGTTTAAGGGAGACTCG
SR101	GCACGAATTCTCCCCGATAAATCC
SR102	TGGGCTTTGCTCCCATCAACTTC
SR103	GGCTCCAGCGCCTGCACCAGCTCCTGCTTTGGTTGTGACGTTG CGC
SR104	GCATCAGTGCCTCCTCTCAGACAGATTGATACGCTCTAATGGA T
SR105	ACATGCCAGCAAATTCCTTCCTG
SR106	CAGGGAAAGGAGGTACGTGACAAG
SR107	CACCGTTCGTTCCAAATGTCG
SR108	TGACATTTCCGCCCATAGCTCAC
SR109	GGCTCCAGCGCCTGCACCAGCTCCTTCGGTTTTCTTCGCACCG
SR110	GCATCAGTGCCTCCTCTCAGACAGCGCTATCGTACTTGAGGTC TC
SR111	GCCCTTTCCCTTTGAGCATATTCC
SR112	GGCATATTGCGTAGCGAGTCTTCG
SR113	GATACAGTTTCCTCCTGCCTTTCC
SR114	TGCCAAACAAGACTCCAGCCTCTC
SR115	GGCTCCAGCGCCTGCACCAGCTCCATGCCGCTTATTATGTCCC ATTG
SR116	GCATCAGTGCCTCCTCTCAGACAGCGAGGATATCGGGTTGGTA AAAAG
SR117	GAAATCCGCTGGAATATGGACGTG
SR118	AACACTCCCTTCTGGCTCGATGTC
SR119	GTCGAAGATGAACCACCGCTCAAG
SR120	CGCTTGGCCTCGGAACAATATCTAC
SR121	GGCTCCAGCGCCTGCACCAGCTCCAGGTTCTTTTTGCTATCTT CCTC
SR122	GCATCAGTGCCTCCTCTCAGACAGATTCCTCTTGGTCTGAGA C

SR123	TTGAAGACTCCGTCGTTTCTGTGG
SR124	TTGTATATGAGCCAGCGACCAAGC
SR125	GATATGCACGCCCTTTTCCAGGTC
SR126	ATCATGGACGTGTTCCCTCGACGTTT
SR127	GGCTCCAGCGCCTGCACCAGCTCCCTTTCCCAGGTACTGCCCC C
SR128	GCATCAGTGCCTCCTCTCAGACAGTGTTTCTAATGCCGTGCAG ATG
SR129	GATGGATTCCCTCACGCTCTGTTTC
SR130	CCTAGTAGCGTTTCGGCCATTCTTC
SR131	TACGTCTTGCATCGTGGACCTTTC
HP116	GGAGCTGGTGCAGGCGCTGGAGCC
LU233	CGCCTCAAACAATGCTCTTC
FN01pyrG	CTGTCTGAGAGGAGGCACTGATGC

Chapter 3. The proteolytic activation and nuclear translocation of the SrbA protein in response to gaseous signaling in *Aspergillus nidulans*

3.1 Introduction

The Sterol Regulatory Element Binding Protein (SREBP) was first identified in mammalian cells as the critical transcriptional regulator of the LDL (Low Density Lipoprotein) receptor gene⁵¹. LDL binds cholesterol to enable its solubility and transport through blood plasma and the LDL receptor is responsible for the cellular uptake of cholesterol-bound LDL. Low cholesterol levels were known to activate transcription at the promoter of the LDL receptor gene (thereby promoting the transport of plasma cholesterol into cells) and high cholesterol repressed transcription of the LDL receptor gene⁵². This suggested the presence of a regulatory transcription factor that bound to the LDL receptor gene promoter in a cholesterol dependent manner. A specific octamer sequence designated SRE-1 (Sterol Regulatory Element 1) was identified in the promoter of the LDL receptor gene as necessary for this cholesterol-dependent regulatory activity⁵³. In a subsequent study, using gel mobility shift assays, a specific protein from rat liver nuclear extracts was identified that specifically bound to SRE-1 oligo sequences⁵¹. This protein called SREBP (Sterol Regulatory Element-1 Binding Protein) and was also isolated from human (HeLa cell) nuclear extracts, sequenced and further characterized⁵⁴. Northern blots of human SREBP mRNA found it expressed in a variety

of tissues like the muscle, kidney and lung with the strongest expression in liver and adrenal tissues. In another study, western blots using anti-SREBP-1 antibodies (directed at the SREBP-1 N-terminus) identified something unexpected:- SREBP-1 protein from HeLa cell nuclei migrated as a at ~68kD while SREBP-1 protein from whole cell extracts containing a SREBP-1 cDNA expression vector, migrated at ~125kD⁵⁵. This suggested that the full-length protein (125kD) was cleaved proteolytically to produce the nuclear form (68kD). Cell fractionation experiments revealed that the full-length SREBP-1 protein was in the membrane-bound fraction while most of the short SREBP-1 protein was in the nuclear fraction. Incubation of HeLa cells with increasing concentrations of sterols resulted in the corresponding reduction of the short nuclear form. It was thus concluded that SREBP-1 was synthesized as a 125kd full-length protein bound to the ER and nuclear envelope and when cholesterol was depleted the full-length protein was cleaved to release the N-terminal protein (68kD) that translocated to the nucleus.

Two SREBP homologous proteins Sre1 and Sre2 were identified in fission yeast *Schizosaccharomyces pombe* based on sequence similarity to SREBP-1⁵⁶. No such homologs have been identified in *Saccharomyces cerevisiae*. Antibodies raised specifically against the N-terminal region of Sre1 were used to analyze the *S. pombe* protein through western blots⁵⁶. The full-length precursor Sre1 protein was detected at ~110kD. Similar to mammalian SREBP, chemical inhibition of ergosterol synthesis in cells resulted in the production of a smaller cleaved Sre1 protein at ~55-80kD. Microarray analysis in WT and Δ sre1 strains, with and without chemical inhibition of ergosterol synthesis, identified numerous genes with differentially expressed RNA⁵⁶.

Many of these genes encoded enzymes that require oxygen for their respective catalytic activities, for example biosynthetic enzymes of ergosterol, heme and sphingolipid^{56,57}, suggesting Sre1 might be required for growth under anaerobic conditions. Deletion of the *sre1* gene resulted in cells that were unable to grow under anaerobic conditions while showing normal growth under aerobic conditions⁵⁶. Using a controlled hypoxia workstation, cleavage of the Sre1 protein was analyzed under different oxygen concentrations. Under 0.2% oxygen very little cleavage was observed, whereas the level of cleaved SrbA protein steadily increased proportional to time spent under anaerobic (~0% oxygen) conditions. The yeast SRE regulatory sequences were identified in a subsequent study using promoter truncations fused to a lacZ reporter⁵⁷. The molecular mechanism of SREBP promoter binding appears to have a high degree of conservation based on the fact that the fission yeast Sre1 protein was able to bind the SRE sequence of the human LDL receptor gene promoter⁵⁷.

The *Aspergillus nidulans* SREBP (Sterol Regulatory Element Binding Protein) was first identified in a screen for hypoxia sensitive mutants³⁷. One of the genes identified in this screen, AN7661 was designated *srbA* based on its sequence homology to the *Aspergillus fumigatus srbA* gene, Afu2g01260. Afu2g01260 was one of several transcription factors identified in a screen of genes transcriptionally induced under hypoxia (through microarray analysis) and was designated *srbA* based on sequence homology to the *S. pombe* Sre1 protein⁵⁸. The *A. nidulans* SrbA protein consists of a polypeptide chain of 1015 amino acids. In the N-terminus of the protein is a basic-Helix-loop-Helix (bHLH) transcription factor domain. The transcription factor domain

constitutes only about one third of the entire SrbA protein (Fig 3.1A). The basic region of this bHLH domain contains a characteristic tyrosine residue (Tyr172) in the place of arginine³⁷. This particular substitution differentiates SREBPs from other bHLH transcription factors. In the mammalian SREBP1, this tyrosine residue was found to be critical for binding to the SRE (Sterol Regulatory Element) in promoters of target genes⁵⁹. In *Aspergillus nidulans*, a single point mutation of Tyr(172)→Ser was sufficient to abolish the hypoxia adaptation activity of SrbA³⁷, suggesting that the functionality of this tyrosine is conserved in fungi. The N-terminal transcription factor domain is immediately followed by at least one transmembrane domain (Fig 3.1A) that keeps full-length SrbA tethered to the endoplasmic reticulum (ER) under normoxia circumstances. The remaining two-thirds of the SrbA protein is of unknown function, though it contains a conserved fungal domain DUF 2014 (DUF = domain of unknown function).

Initially, mammalian SREBP1 protein purified from cell extracts migrated at a much smaller size of ~68kD whereas protein from transiently expressed cDNA vector was ~125kD⁵⁵. This was the first indication of proteolytic cleavage of the SREBP1 protein. Cell fractionation experiments in HeLa cells discovered that the full length precursor SREBP-1 protein was predominantly associated with the membrane fraction while the cleaved, mature form of the protein was in the nuclear extract⁵⁵. An analogous process has been confirmed in *A. nidulans* by microscopy analysis of N-terminally tagged YFP-SrbA protein which, under artificially generated hypoxia (~1% O₂), showed nuclear accumulation of YFP signal while the deletion of the proteolytic genes *sppA* and *dscA* resulted in the absence of this nuclear accumulation³⁷. Thus, when oxygen levels drop

below a threshold for hypoxia, the ER-tethered SREBP undergoes multiple proteolytic cleavages resulting in the release of the transcription factor domain from the ER and its subsequent translocation to the nucleus (Fig 3.1B)^{27,36-38}. Published work in yeast and animal systems have demonstrated SREBP activation in response to low sterol levels^{55,56}. Since sterol synthesis is heavily oxygen dependent, it has been proposed in fission yeast that cells may indirectly sense oxygen levels by sensing the levels of ergosterol⁵⁶.

Recently published work analyzed the self-induced oxygen gradient formed in maturing *Aspergillus* biofilms wherein the bottom-most layer of cells (basal cells) had the lowest oxygen concentration that progressively increased towards the uppermost peripheral layer³¹. The importance that these gaseous microenvironments within biofilms have on regulating cell biology was demonstrated in an earlier study through experiments following microtubule(MT) disassembly and reassembly in response to simple air-exchange in basal biofilm cells³⁴. The presence of the *srbA* gene was also found to be necessary to trigger the MT disassembly process in the developing *A. nidulans* biofilm. Results from a very recent study have expanded the repertoire of biofilm driven cell biological changes dependent on the presence of *srbA*³⁵. In addition to microtubules, ER exit sites, Golgi bodies and actin patches were altered in expression levels and/or localization pattern during biofilm development and these changes failed to take place when *srbA* was deleted.

The presence of the hypoxia-adaptive *srbA* gene seems to be important in regulating fungal cell biology in response to the self-generated hypoxia produced during biofilm maturation. It was therefore worth investigating the expression pattern of the

SrbA protein during biofilm development. Is the SrbA protein activated to release the nuclear localized transcription factor domain during biofilm development? Is the self-generated hypoxia produced by the developing biofilm sufficient to trigger activation of the ER-tethered SrbA? Studies of SrbA activation so far have depended on artificially generated hypoxia through the use of ambient gas chambers or oxygen purging (in liquid media). Does SrbA activation behave as expected under the naturally developing hypoxia in biofilms?

3.2 Results

3.2.1 The Sterol Regulatory Element Binding Protein (SREBP) SrbA undergoes proteolytic activation and nuclear accumulation in basal biofilm cells

To investigate the potential regulatory role of the SrbA transcription factor in biofilm cells the first question to be answered is whether the protein undergoes the canonical proteolytic activation during biofilm development. Since basal biofilm cells produce a hypoxic microenvironment, this should trigger the activation and subsequent nuclear accumulation of the N-terminally SrbA transcription factor domain. Live cell spinning disc confocal microscopy of basal biofilm cells was used to follow the levels and locations of the YFP-tagged SrbA protein over time as the biofilm developed. An *A. nidulans* Δ *srbA* strain containing an ectopic genomic integration of an N-terminally tagged 4X YFP-SrbA construct under the control of the *srbA* promoter was used for this experiment. This strain was obtained from the Chae lab and has already been characterized and published³⁷. To generate the biofilm for microscopy, fungal spores were inoculated in a microscopy cell culture dish containing 3 ml media at a specific

concentration of 2.5×10^5 spores/ml. Incubation resulted in the attachment, germination and growth of multinucleated fungal filaments (mycelia) over the base of the culture dish. Over time the mycelia continue to branch out and grow upward through the media. As the rate of oxygen consumption increases, hypoxia develops in the basal layer of cells because this layer has the highest cell density and is farthest away from the air-media interface (Fig 3.2A). To follow the YFP-SrbA protein fluorescence, spinning disc confocal microscopy of the basal cells was carried out every 3 hours at different stages of biofilm development (Fig 3.2B).

The YFP-SrbA protein was initially observed in the ER at the early stages of biofilm growth (Fig 3.3 18 hours) consistent with published data of SREBP subcellular localization under normoxic conditions in *A. nidulans* and other systems^{27,37,56}. After growth for ~26 hrs at RT (22-24 °C), the YFP signal accumulated in the nuclei of cells accompanied by a loss of signal in the ER (Fig 3.3 26 hours). This is consistent with the SrbA transcription factor domain carrying the N-terminal YFP tag being released from the ER and translocating to nuclei. Interestingly, SrbA protein was not maintained after the activation process and disappeared in the later stages of biofilm formation (Fig 3.3 48 hours).

To capture the SrbA activation process in basal biofilm cells in greater detail, time-lapse microscopy was carried out at the approximate time of activation on a specific field of cells to image the activation process in the same cells over time. Initially the full length precursor SrbA protein was tethered to the ER consisting of the outer nuclear envelope (Fig 3.4A green arrows) and a cytoplasmic ER membranous structure (Fig

3.4A,B white arrows). After 30mins these cells began the activation process. The beginnings of nuclear accumulation of SrbA were clearly visible (Fig 3.4C yellow arrows). The signal distributed over the ER was reduced while small punctate bodies appeared (Fig3.4C pink arrows). 15 minutes later the punctate bodies largely disappeared and the YFP signal was mainly seen only in nuclei (Fig 3.4D). Finally, the intensity of the nuclear signal dropped (Fig 3.4E) and ultimately largely disappeared (Fig 3.4F). The complete process of SrbA activation, from the ER to complete dispersal, took approximately 1 hour during biofilm formation.

These results show that the SrbA protein does indeed translocate to the nucleus in basal biofilm cells. Nuclear translocation of the SrbA N-terminal domain is a process known to be triggered by proteolysis of the ER-tethered full length SrbA protein. This confirms that basal cells in a growing biofilm experience a progressively developing hypoxia such that, when a certain hypoxic threshold is crossed SrbA activation is triggered. After activation, the N-terminal SrbA protein translocated to nuclei of basal cells but did not remain there continuously throughout biofilm development. All YFP signal was completely dissipated approximately 1 hour after activation.

3.2.2 SrbA activation is reversible in basal biofilm cells

The above results established that the SrbA protein was activated in response to the self-generated hypoxia in basal biofilm cells as the biofilm matures. Earlier publications have demonstrated that the simple act of removing the lid of the culture dish results in air exchange that changes the gaseous microenvironment of the basal cells and reverses the cell biological effects experienced by biofilm cells³⁴. To confirm that

proteolysis of SrbA is truly responding to the gaseous microenvironment and not some other trigger, the same type of lid removal experiment was carried out. The lid removal gives more access to ambient oxygen to dissolve in the culture medium thereby altering the oxygen gradient down to the basal layer. In other words, it is thought to relieve the hypoxia developed in the basal cell microenvironment.

The YFP-SrbA strain used in the previous experiment was again followed using microscopy and its activation in a single basal cell was followed during biofilm development. After YFP-SrbA was observed undergoing activation, nuclear accumulation (white arrow) and dispersal in the developing biofilm (Fig 3.5A), the lid of the imaging dish was removed to allow air exchange while the imaging dish was secured to the microscope stage. The YFP-SrbA signal first reappeared in the nucleus (white arrow) and later was observed in its ER tethered form (Fig 3.5B). However, as time passed with the lid off nuclear accumulation of SrbA ceased and only the ER-tethered form was observed.

This demonstrates the reversibility of SrbA activation in basal biofilm cells. These results show that the SrbA activation is clearly responsive to the gaseous microenvironment within developing biofilms. This is also the first piece of evidence demonstrating SrbA activation without any artificially imposed hypoxia and is the closest possible experimental setup to what might be occurring in natural biofilms.

3.2.3 SrbA nuclear accumulation is transiently activated by exogenously supplied nitric oxide

Proteolytic activation of SrbA is clearly responsive to a hypoxic gaseous environment. However, the exact mechanism of hypoxic sensing by SrbA is unknown.

Hypoxic environments affect cellular metabolism in numerous ways. Cells experiencing hypoxia produce specific gaseous molecules like nitric oxide (NO) which then acts as a signaling molecule. The responsiveness of SrbA to air exchange strongly suggests the involvement of a gaseous signal but it is unclear how the absence of oxygen specifically triggers the proteolytic activation and if additional gaseous components might also play a role. One possibility is that SrbA activation is actually triggered by a hypoxia-associated gas like NO that acts as a hypoxic signaling molecule. The question to be asked is whether the SrbA protein can be artificially activated by exogenously supplied nitric oxide when the cell is *not* experiencing hypoxia.

To investigate this, the same N-terminally tagged 4X YFP-SrbA strain as described in previous experiments was used. A ‘nitric oxide releasing compound’ called NOC-18 was used to supply nitric oxide (NO) to the cells⁶⁰. NOC-18 has been characterized as a useful NO-donor to the study the effects of NO on cells in various organisms⁶¹⁻⁶⁸. One advantage of NOC-18 is that it has a long half-life of more than 2 days (depending on the pH) producing a steady release of NO over a long period of time^{60,69}. This is particularly important because NO is a volatile gas making it difficult to elicit cellular responses at low physiological concentrations before the gas dissipates. At the same time, using excessively high concentrations of NO to compensate for the volatility has lethal effects on the cell⁷⁰.

Cells were grown at a lower initial inoculation density (compared to biofilm experiments) and the experiments were carried out at a relatively early stage of growth. This was important to ensure that cells didn’t produce the self-generated hypoxia that

would confound the results from the effects of NO. Fungal spores were inoculated in the imaging dish at a low density of 1×10^5 spores/ml such that the resulting cells (after overnight growth at RT) were adequately spaced apart to maintain a normoxic environment. This was confirmed by the fact that cells at this stage only showed ER localized SrbA protein and no nuclear accumulation.

200 μ M NOC-18 (final concentration in medium) was added to the culture dish after which, time-lapse imaging of YFP-SrbA was immediately carried out using a 5-minute delay between images. The first change was observed about 10 mins after the addition of NOC-18. The subcellular localization of SrbA was altered to numerous small punctate bodies distributed throughout the cell (Fig 3.6), similar to those observed during biofilm activation of YFP-SrbA. At 20 mins, most of the YFP signal accumulated in the nuclei, signifying complete proteolysis and nuclear translocation of the N-terminal transcription factor. However, by the 40 min timepoint, SrbA was no longer accumulated in the nucleus and only ER-tethered SrbA is observed. A control culture dish (inoculated and incubated in parallel with the test dish) that was never treated with NOC-18 was used for comparison. The cells in this dish only showed ER-tethered SrbA signal throughout the duration of the experiment. Therefore, the nuclear accumulation of SrbA observed after the addition of NOC-18 must be due to the effects of nitric oxide and not because of self-generated hypoxia. Although NO did indeed trigger SrbA activation, the timing of activation showed some variation between experimental repeats (within ~20-30 min).

These results provide the first piece of evidence that a gaseous molecule other than oxygen can trigger SrbA activation. NO was able to trigger SrbA activation in

normoxic fungal cells but the activated state was not maintained despite the fact that NO was (presumably) continuously produced by NOC-18. Proteolytic activation triggered by NO was transient with YFP-SrbA reappearing in its ER-tethered unprocessed form. This was unlike the activation observed in the biofilm context where YFP-SrbA completely disappeared after nuclear activation.

3.3 Discussion

The proteolytic activation of the SREBP protein in response to low sterol or low oxygen has been well established in fungi, yeast and mammalian cells. These studies have used a variety of methods, from nitrogen purging to anaerobic gas chambers, to artificially impose a hypoxic environment on cells, thereby triggering SrbA activation and nuclear translocation. Whereas in naturally developing fungal biofilms, the increasing rate of oxygen consumption results in progressively hypoxic gaseous microenvironments, especially for cells furthest from the biofilm periphery. This is the first time that behavior of the SrbA protein in living fungal cells has been observed in real time and in response to the self-generated hypoxia of a developing biofilm. The above experiments have confirmed the activation and nuclear accumulation of the SrbA protein in response to the naturally developing hypoxic microenvironment of *A. nidulans* basal biofilm cells. The fact of this observable nuclear activation of SrbA supports the hypothesis that SrbA plays an important role in the regulation of biofilm cell biology. Closer analysis of the SrbA activation process reveals a potential intermediate transport step between the ER and the nucleus. When SrbA undergoes activation a number of small punctate bodies are observed transiently and ultimately disappear once the fluorescence

signal is mainly nuclear. This observation could be explained by the transport of SrbA protein from the ER to an organelle like the Golgi during the activation process before the release of the fully processed nuclear transcription factor. In fact, the Dsc ubiquitin ligase complex that is required for SrbA proteolysis is known to be localized in the cis-Golgi in fission yeast and the transport of Sre1 from the ER to Golgi was found to be necessary for Dsc complex mediated proteolysis⁷¹. If this process is conserved in *Aspergillus*, it would explain the appearance of the small punctate bodies during activation and is an interesting avenue for further investigation.

Interestingly, after nuclear accumulation of the N-terminal transcription factor domain, the fluorescent signal completely dissipates both in the ER and the nucleus. This unexpected phenomenon may be explained by instability of the cleaved N-terminal domain due to the 4 bulky YFP molecules fused to it though published experiments with this strain has demonstrated the ability of the 4XYFP-SrbA construct to functionally rescue the $\Delta srbA$ strain. If the result is not an artefact of the quadruple tag, this may be evidence of additional nuclear regulation of the SrbA transcription factor in the context of a developing biofilm. Sre1 in *S. pombe* is already known to be regulated by an oxygen dependent prolyl hydroxylase (Ofd1) that specifically degrades nuclear Sre1 protein in the presence of oxygen⁷². However, in this case, perhaps a different mechanism such as anoxic protein turnover plays a role in degrading nuclear SrbA.

Nuclear SrbA appears to be degraded after about 20-30 minutes of accumulating in the nucleus. This suggests that nuclear SrbA function is required only within a very

specific window during the early stages of biofilm development. Alternatively, SrbaA may only be required to initiate downstream processes but not to maintain them.

When air-exchange is allowed via culture dish lid removal, the nuclear SrbaA reappears first (within 5-10 mins) and only after 20-30 mins is ER-tethered SrbaA observed. One possible explanation is that the process of turning over of the nuclear SrbaA is stopped first once the lid is removed, but the conditions are still hypoxic enough for proteolytic activation cleavage to continue. Presumably, the proteolytic pathway in the ER is still active and newly synthesized SrbaA protein is immediately cleaved and therefore only observed in the nucleus. After ~30 mins of air exchange the gaseous microenvironment of the basal cells is no longer below the hypoxic threshold. Consequently, proteolysis of SrbaA stops and only the full-length ER-tethered SrbaA protein is observed with no visible nuclear accumulation.

The fact that exogenously supplied nitric oxide is able to trigger SrbaA activation under normoxic conditions is a novel finding. SrbaA shows clear nuclear accumulation in response to the addition of the nitric oxide donor. However, after a short time of maintaining fully processed nuclear SrbaA, the activation process apparently stops. YFP signal is observed only in the ER at this stage indicating that the YFP-tagged N-terminal domain is no longer cleaved from the full length SrbaA protein tethered to the ER. Since NOC-18 has a half-life of more than 2 days when dissolved in the media, one would expect that the effective NO concentration that the cells are exposed to would be maintained well beyond the duration of the experiment (~3 hours maximum). Yet NO-induced SrbaA activation is transient. In yeast, under normoxic conditions, the oxygen-

dependent prolyl hydroxylase Ofd1 targets nuclear Sre1 protein for degradation⁷² and *Aspergillus nidulans* contains the Ofd1 homolog. Although this protein turnover may explain the loss of nuclear SrbA it does not explain the absence of proteolysis of the ER-tethered protein. In the biofilm context, SrbA activation is also maintained for a short while but then completely disappears, both the nuclear protein and the full-length ER-tethered form. Interestingly, in both the naturally induced (hypoxic biofilm) and the artificially induced (nitric oxide) activation process, the cleaved SrbA transcription factor resides in the nucleus only for a short duration. This is consistent with the idea that the processed SrbA transcription factor may be needed only to initiate downstream regulation but is not necessary after that. This transient nuclear localization of SrbA has not been observed before in either yeast or fungi. This behavior may be specific to the biofilm context or the particular experimental conditions used in the above discussed experiments. Further investigation could provide deeper insight into the nature of SrbA's regulatory role in developing biofilms.

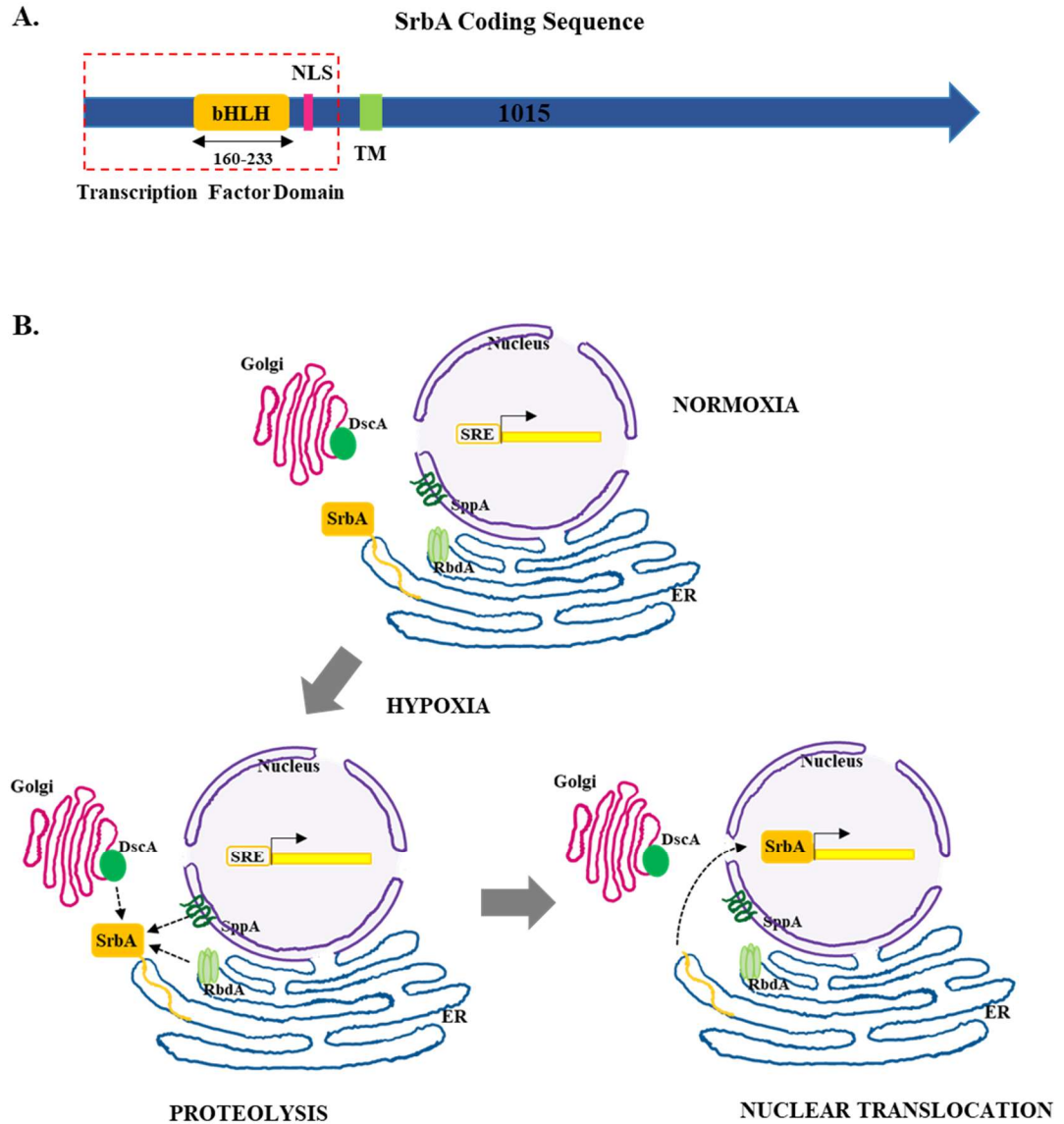


Figure 3. 1 Srba protein structure and regulation A. Schematic of Srba amino acid sequence. Schematic representation of the 1015 amino acid long Srba coding sequence. bHLH = basic Helix-Loop-Helix domain, NLS = Nuclear Localization Signal, TM = Transmembrane domain. Numbers represent amino acid position relative to the first methionine. The red box denotes the transcription factor domain that is released after activation. B. Model of Srba protein proteolytic activation and nuclear translocation. Under normoxia, full length Srba protein is tethered to the ER. Under hypoxia, Srba undergoes proteolysis by the Dsc complex, RbdA and SppA to release the SrbA transcription factor domain from the N-terminal of the protein. The transcription factor translocates to the nucleus where it binds the SRE element in target gene promoters to regulate their transcription.

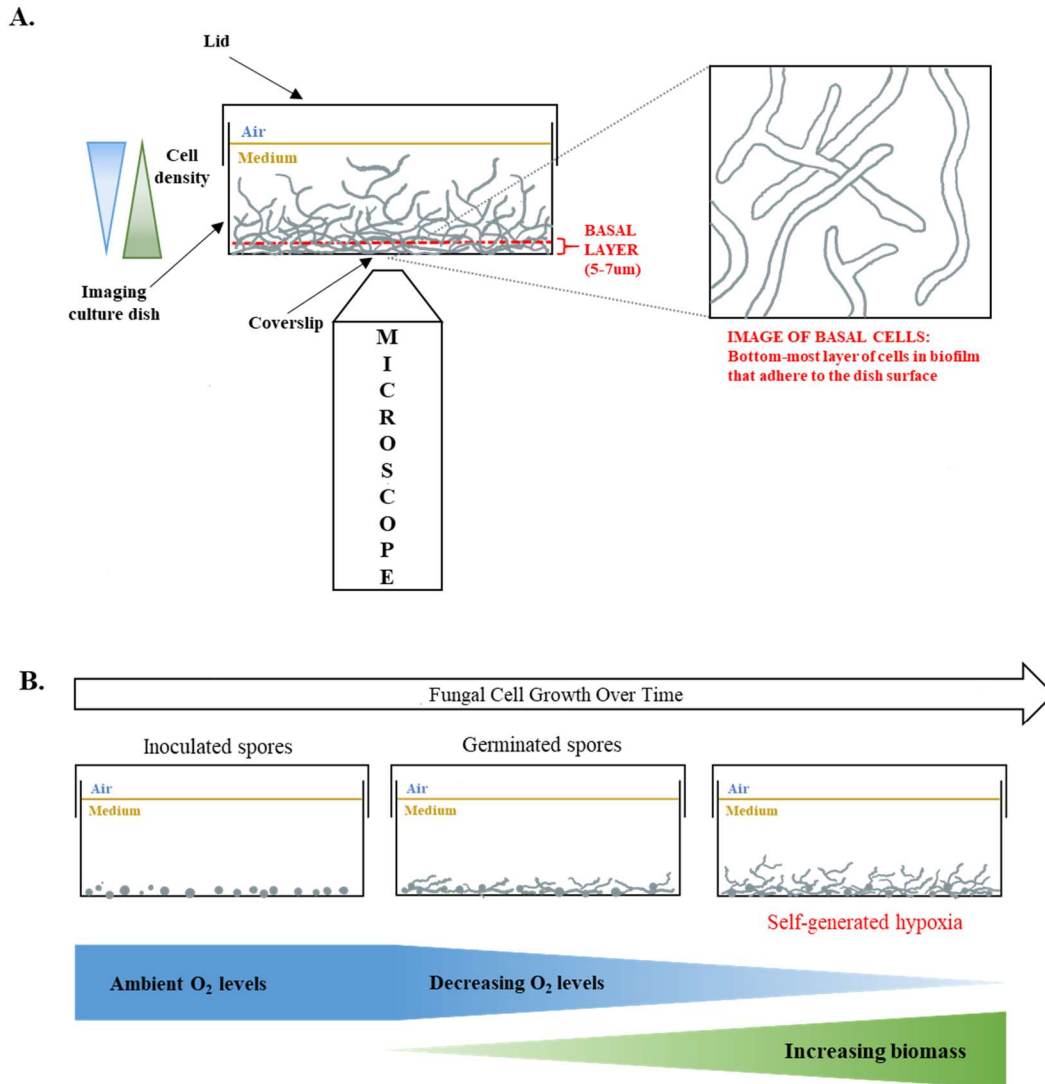


Figure 3. 2 Schematic of experimental setup to track hypoxic biofilm cell biology A. Filamentous fungal cells are grown in a cell culture dish containing a coverslip on the bottom surface. This allows microscopy imaging of the basal layer of cells. Cell density is greatest at the base of the dish and decreases as you move up (green triangle). Due to the oxygen consumption and differential O₂ solubility with distance from the air-media interface, an inverse O₂ gradient is generated (blue triangle). B. Spores inoculated in an imaging culture dish germinate and grow into long, filamentous cells (grey) that adhere to the bottom surface of the dish and continue to grow up through the culture medium. Over time, the basal layer of cells experiences decreasing oxygen levels resulting in a self-generated hypoxia. Tracking cell biological changes in the basal cells during this process gives information on how the cell responds to hypoxia in a natural biofilm.

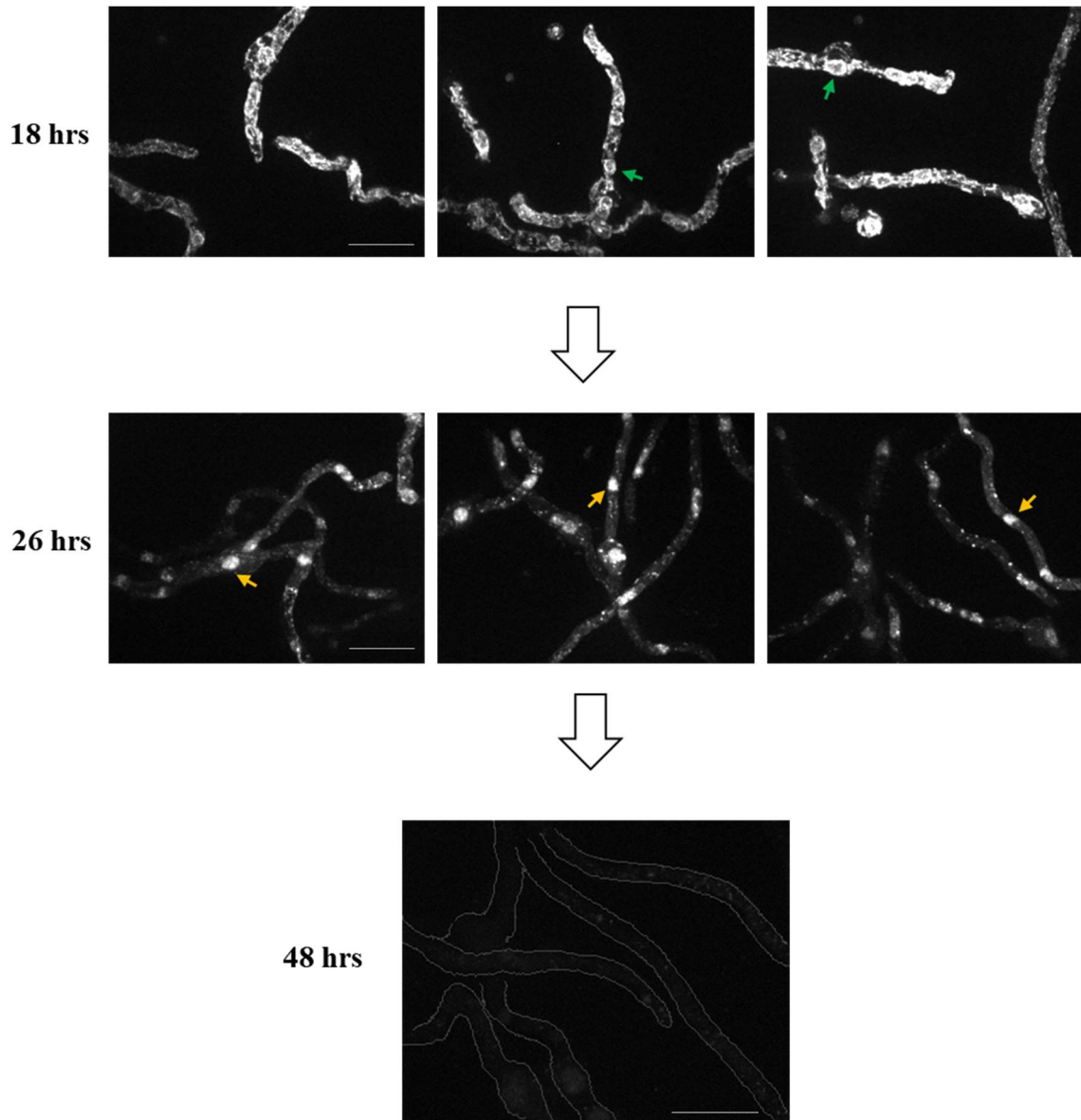


Figure 3. 3 SrbA protein undergoes activation and nuclear translocation in basal cells during the early stages of biofilm development. YFP-SrbA is localized in the ER (green arrow) at 18 hours post inoculation as observed in three separate fields of basal biofilm cells. At approximately 26 hours the basal cells have triggered SrbA activation resulting in nuclear accumulation (yellow arrow) of the YFP-tagged N-terminal domain. The YFP-SrbA signal completely disappears after activation in basal cells as seen at 48 hours post inoculation. Scale bar, 10 μm .

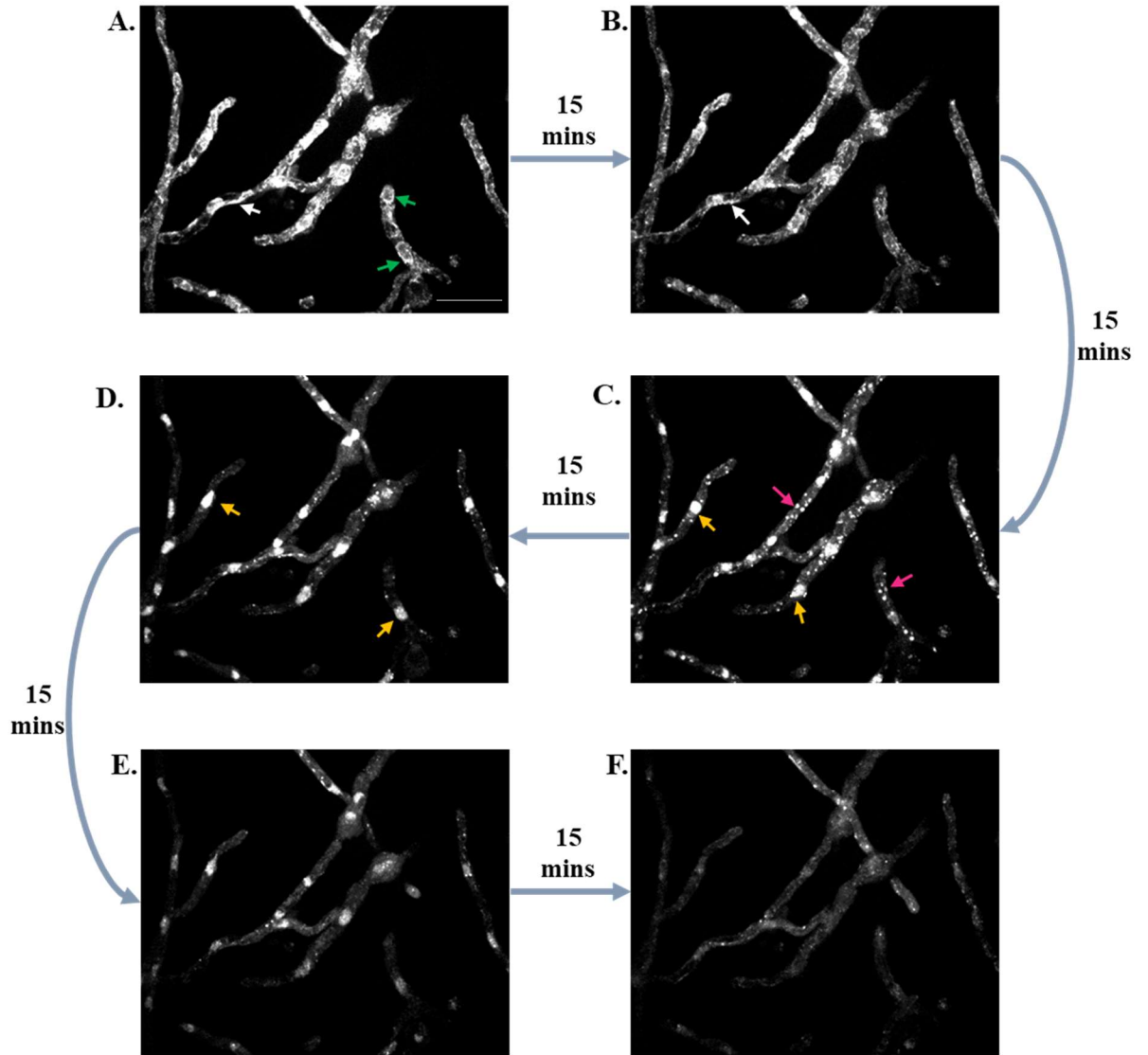


Figure 3. 4 Examination of the Srba activation process within the same basal biofilm cells. The process of Srba activation was captured in a specific field of cells at ~27 hours post inoculation when grown at room temperature. Initially, YFP-Srba is localized in the ER (A, B). Green arrows indicate the nuclear envelope. Cells in the intermediary phase of activation was captured (C) where nuclear accumulation (yellow arrows) is visible as well as small punctate bodies (pink arrows). The punctate bodies eventually disappear (D) leaving only nuclear localized Srba (D, E). Finally, all Srba signal dissipates completely (F). The whole activation process takes approximately 1 hour. Scale bar, 10 μ m

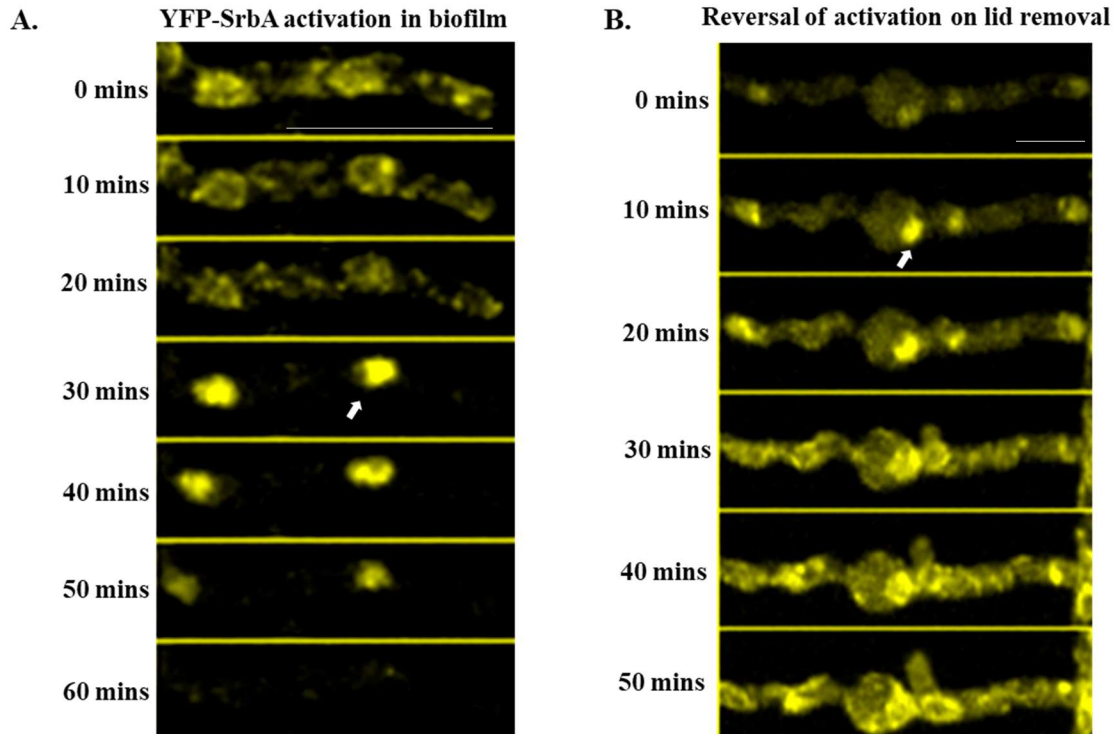


Figure 3.5 *SrbA* activation in basal biofilm cells is reversible in response to air exchange. **A.** *SrbA* activation in a single basal cell was observed in response to self-generated hypoxia in the biofilm. The white arrow indicates nuclear accumulation of *SrbA*. **B.** After nuclear localization and dispersal of YFP signal, lid removal was carried out to allow air exchange. Within the first 10 minutes the YFP signal reappeared predominantly in the nucleus (white arrow). Then nuclear accumulation gradually decreased until finally localized in the ER (30-50 mins). Scale bar, 5 μm .

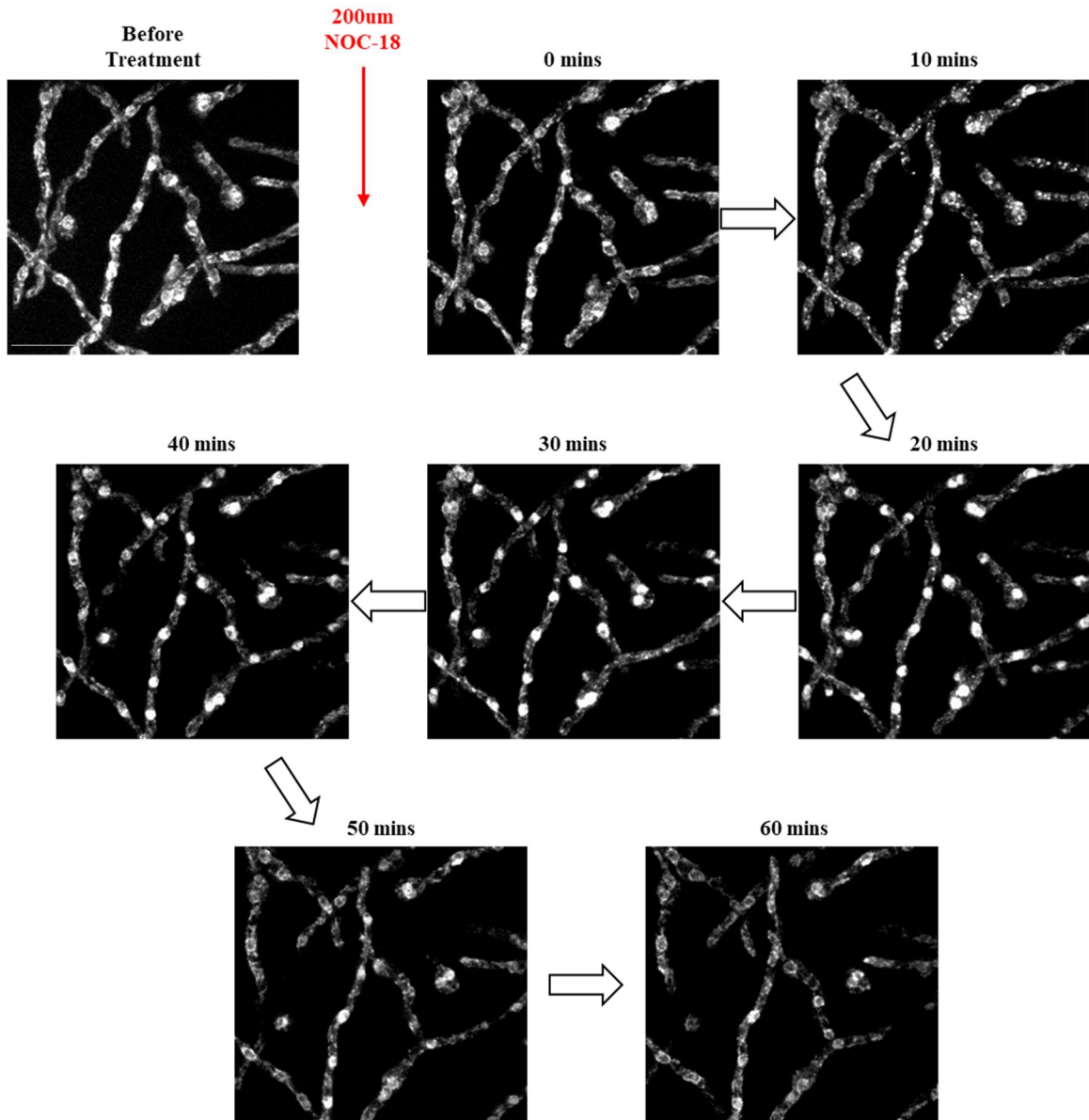


Figure 3. 6 Proteolytic activation of SrbaA is triggered by NOC-18 treatment. Cells grown under normoxic conditions showed the typical ER-localized SrbaA signal (Before treatment). 200 μm of NOC-18 was added to these cells and within 10 minutes a change in localization was observed. The intermediary stage of the activation process was observed wherein small punctate structures appear. By the 20-minute timepoint clear nuclear localization is visible that is maintained up to 40 minutes. Finally, about an hour post-treatment, SrbaA was no longer activated and was ER-localized. Scale bar, 10 μm .

Chapter 4. The role of sterol-regulatory transcription factors in biofilm MT disassembly

4.1 Introduction

Mature fungal biofilms are known to have anoxic cores based on their ability to facilitate growth of obligate bacterial anaerobes^{30,73}. Shukla et al. 2016 demonstrated that in *Aspergillus nidulans*, basal biofilm cells experience a changing gaseous microenvironment in the process of developing into a mature biofilm³⁴. As cells accumulate biomass through growth, their rate of oxygen consumption outpaces supply and the basal cells likely experience increasing self-generated hypoxia. A more recent publication confirmed these findings by measuring the actual oxygen concentration at different depths of the culture dish as well as at different points in time during biofilm development³¹. Shukla et al. found that the gaseous microenvironment can regulate cell biological processes such as microtubule (MT) disassembly and that in the absence of a hypoxic transcription factor, SrbA, this regulation is lost³⁴. Similarly, Lingo et al. 2021 further reported modifications in multiple cell organelles through live-cell imaging of organelle-specific markers in basal cells during biofilm development³⁵. Significant alterations were observed in ER exit sites, early Golgi and endocytic actin patches, while the ER itself remained unchanged. The presence of *srbA* was necessary to trigger these biofilm-driven modifications. Interestingly, exogenous nitric oxide treatment of cells *not*

in a biofilm could produce the same modifications. Thus, gaseous signaling is clearly important during biofilm development and has wide-ranging effects in modifying cell biology.

SrbA is a sterol regulatory element binding protein that is known to be required for hypoxia adaptation through its role as a transcription factor³⁶. The transcription factor domain constitutes only about one third of the entire SrbA protein. It is located at the N-terminal region and is immediately followed by at least one transmembrane domain that keeps full-length SrbA tethered in the endoplasmic reticulum (ER) under normoxia (ambient oxygen levels). The remaining two-thirds of the SrbA protein is of unknown function. When oxygen levels drop below a threshold, the ER-tethered SrbA undergoes multiple proteolytic cleavages resulting in the release of the transcription factor domain from the ER and its subsequent translocation to the nucleus (Fig 4.1A)^{27,36-38}. Thus, there is a tight linkage between hypoxia and SrbA transcription factor activation and release from the ER to the nucleus.

Till date, three separate proteolytic mechanisms have been discovered in *Aspergillus* that are involved in the release of the mature SrbA transcription factor from the endoplasmic reticulum (ER)^{27,37,38}. The first is the Dsc ubiquitin E3 ligase complex that was first identified in *Schizosaccharomyces pombe* as a proteolytic regulator of Sre1⁷¹. The Dsc (defective for SREBP cleavage) complex genes (*dsc1*, *dsc2*, *dsc3*, *dsc4*) were identified in a forward genetic screen in *S. pombe* that were found to be necessary for cleavage of Sre1 and Sre2. Tandem affinity purification demonstrated that all 4 proteins interacted *in*

vivo, likely forming a complex. Sequence analysis identified Dsc1 as a Golgi ubiquitin E3 ligase and GFP-tagged Dsc 2 protein localized in the cis-Golgi. Experiments with Brefeldin A (BFA), which fuses ER and Golgi compartments, demonstrated that the co-mingling of ER-resident Sre1 with Golgi-resident Dsc proteins was sufficient to trigger Sre1 proteolytic cleavage. In *A. fumigatus* and *A. nidulans*, DscA, DscB, DscC, DscD and DscE were identified based on sequence homology to the *S.pombe* proteins^{27,37}. Loss of any one of the *dsc* genes rendered *A. fumigatus* sensitive to hypoxia and azole drugs, consistent with the phenotype of *srbA* deletion mutant. Western blot experiments demonstrated that the full length SrB protein is proteolytically cleaved under hypoxia to the shortened form and that this cleavage is disrupted in the absence of *dscA* or *dscC*. Hypoxic regulation of known SrB targets such as *erg11A* and *erg25A*^{26,74} was also disrupted in the absence of *dsc* genes²⁷. These results provide evidence that the Dsc complex proteolytically activates the ER-tethered SrB full length protein and this activation is necessary for the release and function of the mature SrB transcription factor domain.

A Rhomboid family protease *rbdA* was identified almost simultaneously in hypoxic screens by two separate labs as a regulator of SrB^{38,75}. Though the gene is named *rbdA* by one lab and *rbdB* by the other, they are in fact the same gene Afu6g12750. Loss of *rbdA* phenocopied Δ *srbA* causing sensitivity to hypoxia and azole drug treatments. Northern blots and qPCR experiments found *rbdA* as necessary for hypoxic upregulation of *erg11A* and *erg25A* mRNA. GFP-tagged SrB protein failed to show nuclear localization in the *rbdA* deletion mutant³⁸ while a truncated SrB protein containing the

transcription factor domain alone (that does not require release from the ER) was able to rescue the hypoxic growth and azole sensitivity phenotypes of the *rbdA* deletion mutant⁷⁵.

A signal peptide peptidase *sppA* was identified in a screen for hypoxia sensitive mutants carried out in *A. nidulans*³⁷. SppA is a member of the widely conserved aspartyl proteases family present in plants, animals and fungi⁷⁶ that carry out regulated intramembrane proteolysis. Loss of *sppA* resulted in the typical hypoxia and azole drug sensitive phenotypes, just like loss of *rbdA* or the *dsc* proteins. Loss of *sppA* resulted in the inability of SrbA to localize to the nucleus. YFP-tagged SppA protein was found to be ER-localized but interestingly, BiFC interaction between SrbA and SppA was concentrated only at the periphery of the nucleus or the nuclear envelope. Phenotypic rescue of Δ *sppA* with various N-terminal SrbA truncations identified SppA's proteolytic site between amino acid 381-441 on SrbA.

It is unclear why SrbA requires multiple proteolytic cleavage events to produce the activated transcription factor by release from the ER. The proteolysis events also appear to be sequential. Western blot analysis of SrbA fragments produced in the presence or absence of *dscA* and *sppA* reveal that the Dsc complex cleaves SrbA first, followed by SppA³⁷. It is interesting to note that the Dsc complex interacts with SrbA in the Golgi while SppA-SrbA interaction appears to be limited to the nuclear periphery³⁷ (despite the presence of SppA in the ER). This suggests that for the complete activation of the SrbA transcription factor, a combination of multiple signaling events that trigger proteolysis in different cell organelles are required.

AtrR (ABC transporter regulator) is another transcription factor that is required for hypoxia adaptation^{28,29}. *atrR* was originally discovered in a genetic screen carried out in *Aspergillus oryzae* as one of the genes required for azole drug resistance²⁸. Homologous *atrR* genes were subsequently identified in *Aspergillus fumigatus* and *Aspergillus nidulans* and in both cases presence of *atrR* was found to be necessary for azole drug resistance²⁸. In *A. fumigatus* the deletion of the *atrR* gene resulted in loss of hypoxia (~2-4% O₂) adaptation, similar to deletion of *srbA*. In this experiment the fungal cells were subjected to an artificially generated hypoxia using a sealed pack system with oxygen concentration set at 2%. AtrR transcription factor was found to bind to some promoters of genes also regulated by SrbA, such as the ergosterol biosynthetic genes. Deletion of *atrR* resulted in decreased mRNA of these *erg* genes.

An in-depth ChIP analysis aiming to identify genomic targets of the AtrR transcription factor, helped identify the AtrR Response Element (ATRE). AtrR also binds to the promoter of *SrbA* as well as its own promoter. Analysis of the subset of genes commonly regulated by *SrbA* and AtrR revealed that the AtrR and *SrbA* transcription factors have adjacent binding sites on promoters of genes, implying co-regulation²⁹. However, the role of *SrbA* and AtrR in azole resistance is not redundant. A hyperactive *atrR* allele is able to increase azole resistance in a WT strain, yet it cannot rescue the azole sensitivity of the *srbA* deletion strain²⁹.

Previously published work by Shukla et al. 2016 identified *srbA* as necessary to trigger MT disassembly in basal cells of developing biofilms³⁴. The MT disassembly in biofilm cells responded to air exchange brought about by the simple act of removing the lid of the

culture dish. The results implied that a major change in cell biology such as MT disassembly was responsive to the gaseous microenvironment of the biofilm cells. Basal biofilm cells are known to experience increasing self-generated hypoxia³¹ and *srbA*, an established hypoxia-adaptive gene, was required to trigger MT disassembly, a process also potentially responsive to the self-generated hypoxia of the basal cells. Additionally, *srbA* and *atrR* are necessary for fungal resistance to azole drugs that are used to treat clinical infections, many of which demonstrate biofilm-like growth in the host^{2,17}. The role of *srbA* regulation in response to hypoxia within a developing fungal biofilm is therefore worth investigating further.

4.2 Results

4.2.1 Complete proteolytic processing of SrbA protein is required to trigger MT disassembly in basal biofilm cells

In Shukla et al. 2016, the presence of the *srbA* gene was identified as necessary to trigger MT disassembly, a process demonstrably responsive to changes in the gaseous microenvironment of cells. The next question is whether *srbA* is needed specifically for its activated transcription factor activity which would be dependent on its activating proteases for release from the ER to nuclei. Full length inactive SrbA protein is tethered to the ER under normoxic conditions via SrbA's transmembrane domain^{27,37}. Activation of SrbA requires three separate proteolytic pathways, where the first cleavage is necessary for the second cleavage which in turn is necessary for the third, to release the N-terminal transcription factor domain (Fig 4.1A)^{27,37,38,71,75}. To test whether complete proteolytic processing of SrbA transcription factor is necessary for MT dispersal, the gene deletions of *sppA*, *dscA* and *rbdA* were carried out. Loss of each of these genes is

sufficient to disrupt one of the three proteolytic pathways involved in *SrbA* activation^{27,37,38}. Each proteolytic gene was deleted in a strain containing unmodified endogenous *srbA* and C-terminally tagged Eb1-GFP. Eb1 is a protein that specifically binds to the actively polymerizing '+' ends of MTs. Eb1-GFP, tagged at the endogenous genomic locus, allows for MT dynamics to be followed by tracking Eb1 comets that are formed only at the growing '+' ends of MTs (Fig 4.1B).

The Eb1-GFP comets of WT, Δ *sppA*, Δ *dscA* and Δ *rbdA* strains were imaged using confocal-laser microscopy at 3-hour intervals during the course of biofilm development. The control wildtype (WT) strain initially had actively polymerizing MTs as represented by the presence of Eb1 comets (Fig 4.2A 27hrs). By the 36hr timepoint all WT cells completely dispersed their MTs represented by the complete absence of Eb1 comets (Fig 4.2A 36hrs). The three proteolytic deletion strains, Δ *sppA*, Δ *dscA* and Δ *rbdA* failed to disassemble MTs and Eb1-GFP remained as comets just like Δ *srbA* biofilm cells (Fig. 4.2A). This change in MT status was quantified by counting the number of comets relative to cell area. This quantification of comets was plotted at intervals of 3 hours over a 12-hour window during biofilm development. The plot shows a progressive reduction in the number of comets in WT cells over 6 hours to finally reach the stage when all cells have completely dispersed their MTs and have no Eb1 comets (Fig 4.2B). The comparatively large error bars for the timepoint 33hrs is because a large variation in MT status existed at this stage among individual cells in the basal layer of the WT biofilm. In this transitional stage, some cells had Eb1 completely dispersed while others still had active Eb1 comets. However, strains in which *srbA* or any one of the proteolytic genes

was deleted, maintained a high number of comets per unit area of the cell throughout the experiment (Fig 4.2B). This is despite the fact that *ΔsppA*, *ΔdscA* and *ΔrbdA* strains all have the unmodified native *srbA* genomic locus that expresses wild type SrbA protein. One possibility is that deletion of any of the proteolytic genes may result in an unstable partially processed SrbA protein that gets degraded, effectively becoming an SrbA null mutant. However this is unlikely because published work has detected YFP-SrbA (under its endogenous promoter) expression under a microscope as well as by western blots in *ΔsppA* and *ΔdscA A. nidulans* mutants³⁷ while in the *A. fumigatus ΔrbdA* mutant strain GFP-tagged SrbA (under an artificial promoter) was detectable using confocal laser microscopy⁷⁵. This indicates that the presence of the *srbA* gene alone is not sufficient but complete proteolytic activation of the SrbA protein is necessary to trigger MT disassembly in basal biofilm cells. Since the activated SrbA protein consists of a transcription factor domain that translocates to the nucleus, it appears that SrbA's transcriptional regulation of target gene promoters must play an important role.

4.2.2 An additional hypoxic transcription factor, AtrR, is required for MT disassembly in basal biofilm cells

AtrR is a transcription factor that, like SrbA, is required for hypoxia adaptation in *Aspergillus*²⁸. Though each of these transcription factors regulate hundreds of gene promoters, there is evidence that SrbA and AtrR co-regulate a common subset of target genes^{28,29}. Unlike SrbA, AtrR protein is not known to undergo any hypoxia induced proteolysis. The question is whether *atrR* is also required to trigger the hypoxia-responsive process of MT disassembly in basal biofilm cells. To investigate this, the *atrR* gene was deleted in a strain containing endogenously tagged Eb1-GFP. A double deletion

of *srbA* and *atrR* was also created in an Eb1-GFP background. Eb1-GFP dynamics was observed in the control WT as well as $\Delta srbA$, $\Delta atrR$, and $\Delta srbA\Delta atrR$ strains over the course of biofilm development at 2-hour intervals. In the absence of *srbA*, *atrR* or both, cells failed to disassemble MTs and disperse Eb1-GFP comets while the WT strain transitioned from actively polymerizing MTs (Fig 4.3A 27hrs) to complete disassembly of MTs (Fig 4.3A 33hrs) during biofilm development. Quantification of this change in Eb1-GFP dynamics was done by counting the number of comets in all cells imaged relative to cell area. As the WT biofilms matured, the basal cells transitioned from having a high number of Eb1-GFP comets (actively polymerizing MTs) to none (disassembled MTs) (Fig. 4.3B). The deletion strains, on the other hand, failed to undergo this transition and maintained a high number of Eb1 comets till the end of the experiment. These results indicate that the presence of both hypoxia-adaptive transcription factors, *SrbA* and *AtrR*, is required to trigger MT disassembly in developing biofilms.

4.2.3 WT cells can create the gaseous microenvironment that triggers MT dispersal in $\Delta srbA$ and $\Delta atrR$ cells

The next question investigated was what caused the $\Delta srbA$ and $\Delta atrR$ strains' inability to disassemble MTs. MT biofilm disassembly appears to be triggered by some kind of self-generated gaseous signaling, most likely hypoxia³⁴. So, is the lack of MT dispersal in $\Delta srbA$ and $\Delta atrR$ strains due to their inability to produce the gaseous signal or the inability to respond to it?

The approach used to investigate this involved the use of a co-culture of WT and $\Delta srbA$ cells in the same culture dish such that both types of cells would be exposed to the same gaseous microenvironment within the same developing biofilm. Quantification of the

spores inoculated for each strain allowed for the creation of co-cultures composed of specific ratios of the two strains. In the first experiment, a co-culture was inoculated with 80% WT and 20% Δ *srbA* spores. Each strain contained Eb1-GFP while the Δ *srbA* strain alone contained an additional red tag (PH^{OSBP}-mRFP, a Golgi marker) to help differentiate the two types of cells within the co-culture. The MT dynamics of this co-culture was followed by imaging Eb1-GFP over the course of biofilm development. In the co-culture, Eb1-GFP comets readily dispersed in both WT cells (Fig 4.4A purple arrow) and Δ *srbA* cells (Fig 4.4A yellow arrow). In contrast, the control Δ *srbA* strain grown in an independent dish retained active Eb1-GFP comets (Fig 4.4A).

A similar co-culture experiment was carried out between WT Eb1-GFP and Δ *srbA* Eb1-GFP, Δ *atrR* Eb1-GFP and Δ *srbA Δ *atrR* Eb1-GFP respectively. In this case, no red tag was used to differentiate cells, however, each of these co-cultures were composed of 1% WT and 99% Δ -strain spores i.e., the vast majority of spores initially in each dish are those of the deletion strain. In this experiment, again, all cells underwent MT dispersal in the co-cultures while the independently grown Δ *srbA*, Δ *atrR* or Δ *srbA Δ *atrR* did not (Fig 4.4B). These results show that cells lacking *srbA* or *atrR* are perfectly capable of responding to the MT dispersal signal but seem unable to produce the signal independently. Although all deletion strains underwent MT dispersal when co-cultured with WT cells, the percentage of WT cells determined the time taken to induce dispersal. When WT cells were 80%, MT dispersal took place at an earlier stage of biofilm development, whereas when WT cells were 1%, MT dispersal took place at a much later stage.**

4.2.4 $\Delta srbA$ cells respond to a lower threshold of the MT dispersal signal

While both WT and $\Delta srbA$ cells dispersed MTs in the co-culture biofilm, close observation of the transition stage (when cells are just beginning to undergo Eb1 disassembly from comets) revealed something unexpected. In this experiment Eb1-GFP was observed in two different co-cultures of the following spore inoculum ratios:

i) 80%WT and 20% $\Delta srbA$

ii) 20%WT and 80% $\Delta srbA$

$\Delta srbA$ cells were differentiated by the presence of an additional red tag (PH^{OSBP}-mRFP, a Golgi marker). During the transition stage, in both co-cultures irrespective of the relative ratios of spores, $\Delta srbA$ cells began to disperse Eb1-GFP comets *before* WT cells.

Quantification of the number of dispersed cells relative to the number with comets shows that a clear majority (>75%) of $\Delta srbA$ cells were dispersed while a majority of WT cells had active comets at this identical stage (Fig 4.5). This means that $\Delta srbA$ cells are actually *more* sensitive to the MT dispersal signal than WT cells. Eventually all the cells, WT and $\Delta srbA$, in both the co-cultures underwent MT disassembly as shown in the previous section.

Additional experiments were carried out with the co-cultures i and ii, once both WT and $\Delta srbA$ cells had dispersed Eb1-GFP comets in the biofilm. The lid of the culture dish was removed to allow air exchange while the culture dish was secured to the microscope stage. Subsequent changes in Eb1-GFP dynamics were captured at 5-minute intervals (as carried out in Shukla et al. 2016 who showed that lid removal led to MT reassembly and return of Eb1-GFP comets). Within 5 minutes of lid removal, the beginnings of MT

reassembly could be observed (Fig 4.6A). Nucleation of tubulin dimers at microtubule organizing centers (MTOCs) is characteristic of the MT reassembly process. This phenomenon was observed as nucleation of Eb1-GFP at MTOCs first in the WT cell (Fig 4.6A at 5mins, purple arrow) while in the $\Delta srbA$ cells (yellow arrow) Eb1-GFP was still dispersed. At 10mins, Eb1 comets reappeared in both WT and $\Delta srbA$ cells. Next, the lid was replaced to recreate the gaseous microenvironment to disperse MTs and subsequent changes in MT dynamics were captured in 5-minute intervals. This time $\Delta srbA$ cells dispersed MTs *before* WT cells (Fig 4.6B). At 0 mins, both WT and $\Delta srbA$ cells have Eb1 comets. At 5mins, $\Delta srbA$ cell (yellow arrow) has completely lost comets with the Eb1-GFP signal being dispersed throughout the cell while the WT cell (purple arrow) still retains Eb1-GFP comets. Finally at 10 mins, both WT and $\Delta srbA$ cells have lost all comets. In summary, both WT and $\Delta srbA$ biofilm cells were able to respond to the changes in their gaseous microenvironments. When the lid was removed, $\Delta srbA$ cells repolymerized MTs *after* WT cells. When the lid was replaced to allow hypoxia to regenerate, $\Delta srbA$ cells dispersed their Eb1-GFP comets *before* the WT cells. These experiments involving the co-culture biofilm along with the lid removal and replacement tests indicate that $\Delta srbA$ cells are more sensitive to the gaseous dispersal signal than WT cells and are likely responding to a lower signal concentration threshold relative to WT (Fig 4.6C).

4.2.5 $\Delta srbA$ and $\Delta atrR$ can independently trigger MT disassembly in shaken cultures

Shukla et al. 2016 investigated WT MT disassembly dynamics under agitated conditions relative to static conditions and no significant difference was found in MT disassembly³⁴.

In a shaking culture, continuous mixing of the culture medium results in increased dissolved oxygen concentration compared to static cultures because the passive diffusion rate of oxygen through water-based liquid media is very low²⁴. In this experiment, culture dishes were rapidly transferred from actively-oxygenated shaking conditions to poorly oxygenated static conditions. This setup was used as an alternate method of inducing hypoxia in real-time to follow subsequent changes in MT dynamics.

WT, $\Delta srbA$ and $\Delta atrR$ strains, containing endogenously tagged Eb1-GFP, were inoculated at biofilm concentration (2.5×10^5 spores/ml) and incubated in static cultures overnight (~18hrs) to allow cells to germinate and adhere to the bottom of the culture dish. Next, the imaging culture dishes were placed on an orbital shaker set at 100 rpm adjacent to the microscope so that dishes may be transferred rapidly to the microscope stage to capture MT dynamics. Once on the shaker, cells were imaged every 3 hours over the course of about 12 hours. For each strain, two images were taken: one immediately after transfer to microscope stage (0 mins) and another, after allowing the dish to sit still on the stage for 5 mins (Fig 4.7).

In the earlier stages, no change was observed in the status of the actively polymerizing MTs when transferred from shaking to still conditions. At a specific intermediate stage of biofilm growth the following results were observed. The WT, $\Delta srbA$ and $\Delta atrR$ strains had active Eb1-GFP comets at 0 mins, immediately after the transfer from the shaker. However, after sitting still for 5 mins (static condition), all three strains including $\Delta srbA$ and $\Delta atrR$ dispersed MTs. (Fig 4.). Visual inspection of the culture dishes at the end of the experiment compared with identical cultures that had never been on the shaker were

carried out. The $\Delta srbA$ strain grown with shaking had WT levels of biofilm development while the static $\Delta srbA$ showed typical defective biofilm formation.

These unexpected results demonstrate the ability of shaking cultures to rescue the growth defect in $\Delta srbA$ and $\Delta atrR$ and to independently trigger MT disassembly.

4.3 Discussion

Previously published work identified that reversible MT disassembly is a process that responds to the gaseous microenvironment within a developing biofilm³⁴. In addition, the *srbA* gene was found to be necessary to trigger MT disassembly. Results from the previous chapter show that the SrbA protein itself responds to self-generated hypoxia during early biofilm growth and undergoes proteolytic activation. These two independent processes alter biofilm cell physiology and show dynamic responses to changing gaseous environments. The fact that different physiological phenomena respond dynamically to changing gaseous environments within the developing biofilm emphasizes the importance of gaseous signaling in regulating cell biology.

Aspergillus SrbA is known to require at least 3 sequential proteolytic cleavage steps to release the fully processed mature transcription factor from ER to nuclei^{27,37,38,75}. The results discussed above demonstrate that the disruption of any one of the 3 proteolytic cleavage events of SrbA protein is sufficient to prevent Eb1-GFP dispersal from MTs in the biofilm. In other words, fungal cells with proteolysis disrupted produce the same phenotype as the complete deletion of the *srbA* gene. This indicates that the transcriptional regulatory activity of the fully processed mature SrbA transcription factor is critical in a static culture. SrbA's transcriptional regulatory activity appears to be

necessary, in a static culture, to produce the gaseous environment required to trigger MT disassembly in the biofilm.

Since gaseous signaling involving hypoxia appears to be a significant factor, the role of another hypoxic transcription factor, AtrR in regulating biofilm MT dynamics was also investigated. Experiments with the *atrR* deletion strain showed that AtrR is also required to trigger MT disassembly in the late biofilm. The double deletion strain of *srbA* and *atrR* showed a phenotype no different from either of the single deletions. Although both SrbA and AtrR transcription factors are each known to regulate hundreds of genes, a subset of these overlap. Regulatory target genes common to both transcription factors are therefore implicated in downstream processes leading to MT disassembly in the biofilm. The fact that two unrelated hypoxia adaptive transcription factors are necessary emphasizes the importance of hypoxia adaptation in regulating major cell biological changes within basal biofilm cells. This is understandable, considering that basal biofilm cells experience steadily decreasing oxygen concentrations as the growing fungal biomass rapidly consumes more and more oxygen^{31,34}.

The co-culture experiments revealed several interesting pieces of information:

- i) $\Delta srbA$ and $\Delta atrR$ cells are capable of responding to the MT dispersal signal but are unable to generate the dispersal signal on their own in static cultures
- ii) WT cells are capable of providing the signal that can trigger MT disassembly in adjacent cells i.e., through a non-cell autonomous mechanism.
- iii) $\Delta srbA$ cells actually have a greater sensitivity to the MT dispersal signal than WT cells.

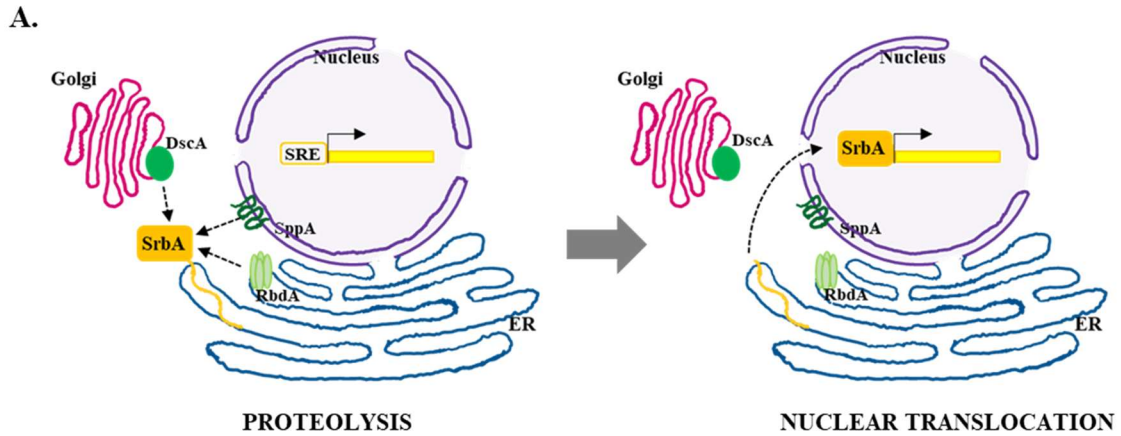
One possible explanation is that $\Delta srbA$ and $\Delta atrR$ cells have defective growth under oxygen limitation. This growth defect is evident in static cultures between WT and $\Delta srbA$ (Fig 4.7C). Such cells will be unable to generate sufficient biomass to produce the self-generated hypoxia the way WT cells do. So *srbA* and *atrR* cells cannot independently disassemble MTs because they are unable to generate the requisite gaseous microenvironment to trigger the process. However, when they are grown alongside WT cells in the same dish, the $\Delta srbA$ and $\Delta atrR$ cells are exposed to the hypoxia generated by the growing WT cells and therefore undergo MT dispersal.

The fact that the MT dispersal responds rapidly to the minimal perturbation of air exchange and the fact that the dispersal signal appears to be non-cell autonomous is suggestive of a gaseous signaling molecule. Small non-polar gaseous molecules such as O₂ can easily diffuse through the lipid bilayer of the cell membrane. Such a signaling molecule could elicit very fast and dynamic changes in cell biology in response to changes in the environment. The MT dispersal signal could be hypoxia i.e., the drop in O₂ molecule levels. Alternatively, a gaseous signaling molecule like nitric oxide that is produced under hypoxia may be the actual MT dispersal signal.

Finally, the completely unexpected result of $\Delta srbA$ cells being significantly more sensitive to the MT dispersal signal is worth further investigation. $\Delta srbA$ cells in co-culture underwent MT disassembly *before* WT cells during biofilm development. Lid removal and replacement performed on this co-culture showed $\Delta srbA$ cells disperse MTs before WT cells do and $\Delta srbA$ cells repolymerize MTs after WT cells do. $\Delta srbA$ cells seem to respond to a lower threshold of the MT dispersal signal than the WT cells (Fig

4.6). SrbA is a transcription factor with hundreds of regulatory target genes. The most well studied and interesting set of targets with respect to this question are those of the ergosterol biosynthetic pathway. The absence of *srbA* would produce multiple perturbations along the ergosterol pathway, ultimately affecting the sterol composition of the cell membrane. Modified membrane sterols could result in a cell membrane having increased permeability to gaseous signaling molecules, thereby explaining why Δ *srbA* cells are more sensitive to the MT dispersal signal relative to WT cells.

All biofilm experiments investigated thus far were grown under static conditions. Here the self-generated hypoxia produced as a result of the increasing rate of oxygen consumption by the accumulating biomass. The shaking culture experiment was an alternate method of producing hypoxia in real-time by inducing a sharp drop in dissolved oxygen when transferring culture dishes from shaking to static conditions. WT cells responded in the expected fashion to this sudden drop in oxygen by dispersing MTs as previously published³⁴. The big surprise was that Δ *srbA* and Δ *atrR* also responded exactly as WT cells when transferred from shaking to static conditions. One possible explanation of this phenomenon is that under the well-oxygenated shaking conditions Δ *srbA* and Δ *atrR* don't have defective growth. Δ *srbA* and Δ *atrR* are able to grow as well as WT cells and this growth is necessary to produce the self-generated gaseous microenvironment necessary to trigger MT dispersal. Whereas in static biofilm cultures, the poorly oxygenated media does not allow Δ *srbA* and Δ *atrR* to accumulate sufficient biomass needed to trigger MT disassembly (Fig 4.7C). Defective growth under hypoxia is a well-established phenotype for Δ *srbA* and Δ *atrR*^{28,37}.



B.

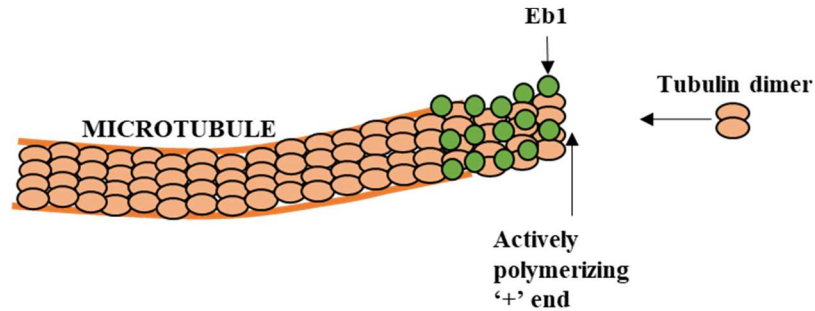


Figure 4. 1 Model of Srba protein proteolytic activation and Eb1 protein tracking.
 A. Under normoxia, full length Srba protein is tethered to the ER. Under hypoxia, Srba undergoes sequential proteolysis by the Dsc complex, RbdA and SppA to release the Srba transcription factor domain from the N-terminal of the protein. The transcription factor translocates to the nucleus where it binds the SRE element in target gene promoters to regulate their transcription. B. Schematic representation of Eb1 protein tracking active MT polymerization. The orange circles represent tubulin monomers that polymerize to form the elongated microtubule (MT). Tubulin dimers are added to one specific end of the MT called the '+' end. Eb1 protein (green circles) specifically bind to the growing + end, thereby acting as a marker for actively polymerizing MTs.

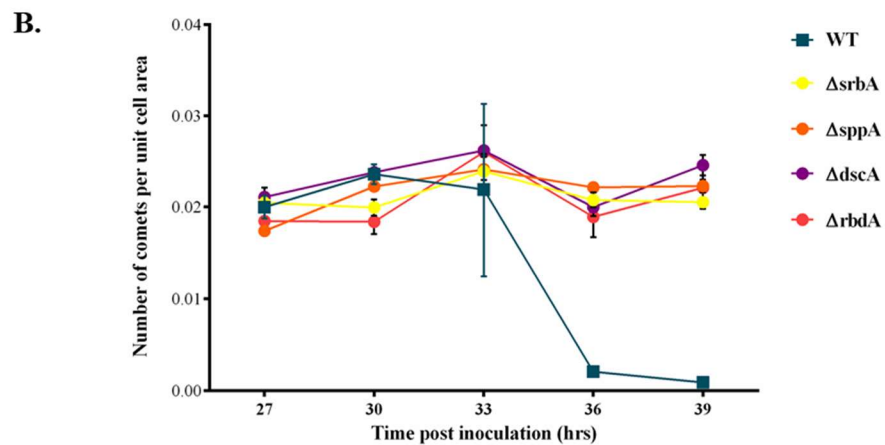
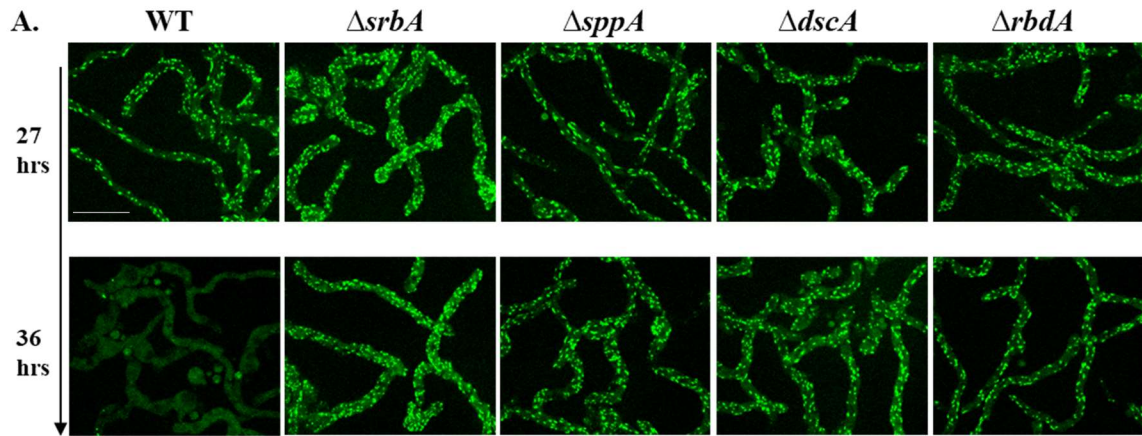


Figure 4. 2 Fully processed *SrbA* transcription factor is required for MT dispersal in basal biofilm cells. Active MTs were analyzed using Eb1-GFP, visualized as GFP comets within cells. Microtubule disassembly resulted in the loss of Eb1 comets. A. Wild type (WT) basal cells in a biofilm dispersed their MTs by ~36hrs while $\Delta srbA$ cells did not. Similarly, $\Delta sppA$, $\Delta dscA$ and $\Delta rbdA$ also failed to disperse MTs like $\Delta srbA$. B. Quantitation of the number of comets per unit area of cells was carried out for all cells in three separate image fields at a given time point. The plot demonstrates the complete disappearance of comets in WT cells while the deletion strains show a maintenance of comet number. Scale bar, 10 μ m.

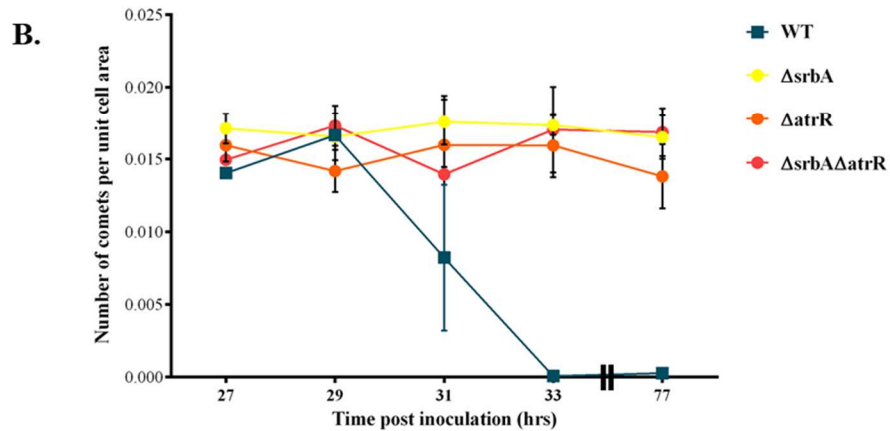
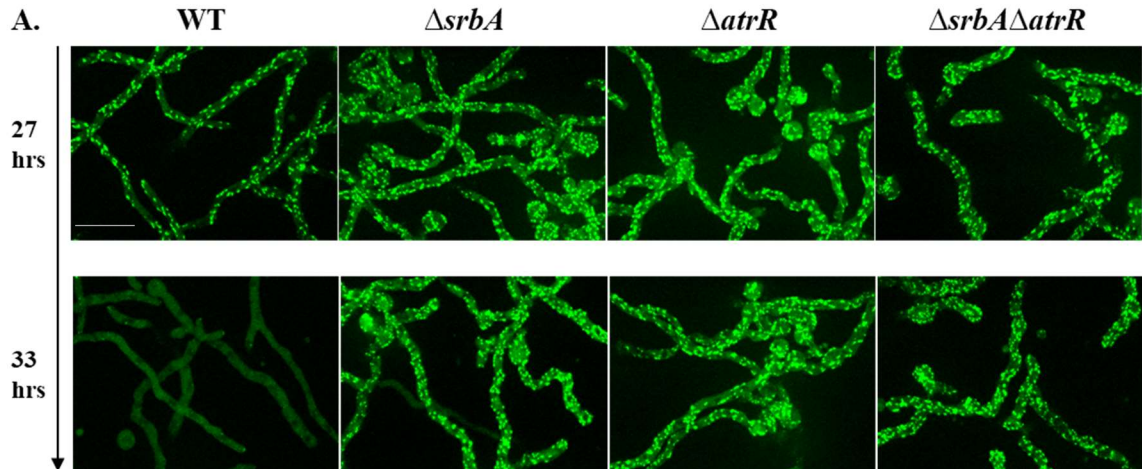


Figure 4. 3 *srbA* and *atrR* are required for progression of biofilm cells to MT disassembly stage. Growing MTs are visualized using endogenously tagged Eb1-GFP that appears as numerous, mobile comet-like structures in cells. Microtubule disassembly results in the loss of Eb1 comets, allowing for clear distinction between MTs in active and dispersed states. Wild type (WT) basal cells (A.) in a biofilm undergo microtubule (MT) dispersal between 29 to 33 hours after inoculation. When *srbA*, *atrR* or both are deleted basal cells fail to disperse their microtubules. Quantitation (B.) of the number of comets per unit area of cells was carried out for all cells in three separate image fields at each time point. The plot demonstrates the complete disappearance of comets in WT cells while the deletion strains show a maintenance of comet number. Scale bar, 10 μ m.

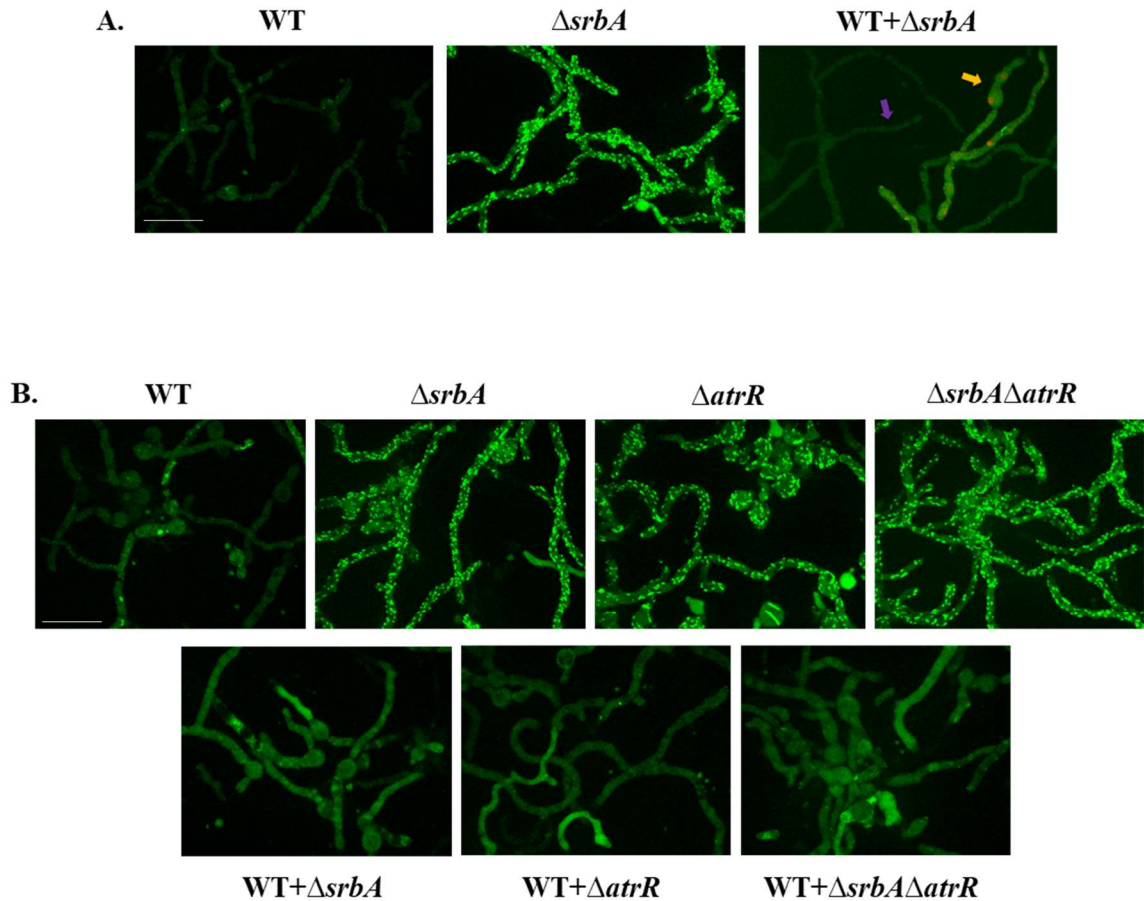
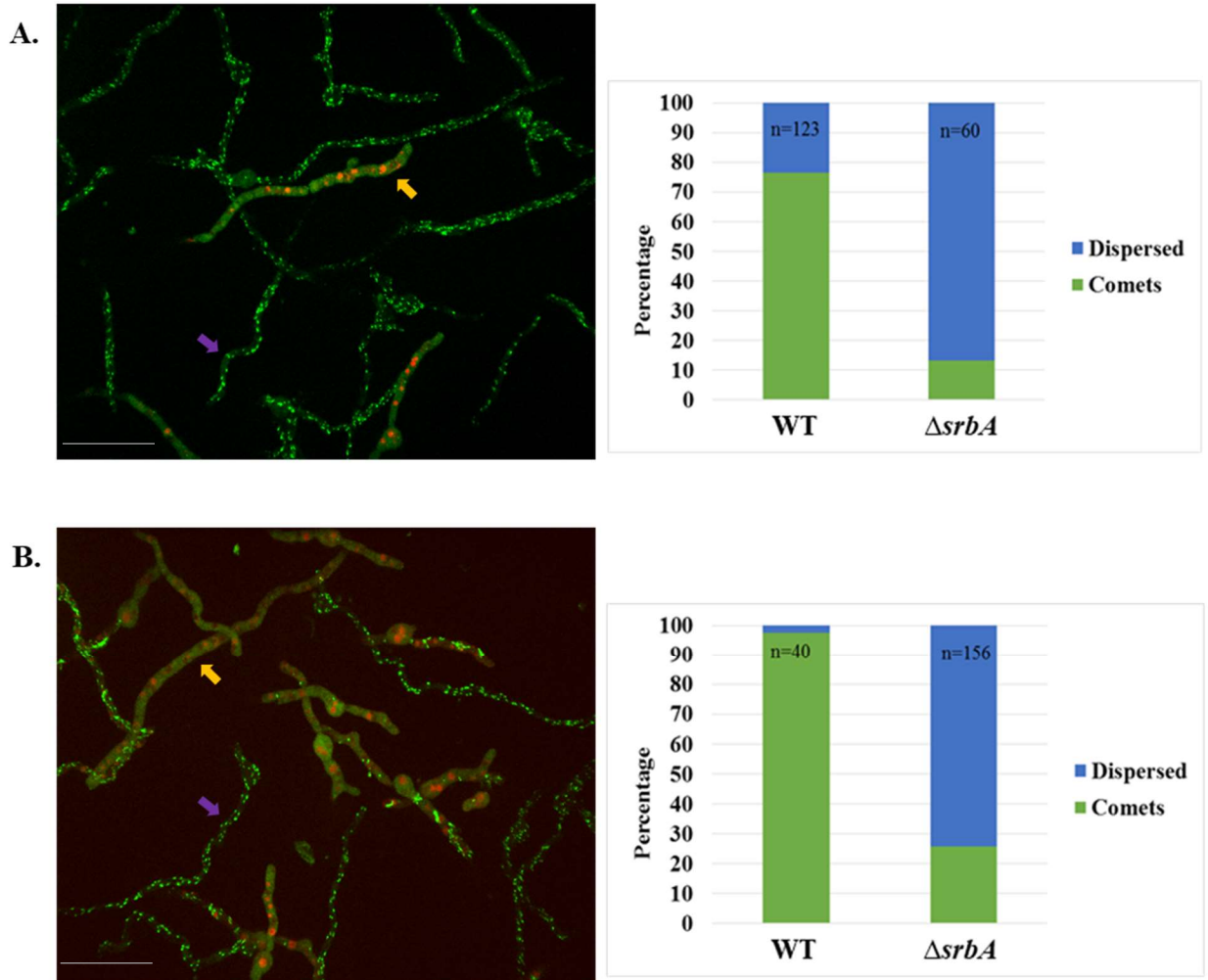


Figure 4. 4 WT cells can create the gaseous microenvironment that triggers MT dispersal in $\Delta srbA$ and $\Delta atrR$ cells. A. WT cells disperse MTs and $\Delta srbA$ cells maintain active MTs when grown independently. When WT cells (purple arrow) and $\Delta srbA$ cells (yellow arrow) are grown in a co-culture (80%WT+20% $\Delta srbA$) both types of cells undergo MT dispersal. WT and $\Delta srbA$ cells were differentiated by the presence of an additional mRFP tagged gene present only in the $\Delta srbA$ strain. B. MT dispersal is also observed in all cell types when WT is cultured with $\Delta srbA$, $\Delta atrR$ or $\Delta srbA\Delta atrR$ respectively (1%WT+99% Δ). All strains used in this experiment contain only Eb1-GFP with no other tagged genes. Scale bar, 10 μ m.



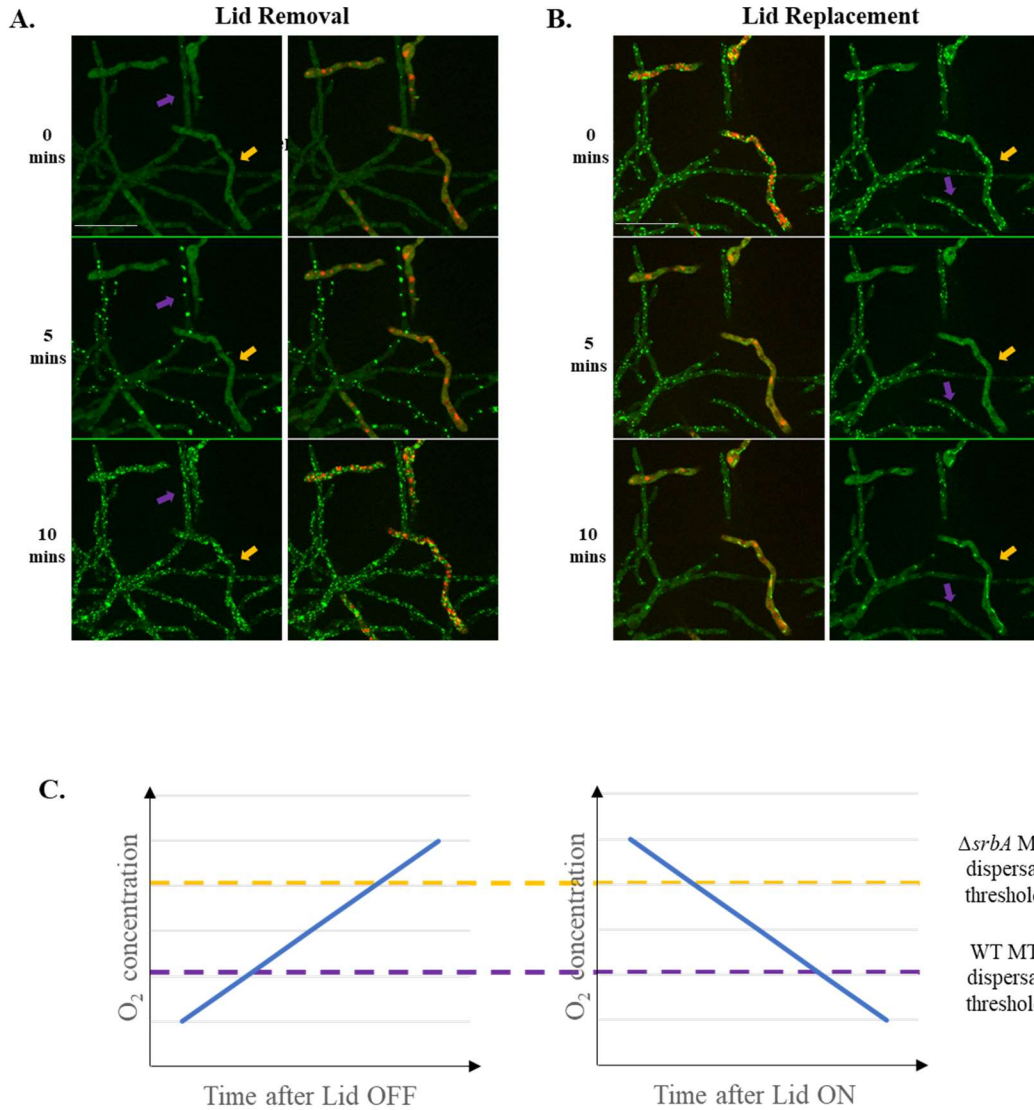


Figure 4. 6 Reversal of MT dynamics by lid removal and replacement. MT dispersal dynamics were followed with Eb1-GFP in WT (purple arrow) and $\Delta srbA$ (yellow arrow) cells grown in a co-culture (80%WT + 20% $\Delta srbA$). The mRFP tag was present only in the $\Delta srbA$ cells. Each montage is presented in two forms: one with only the green channel and the other as an overlay of red and green channels. Images of a specific field were captured at 0, 5 and 10 minutes after lid removal or lid replacement. A. Eb1 comets reappeared first in WT cells followed by $\Delta srbA$ cells after lid removal. B. Once comets reappeared in all cells, the lid was replaced, and images of the same field captured similarly. $\Delta srbA$ cells lose comets first followed by WT cells after lid replacement. C. Model demonstrating WT and $\Delta srbA$ cell sensitivity in response to lid removal/replacement. Scale bar, 10 μ m.

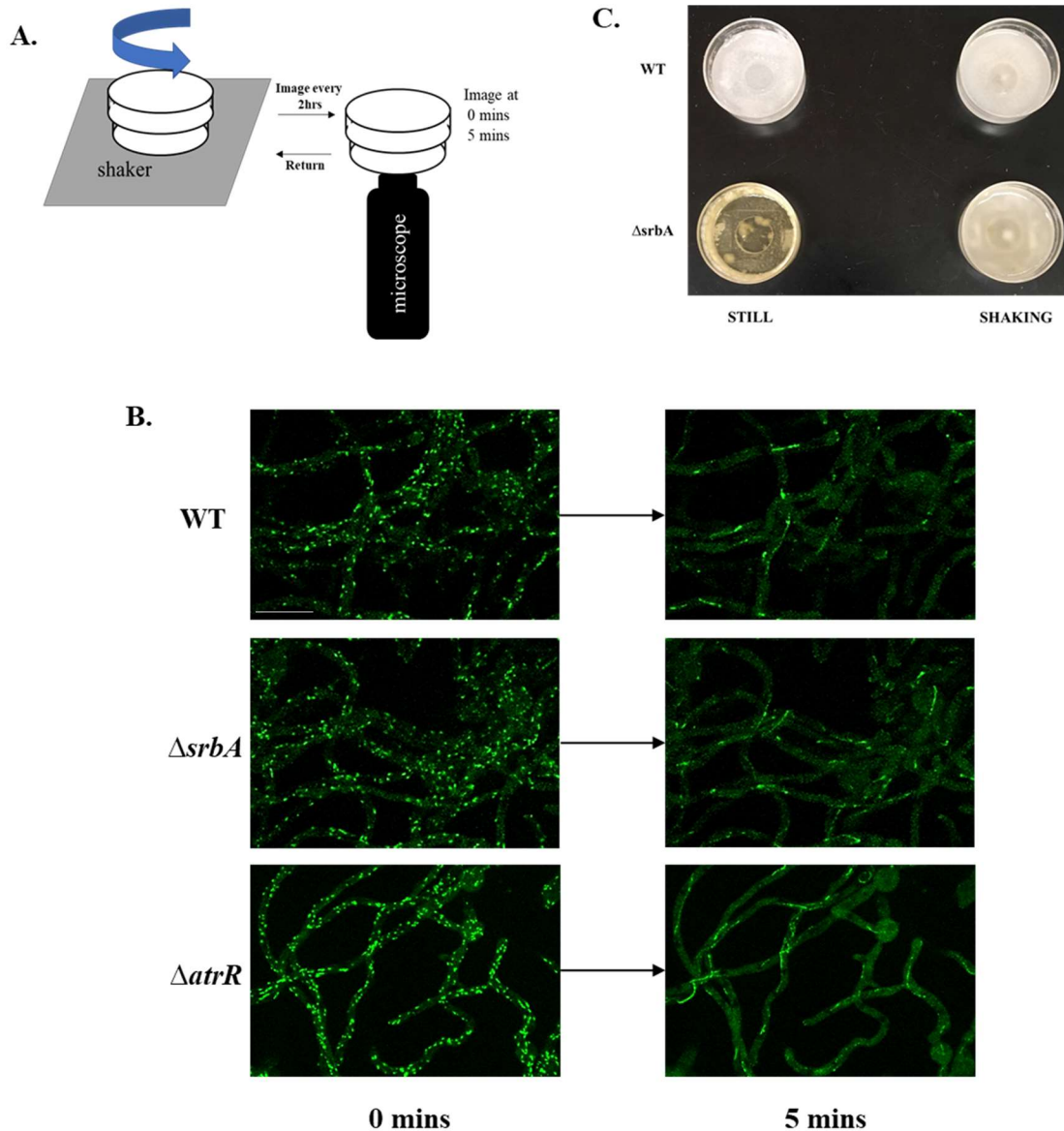


Figure 4. $\Delta srbA$ and $\Delta atrR$ cells can disperse MTs after shaking treatment. A. Schematic of experimental set-up:- cells grown in an imaging dish are placed on an orbital shaker (100rpm) immediately adjacent to the microscope. At 2hr intervals, each dish is transferred to the microscope stage and 2 sequential images are captured: one immediately after transfer to stage (0 mins) and one after allowing dish to sit still (5mins). B. WT, $\Delta srbA$ and $\Delta atrR$ basal biofilm cells show active MTs in the form of Eb1-GFP comets under the shaking condition (0mins). The WT and deletion strains disperse MTs within 5 minutes after transfer from shaking to still condition as apparent by the loss of Eb1 comets (5mins). C. Biofilm growth of WT and $\Delta srbA$ strains under static and shaking conditions. Scale bar, 10 μ m.

Chapter 5. Protein expression analysis of ergosterol biosynthetic genes that are targets *SrbA* and *AtrR* transcriptional regulation

5.1 Introduction

The results from the previous chapters demonstrate that the *srbA* and *atrR* genes play a significant role in mediating specific cell biological changes occurring in basal biofilm cells. More specifically,

- i) the *SrbA* protein undergoes proteolytic activation in basal cells during biofilm development causing its basic helix-loop-helix leucine zipper DNA binding domain N-terminal region to transition from the ER into nuclei as biofilms develop
- ii) the *SrbA* activation process responds to changes in the gaseous microenvironment of basal cells as demonstrated by its reversibility after aeration above the developing biofilm cells
- iii) the deletion of either *srbA* or *atrR* gene results in an increased cell sensitivity to the intercellular gaseous signaling in basal biofilm cells.

SrbA, a basic helix-loop-helix leucine zipper DNA binding domain protein, and *AtrR*, a Zn_2 -Cys₆ DNA binding domain protein, are both known to regulate transcription of target genes by binding to specific regulatory sequence motifs in the target gene's promoter^{28,29,39}. It is therefore important to investigate the common transcriptional target

proteins of these genes to help throw further light on the potential role of SrbA and AtrR in regulating cell biology during fungal biofilm development.

SrbA and AtrR are known transcriptional regulators of ergosterol biosynthetic enzymes^{28,29,38,57}. In *Schizosaccharomyces pombe*, the SrbA ortholog Sre1p was found to be necessary for the anaerobic upregulation of several ergosterol biosynthetic enzyme gene RNAs such as *erg11*⁺, *erg24*⁺, *erg25*⁺, *erg27*⁺, *erg6*⁺, *erg2*⁺, *erg3*⁺ and *erg5*⁺⁵⁷. This regulation is likely conserved in filamentous fungi because in *Aspergillus fumigatus* hypoxic mRNA upregulation of *erg24*, *erg11A*, *erg25* and *erg3* genes was found to require *srbA*^{39,58} while loss of *atrR* resulted in decreased mRNA for *erg11A*, *erg24A*, *erg25A* and *erg3B*²⁸ in this fungus. Similarly, in *Aspergillus nidulans*, loss of *srbA* resulted in decreased RNA for *erg11A* and *erg25A* as determined by northern blot analysis³⁷. The prevailing model proposes that SrbA function is necessary under oxygen limitation to maintain oxygen-intensive chemical reactions by increasing the levels of enzymes involved to better utilize the limited oxygen available. Ergosterol biosynthesis is an oxygen intensive process, requiring 12 molecules of O₂ to manufacture a single molecule of ergosterol (Fig 5.1). Therefore, current model of SrbA's regulatory function in the sterol biosynthetic pathway is as follows: Under ambient oxygen levels (~21% oxygen), sufficient oxygen is available for the ergosterol biosynthetic enzymes expressed at base level to maintain ergosterol production. But when conditions turn hypoxic (~1% oxygen), the scarcity of oxygen will inhibit ergosterol biosynthesis and normal cell growth, since ergosterol is an important component of the lipid cell membrane. To compensate for low oxygen, SrbA gets activated wherein the released SrbA transcription

factor binds to the promoters of multiple ergosterol biosynthetic genes and upregulates their expression. These increased concentrations of ergosterol enzymes have a higher likelihood of capturing scarce oxygen molecules thereby maintaining ergosterol production and cell growth even under hypoxia³⁶.

AtrR is a Zn₂-Cys₆ zinc finger domain-containing transcription factor that was recently identified in *Aspergillus oryzae* as a factor required for wild-type tolerance to azole drugs²⁸. AtrR, unlike SrbA, is not known to undergo a proteolytic activation process in the ER although its protein sequence does contain a predicted transmembrane domain. Loss of the respective *atrR* orthologs in *A. nidulans* and *A. fumigatus* also resulted in a hypersensitivity to azole drugs and an inability to grow under hypoxia. The azole class of drugs specifically bind to and inactivate the enzyme lanosterol- α -14-demethylase in the ergosterol biosynthetic pathway i.e., the protein product of *erg11*. Further investigation in *A. fumigatus* revealed that RNA levels of *erg24A*, *erg11A*, *erg25A* and *erg3B* were reduced in the absence of *atrR*²⁸. Chromatin Immunoprecipitation (ChIP) experiments identified AtrR binding at the promoter of *erg11A*^{28,29}. The AtrR response element (ATRE) was identified in the promoters of *erg11A*, *erg25*, *erg5*, *erg6* in *A.fumigatus*, adjacent to the previously identified SrbA response element (SRE)^{29,39}. These findings imply that SrbA and AtrR are likely to function as co-regulatory transcription factors of these ergosterol biosynthetic genes.

SrbA and AtrR have been identified specifically as genes required for growth under hypoxia as well as co-regulators of oxygen-dependent ergosterol biosynthetic enzymes. Loss of either *srbA* or *atrR* also results in increased sensitivity to azole drugs.

Many antifungal drugs prescribed in clinical settings specifically target the ergosterol pathway⁷⁷. The azole class of antifungal drugs specifically binds the catalytic domain of Erg11/Cyp51 resulting in loss of catalytic function and accumulation of toxic intermediates^{78,79}. However, the growing resistance of fungal infections to these drugs has become a major problem and one possible explanation is the difference in drug resistance between biofilm cells and free living cells^{17,80}. Fungal cells in a biofilm can have as much as 100X the resistance to antifungals relative to planktonic (free-living) cells^{80,81}. Drug development and testing in labs is not typically carried out on biofilm cells while fungal growth during pathogenesis is frequently in biofilm form. Investigating the expression patterns and regulation of these Erg proteins within the developing biofilm can potentially throw light on this problem.

Results from the previous chapter identified a differential sensitivity of WT and Δ *srbA* cells to gaseous signaling in basal biofilm cells. In animals, cholesterol, the analogous sterol molecule to ergosterol, has been shown to alter membrane permeability to small gaseous molecules like oxygen⁸²⁻⁸⁷. Since ergosterol, like cholesterol, may influence the permeability of the cell membrane, the cell sensitivity in our experiments could be explained by the altered membrane permeability of Δ *srbA* cells brought about by the mis-regulation of ergosterol biosynthesis due to the absence of SrbA regulation. Gradually developing self-generated hypoxia is a significant feature of biofilms, especially in the biofilm basal founder cells³¹. The question addressed in this chapter is how the oxygen-dependent ergosterol enzymes are expressed and regulated during hypoxic biofilm development and what role SrbA plays in this process.

5.2 Results

5.2.1 Ergosterol proteins previously shown to be transcriptionally regulated by SrbA and AtrR show unique protein expression patterns during biofilm development

To better understand the role of ergosterol synthesis during biofilm development, 7 ergosterol biosynthetic genes were selected for analysis. The promoters of these *erg* genes or their paralogs were previously identified as targets of transcriptional regulation by both SrbA and AtrR in *Aspergillus*²⁸. The protein products of these *erg* genes are enzymes that catalyze specific oxygen-intensive biosynthetic steps in the latter half of the ergosterol pathway (Fig 5.2A).

The “Erg” proteins Erg24, Erg11A, Erg11B, Erg25A, Erg25B, Erg3A, Erg3B were tagged with GFP on their C-terminal ends. This was carried out by genetic modification of the endogenous genomic loci of the respective genes through homologous recombination⁴⁵. All seven Erg proteins were expressed in an ER-like pattern consistent with published data. Erg24-GFP has previously been used as ER marker in *Aspergillus nidulans*⁸⁸. In *A. fumigatus* Erg11A and Erg11B were successfully tagged with GFP on their C-terminal ends to analyze subcellular localization⁸⁹. In fission yeast, ERG24, ERG25 and ERG3 proteins have been successfully tagged on their C-terminal ends to analyze cell localization patterns⁹⁰.

To follow real-time levels of these Erg proteins during biofilm development, basal biofilm cells were imaged using spinning disc confocal laser microscopy during the course of biofilm development (Fig 5.2B). Fungal spores inoculated in an imaging cell-

culture dish were allowed to germinate and grow at the bottom of the culture dish on the surface of the embedded microscope coverslip. As the biomass in the dish increases, so does the rate of oxygen consumption and consequently the concentration of dissolved oxygen decreases around the growing cells³¹. By following the cell biology of basal cells in early, middle and late stages of biofilm development, it was possible to observe how SrbA regulated ergosterol proteins actually behave in the self-generated hypoxia of a developing biofilm. Importantly, we have found that SrbA is proteolytically activated and moves from ER to nuclei during the transition from early to middle stages of biofilm formation. In addition, Erg protein levels in newly germinated cells (germlings) was captured during early stage normoxia (normal O₂ concentration at atmospheric pressure) growth conditions.

Step I (Erg11A, Erg11B, Erg24): Erg11A (AN1901) and Erg11B (AN8283) are paralogs that are putative sterol 14- α demethylases while Erg24 (AN4094) is a putative C-14 sterol reductase. Together they catalyze one of the first oxygen dependent steps of the ergosterol biosynthetic pathway at the carbon in position 14 of eburicol (Fig 5.2A). Erg24 contains 8 predicted transmembrane domains distributed throughout the length of the protein. Erg11A has one predicted transmembrane domain near its N-terminus while Erg11B had two predicted transmembrane domains, also near its N-terminus. Erg11A and Erg11B are members of the widely conserved cytochrome P450 monooxygenases family and contain a conserved heme-binding domain near the C-terminus. The first 15 and 32 amino acids of Erg11A and Erg11B respectively do not

align and potentially contain signal peptides. Erg11B contains an ER-retention signal at its C-terminus but Erg11A does not.

During biofilm development, Erg24-GFP protein accumulated in the ER in normoxic germlings (Fig 5.3C) and in early biofilm stages (Fig 5.3A) but dropped to half the levels in the middle stage biofilm (Fig 5.3B). Erg11A-GFP protein was undetectable in normoxic germlings (Fig 5.4C) as well as in the early stages of biofilm growth (Fig 5.4A). SrbA proteolytic activation, which takes place ~24 hours post inoculation, has not yet taken place in the early stages of the biofilm (18-24hrs post inoculation) probably because the hypoxic threshold has not been crossed. However, in the middle to late stage biofilm Erg11A protein showed increasing accumulation in basal cells (Fig 5.4A, B). These results are consistent with the published literature on SrbA-dependent *erg11* mRNA expression patterns. The large error bars in the quantification graph of Erg11A expression is due to variation in signal intensity among different basal cells. In contrast, Erg11B, the paralog of Erg11A, was expressed in normoxic germlings (Fig 5.5C) and during biofilm growth showed relatively little change in protein levels (Fig 5.5A, B)

Step II (Erg25A, Erg25B): Erg25A (AN8907) and Erg25B (AN6973) are part of a complex of Erg proteins (Erg26, Erg27 and Erg28) involved in the two subsequent oxygen dependent steps (Fig 5.2A). Erg25A and Erg25B are paralogs that encode putative C-4 sterol methyl oxidases and function as part of the complex to remove two methyl groups at the carbon 4 position. Removal of each methyl group utilizes 3 O₂ molecules. Erg25A and Erg25B don't contain any predicted transmembrane domains but they do have ER retention signals on their respective C-termini.

The Erg25A protein, like Erg11A, was undetectable in normoxic germlings (Fig 5.6C) and early biofilm stages (Fig 5.6A) but showed increased expression in the middle and later stages (Fig 5.6A, B). Again, like Erg11A, there was significant variation in signal intensity between basal cells, hence the large error bar in the quantification graph. This phenomenon was not observed in any of the other Erg proteins and appears to be specific only to Erg11A and Erg25A. This suggests a cell-specific or region-specific role for Erg11A and Erg25A within the basal layer of the biofilm. The Erg25B protein, on the other hand, showed constant expression both in germlings (Fig 5.7C) and during biofilm development (Fig 5.7A, B).

Step III (Erg3A, Erg3B): Erg3A (AN6506) and Erg3B (AN3638) catalyze the last oxygen dependent step to produce the final sterol product, ergosterol (Fig 5.2A). They are putative C-5 sterol desaturases, which introduces a double bond between the carbons at position 5 and 6. Erg3A has 3 predicted transmembrane domains while Erg3B has 4 predicted transmembrane domains distributed over the length of the protein. Erg3B has an additional putative signal peptide at its N-terminal end that is absent in Erg3A. Erg3A has a 14 amino acid sequence near its N-terminal and a 32 amino acid sequence at its C-terminal that are absent in Erg3B. Both proteins also have ER-retention signals at their respective C-terminal ends.

Erg3A protein, like Erg11B, was constantly expressed both in germlings (Fig 5.8C) and throughout biofilm development (Fig 5.8A, B). Erg3B protein, however, was undetectable in germlings (Fig 5.9C) as well as in the early stages of the biofilm (Fig 5.9A). As the biofilm developed Erg3B protein accumulated to higher and higher levels

(Fig 5.9A, B). At 2 days of biofilm growth Erg3B protein showed the strongest expression levels of all proteins analyzed in this study.

5.2.2 Ergosterol protein expression in the presence and absence of *srbA* provides novel insights into the regulatory mechanism

To understand the role of SrbA regulation on the expression of these Erg proteins during biofilm development, the same analysis (refer 5.2.1) of the respective tagged Erg proteins was carried out in a Δ *srbA* background.

Step I (Erg11A, Erg11B, Erg24): Erg24 protein continued to show an ER-like expression pattern even in the absence of *srbA* (Fig 5.3A) but in this case the protein accumulated to levels only half of that in the WT background (Fig 5.3B). This reduced protein level was maintained in normoxic germlings (Fig 5.3C) and throughout biofilm development in the Δ *srbA* background (Fig 5.3A).

In the absence of *srbA*, Erg11A failed to show activation of protein expression during biofilm development as seen in the WT background (Fig 5.4A). This result is consistent with the published literature that identified SrbA protein activation under artificially induced hypoxia and the subsequent upregulation of *erg11* RNA. However, Erg11B, despite being a paralog of Erg11A with presumed redundancy of function, showed no significant difference in protein expression in the presence or absence of *srbA* (Fig 5.5A, B). Erg11B protein showed an ER-like expression pattern in both WT and Δ *srbA* backgrounds and its protein expression was maintained at relatively constant levels in normoxic germlings (Fig 5.5C) and throughout biofilm development.

Step II (Erg25A, Erg25B): In the WT background, Erg25A protein was undetectable in germlings as well as in the early biofilm but showed significant protein accumulation in

the middle to late stages (Fig 5.6). This is presumably because the middle to late stage biofilm is the time frame after *SrbA* activation (~24hrs post inoculation). However, just like *Erg11A*, *Erg25A* also failed to show this protein accumulation when *srbA* was deleted (Fig 5.6A). Thus, *Erg25A* protein showed an *SrbA*-dependent activation process during the development of the hypoxic biofilm, consistent with published data. *Erg25B* protein, despite being a paralog of *Erg25A*, behaved differently. In the WT background, *Erg25B* protein was expressed at constant levels both in germlings and during biofilm growth (Fig 5.7). In Δ *srbA*, *Erg25B* protein expression was unexpectedly higher (~3-4 fold) than in the WT background (Fig 5.7A, B). This high level of protein expression was consistently expressed in both germlings (Fig 5.7C) and the biofilm with little variation. This result suggests that *SrbA* may directly or indirectly cause the negative regulation of *Erg25B* protein. The high protein level is observed even in Δ *srbA* germlings, a stage at which *SrbA* protein is tethered to the ER and cannot regulate promoters even in the WT background. This means that *SrbA*'s influence on *Erg25B* protein is probably not through regulation of the *erg25B* promoter. Since both *SrbA* and *Erg25B* protein localize in the ER, it is possible that *SrbA*'s negative regulation of *Erg25B* may take place through direct protein-protein interaction and would be an interesting avenue for future study.

Step III (*Erg3A*, *Erg3B*): As in the case of the WT background, the absence of *srbA* had no significant effect on *Erg3A* protein levels (Fig 5.8). *Erg3A* protein was expressed at constant levels in normoxic germlings (Fig 5.8C) as well as during growth of the hypoxic biofilm (Fig 5.8A) and very little variation in protein level was found between WT and Δ *srbA* (Fig 5.8B). On the other hand, the paralogous *Erg3B* behaved very differently

from all the other Erg proteins investigated here. In the WT background Erg3B was undetectable in germlings (Fig 5.9C) but showed increased protein accumulation as the hypoxic biofilm developed (Fig 5.9A). In the absence of *srbA*, Erg3B protein was surprisingly still able to accumulate as the biofilm developed. However, the protein accumulation in $\Delta srbA$ was exponentially higher than in the WT background (Fig 5.9B). This result again suggests a potential negative regulatory role for SrbA, though the nature of this regulation is still unclear and has potential for further study. A quantitative comparison of all the Erg protein levels analyzed in this study can be visualized in Fig 5.10.

5.3 Discussion

One of the major sets of genes commonly regulated by SrbA and AtrR are those of the ergosterol pathway. The current model is that under hypoxia, Erg proteins functioning in oxygen-intensive catalytic steps are upregulated to compensate for low oxygen availability. Notably, little work has been done to follow the protein levels of the regulated *erg* genes during imposed artificial hypoxia. We had assumed that *erg* gene protein levels during biofilm formation would be regulated in a manner similar to the mRNA levels during imposed hypoxia. However, the experimental results above demonstrate that Erg proteins of established SrbA/AtrR *erg* gene targets are *not* universally upregulated in response to hypoxic SrbA activation in the biofilm context.

Erg11A, Erg25A and Erg3B proteins do accumulate during biofilm development while being undetectable in normoxic germlings. In fact, Erg11A and Erg25A demonstrate the classical SrbA-dependent activation as seen for mRNA levels in

response to artificially imposed hypoxia^{28,39} but, as reported here, at the protein level in biofilm cells. Erg3B protein also shows an accumulation of protein levels in basal cells as the biofilm matures but it also appears to be activated in the absence of *srbA* unlike Erg11A and Erg25A. Published work in *Aspergillus fumigatus* report that Erg3B mRNA shows a significant decrease in the absence of *srbA*^{26,28,58}. Whereas in the biofilm experiments discussed above, Erg3B protein was found to accumulate to an exponentially higher extent in the absence of *srbA* relative to that in the presence of *srbA*. This effect may be due to a direct role of SrB suggesting a novel negative regulation by SrB or it may be an indirect result of *srbA*'s absence. The fact that Erg11A, Erg25A and Erg3B were undetectable in normoxic germlings suggests that they perform functions specifically required during biofilm development.

The paralogs Erg11B, Erg25B and Erg3A, on the other hand, did not show the same biofilm-specific expression profiles; they were expressed both under normoxia (as observed in germlings) as well as in the biofilm with no significant change in protein levels during the process. Erg11B and Erg3A also show no change in protein levels in response to the presence or absence of *srbA*. These paralogs do not appear to be regulated by *srbA* in the biofilm context despite published data showing SrB binding to their promoter sequences in *A. fumigatus*³⁹. It can also be concluded that *erg* gene paralogs are not merely redundant, as has been generally presumed thus far.

Previous publications identified SrB binding to *erg25B* promoter through ChIP-seq and decreased mRNA levels in the absence of *srbA*³⁹. Whereas, in biofilm experiments discussed above, Erg25B protein was significantly increased in the absence

of *srbA* relative to WT. The increased protein was observed in normoxic germlings as well as in the early biofilm i.e., stages at which the SrbA protein would not have undergone proteolytic activation even if present. This suggests that the ER-tethered “inactive” form of SrbA may have functions beyond its transcription factor domain. Both SrbA and all the studied Erg genes are localized in the ER. It is possible that SrbA influences protein levels in the ER through direct protein-protein interaction. It is worth noting that almost two-thirds of the SrbA amino acid sequence near the C-terminal contains a conserved fungal domain of unknown function and could function as a protein-interacting domain. This result is another example of a potential negative regulatory role for SrbA.

Erg24 protein levels are higher in WT relative to Δ *srbA*. At first glance this appears to be consistent with published data showing decreased *erg24* mRNA in the absence of *srbA*^{28,58}. However, in these results Erg24 protein is higher in WT at the early stage, at a time when SrbA protein is unlikely to be activated. Similar to Erg25B, this suggests the possibility of direct protein-protein interaction of SrbA with a target Erg protein instead of transcriptional regulation. ER-tethered SrbA protein could interact directly with Erg24 protein that is also in the ER, perhaps influencing protein stability. Putting all these results together, a revised model of SrbA-dependent Erg protein expression has been outlined in Fig 5.11.

Many studies of SrbA regulation of *erg* genes under artificial hypoxia have identified a predominantly activating function for the transcription factor. However, transcriptomic studies in *C. albicans* biofilms have found distinct ERG genes either

upregulated or downregulated relative to planktonic cells⁹¹, similar to our findings. This suggests that the behavior of Erg proteins under artificial hypoxia may not be equivalent to that of biofilm-generated hypoxia.

The question is why such regulation of the ergosterol pathway should take place under biofilm conditions. Shukla et al. showed that basal biofilm cells stop growth early on in biofilm development³⁴. It is, therefore, surprising that ergosterol synthesis continues in cells that are no longer growing. One possible explanation is that ergosterol synthesized in basal cells is transported to supplement the growth of cells at the periphery of the biofilm. Alternatively, the regulation of ergosterol genes in basal biofilm cells may be important, not for cell growth, but to alter permeability of the cell membrane. Our data shows that the loss of *srbA* results in increased cell sensitivity to gaseous signals as well as an altered expression profile of multiple Erg proteins. The regulation of the ergosterol pathway during hypoxia may, therefore, be necessary to modulate the cell's responsiveness to the gaseous signal.

Membrane permeability is one of the characteristics attributed to the presence of sterol in the plasma membrane. Cells may have evolved sterol molecules to function as a barrier to O₂ entry to protect the internal redox mechanism from excess oxygen^{82,84}. Various pieces of evidence across the animal and plant kingdoms show a negative correlation between membrane sterol levels and its permeability to gases like O₂^{85,92}. Studies of animal red blood cells show that increased membrane cholesterol reduces the ability of O₂ to permeate the cell membrane^{86,87}. Membrane permeability could also be modified by changing the type of sterol molecule predominant in the plasma membrane.

The data in this study shows different Erg proteins going up, down or remaining unchanged over the course of biofilm formation and maturation. This could mean that the end product, under these circumstances, is not ergosterol but some other sterol intermediate. In *C. albicans* biofilms, ergosterol levels actually drop by 50% between early and mature stages while other intermediates accumulate¹². Experiments in yeast suggest that replacing membrane ergosterol with sterol intermediates from the late steps of the pathway alter the cell's tolerance to oxidative stress⁹³. So, the selective regulation of ergosterol biosynthetic enzymes that we observe in the developing biofilm may be to alter the type of sterol molecule produced which then confers different permeability characteristics to the plasma membrane. This special permeability of the cell membrane would allow cells to respond to gaseous signaling within a biofilm context in a way that planktonic cells cannot. Thus, the altered sterol composition of biofilm cell membranes may be an adaptation to the interconnected, cooperative lifestyle within the fungal biofilm.

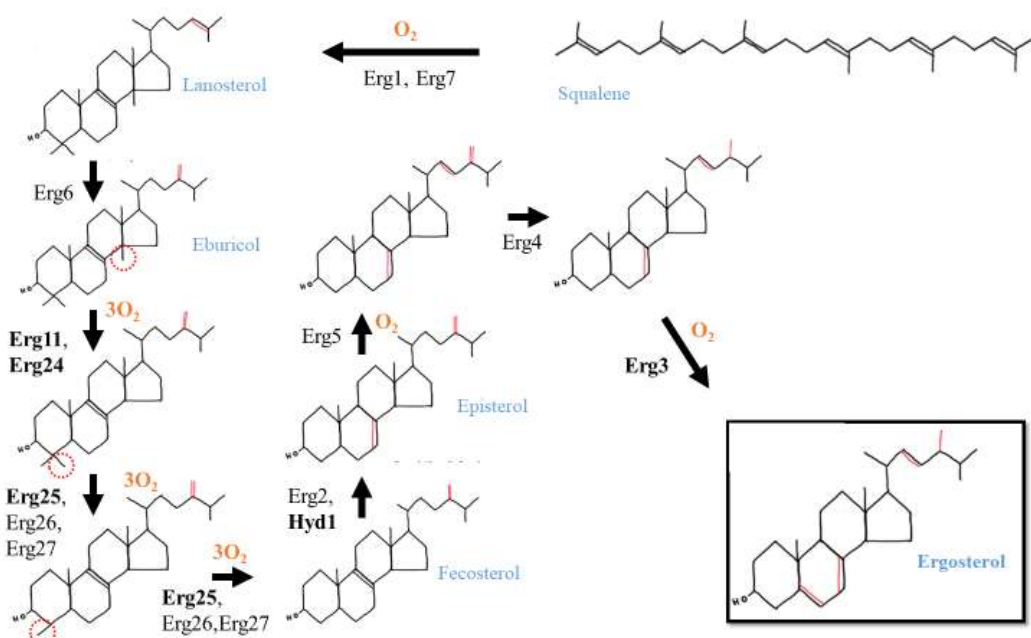


Figure 5. 1 *Aspergillus* ergosterol biosynthetic pathway. Pathway adapted from the *Aspergillus fumigatus* ergosterol pathway^{94–96}. Chemical structures of intermediates deduced based on predicted catalytic function of respective Erg proteins. Erg proteins marked in bold-face are the proteins tested in this study. The chemical modification of the sterol substrate is marked in red at each catalytic step of the pathway.

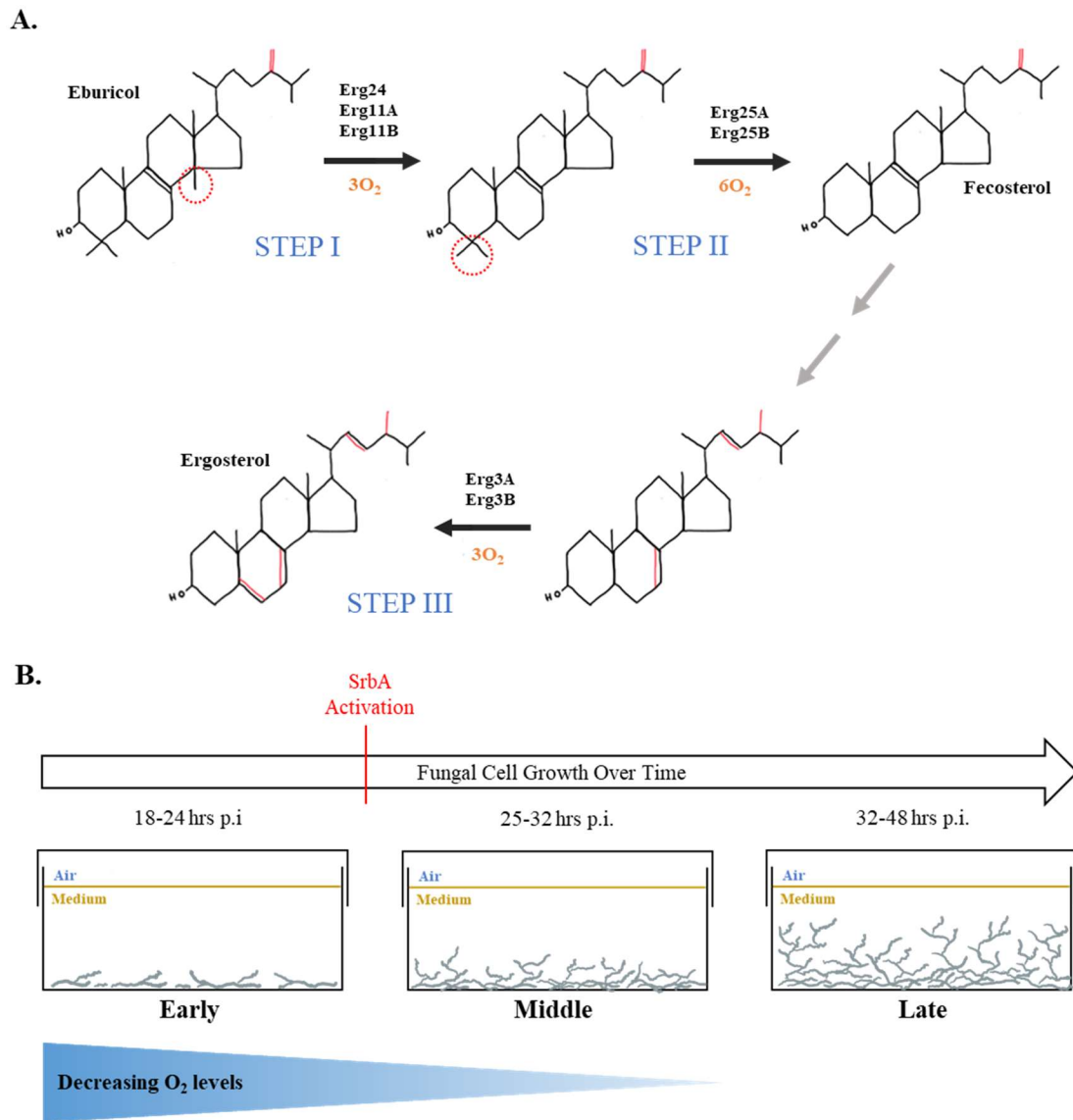


Figure 5. 2 Ergosterol proteins of 3 oxygen dependent catalytic steps investigated during biofilm development. A. The late steps of the ergosterol biosynthetic pathway, with the 7 “Erg” proteins relevant to this study, are depicted. Parts of the sterol molecule’s structure undergoing chemical change and highlighted in red. The grey arrows indicate intermediate steps not involving any of the 7 “Erg” proteins. B. Schematic of biofilm development in an imaging culture dish over time. p.i = post inoculation. As the hyphae grow and accumulate biomass, the rate of oxygen consumption increases resulting in decreasing O₂ levels in the gaseous microenvironment of basal cells. SrbA activation takes place approximately between Early and Middle stages.

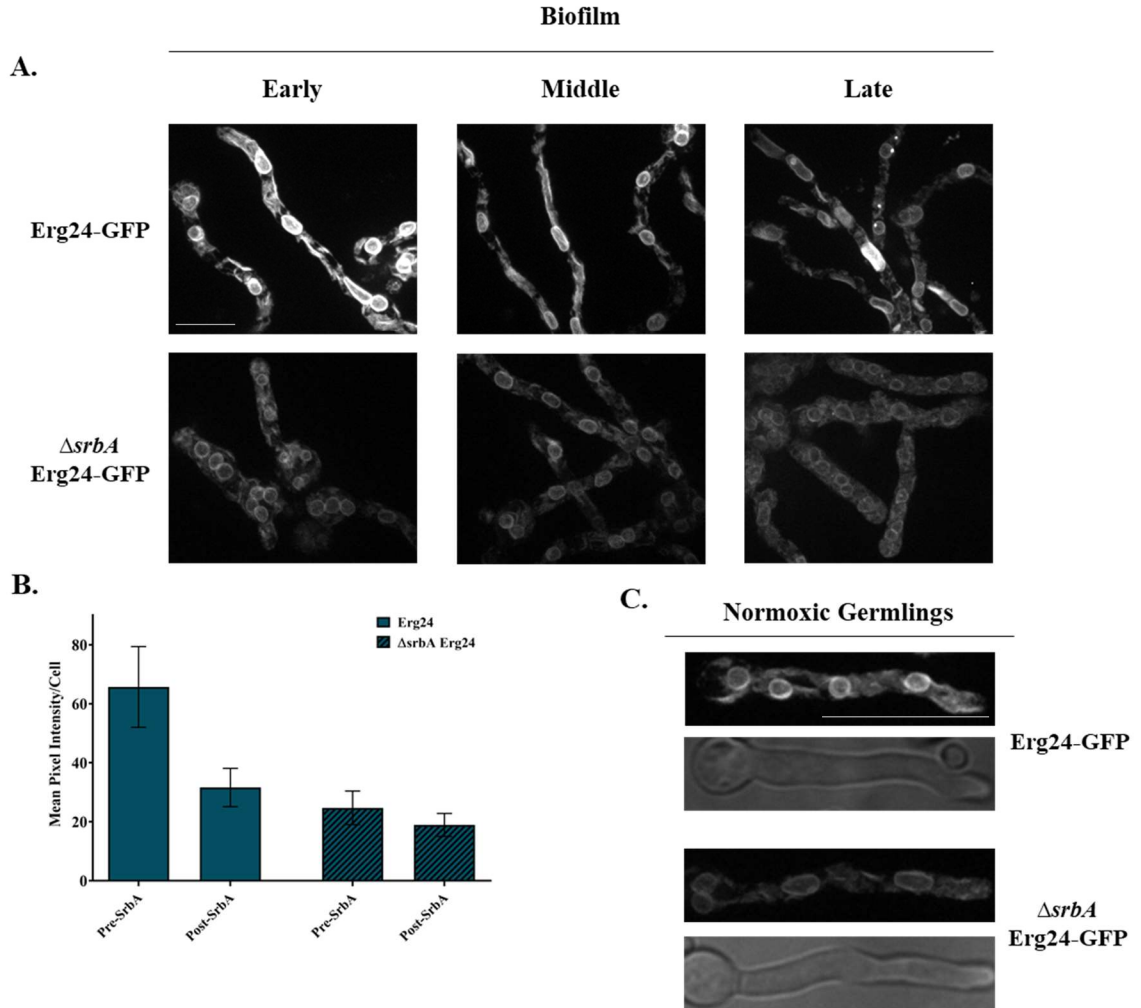


Figure 5. 3 Real-time expression of GFP-tagged Erg24 protein in living *A. nidulans* cells. A. GFP-tagged protein levels in basal cells during early (18-24 hrs), middle (25-32 hrs) and late (32-48 hrs) stage biofilm development. B. Quantification of protein levels by measurement of total GFP intensity within cells (n=3) before Srba activation (Pre-Srba or Early stage biofilm) and after Srba activation (Post-Srba or Middle stage biofilm). C. Protein expression in newly germinated cells (germlings) not in a biofilm i.e., under normoxia. Scale bar, 10 μ m.

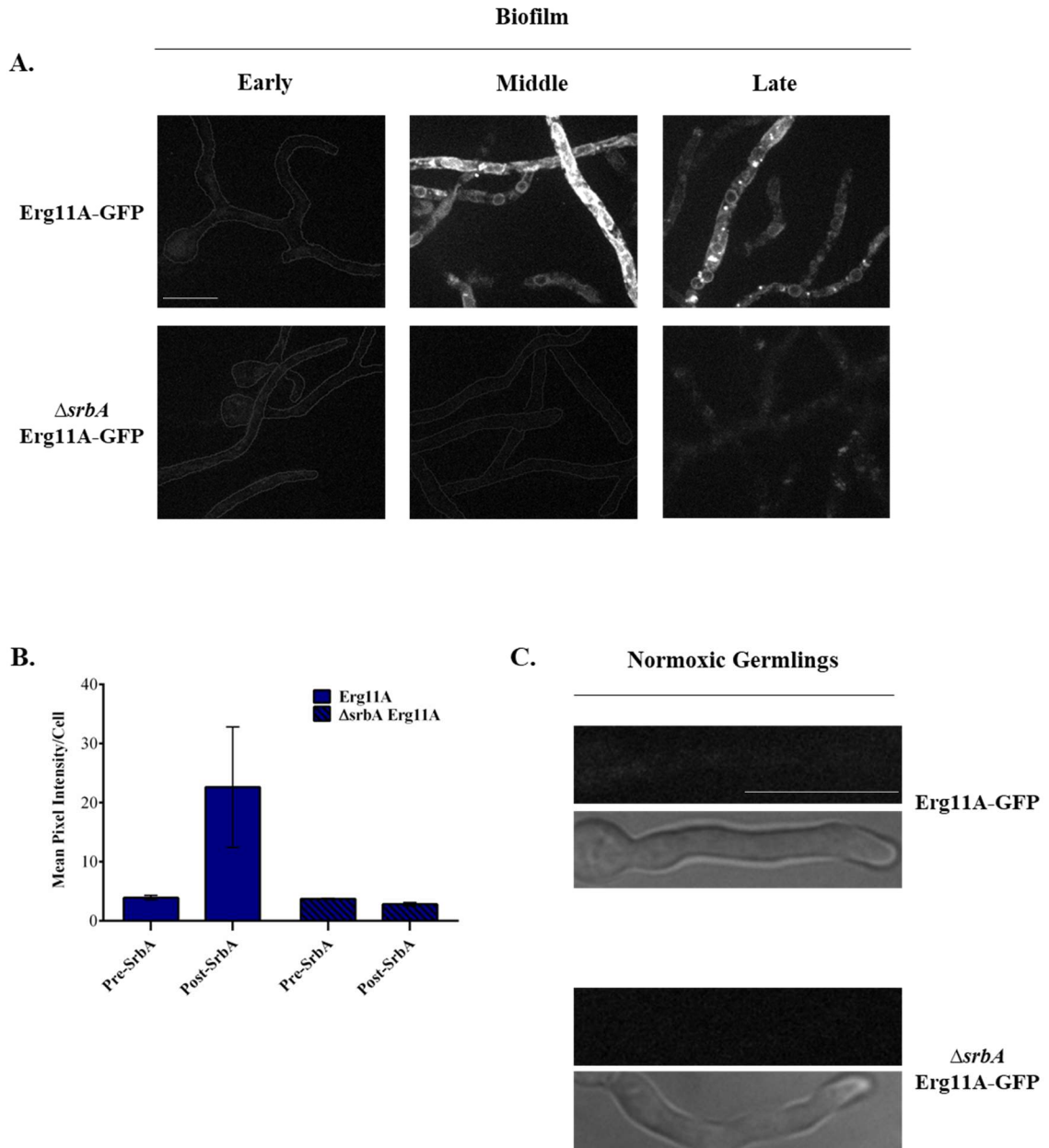


Figure 5. 4 Real-time expression of GFP-tagged Erg11A protein in living *A. nidulans* cells. A. GFP-tagged protein levels in basal cells during early (18-24 hrs), middle (25-32 hrs) and late (32-48 hrs) stage biofilm development. B. Quantification of protein levels by measurement of total GFP intensity within cells (n=3) before SrbA activation (Pre-SrbA or Early stage biofilm) and after SrbA activation (Post-SrbA or Middle stage biofilm). C. Protein expression in newly germinated cells (germlings) not in a biofilm i.e., under normoxia. Scale bar, 10 μ m.

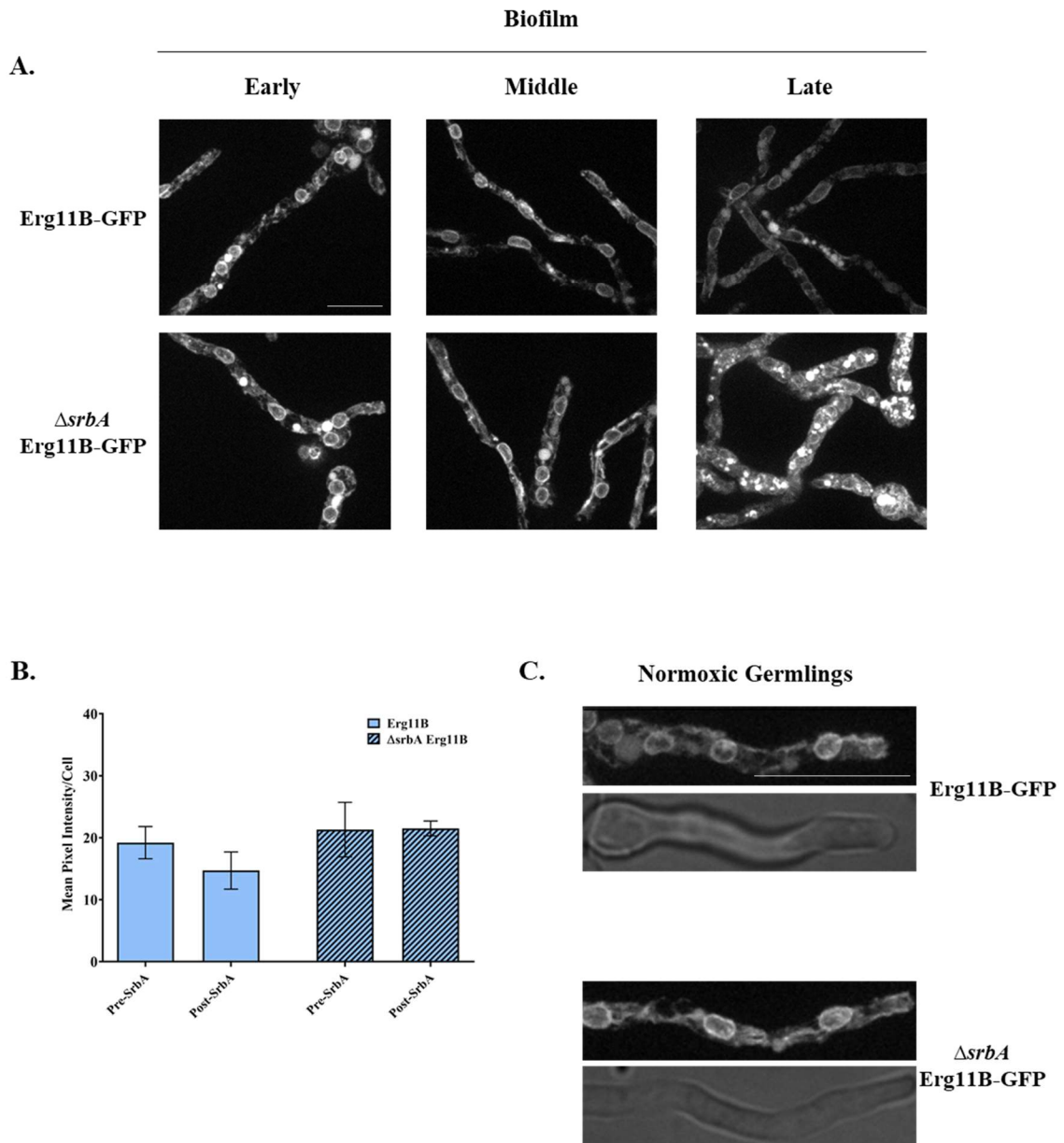


Figure 5. 5 Real-time expression of GFP-tagged Erg11B protein in living *A. nidulans* cells. A. GFP-tagged protein levels in basal cells during early (18-24 hrs), middle (25-32 hrs) and late (32-48 hrs) stage biofilm development. B. Quantification of protein levels by measurement of total GFP intensity within cells (n=3) before SrbA activation (Pre-SrbA or Early stage biofilm) and after SrbA activation (Post-SrbA or Middle stage biofilm). C. Protein expression in newly germinated cells (germlings) not in a biofilm i.e., under normoxia. Scale bar, 10 μ m.

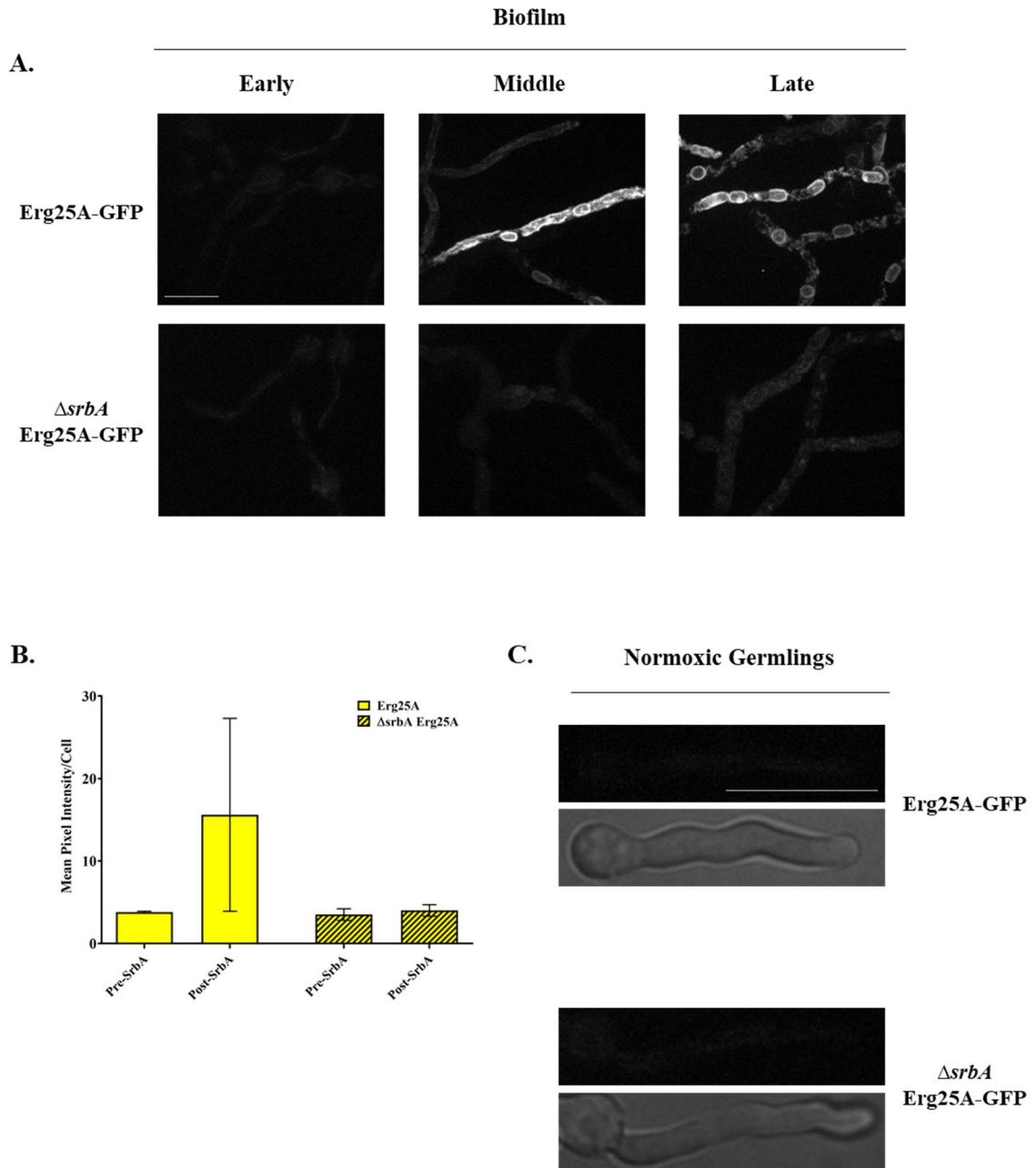


Figure 5. 6 Real-time expression of GFP-tagged Erg25A protein in living *A. nidulans* cells. A. GFP-tagged protein levels in basal cells during early (18-24 hrs), middle (25-32 hrs) and late (32-48 hrs) stage biofilm development. B. Quantification of protein levels by measurement of total GFP intensity within cells (n=3) before SrB activation (Pre-SrB or Early stage biofilm) and after SrB activation (Post-SrB or Middle stage biofilm). C. Protein expression in newly germinated cells (germlings) not in a biofilm i.e., under normoxia. Scale bar, 10 μ m.

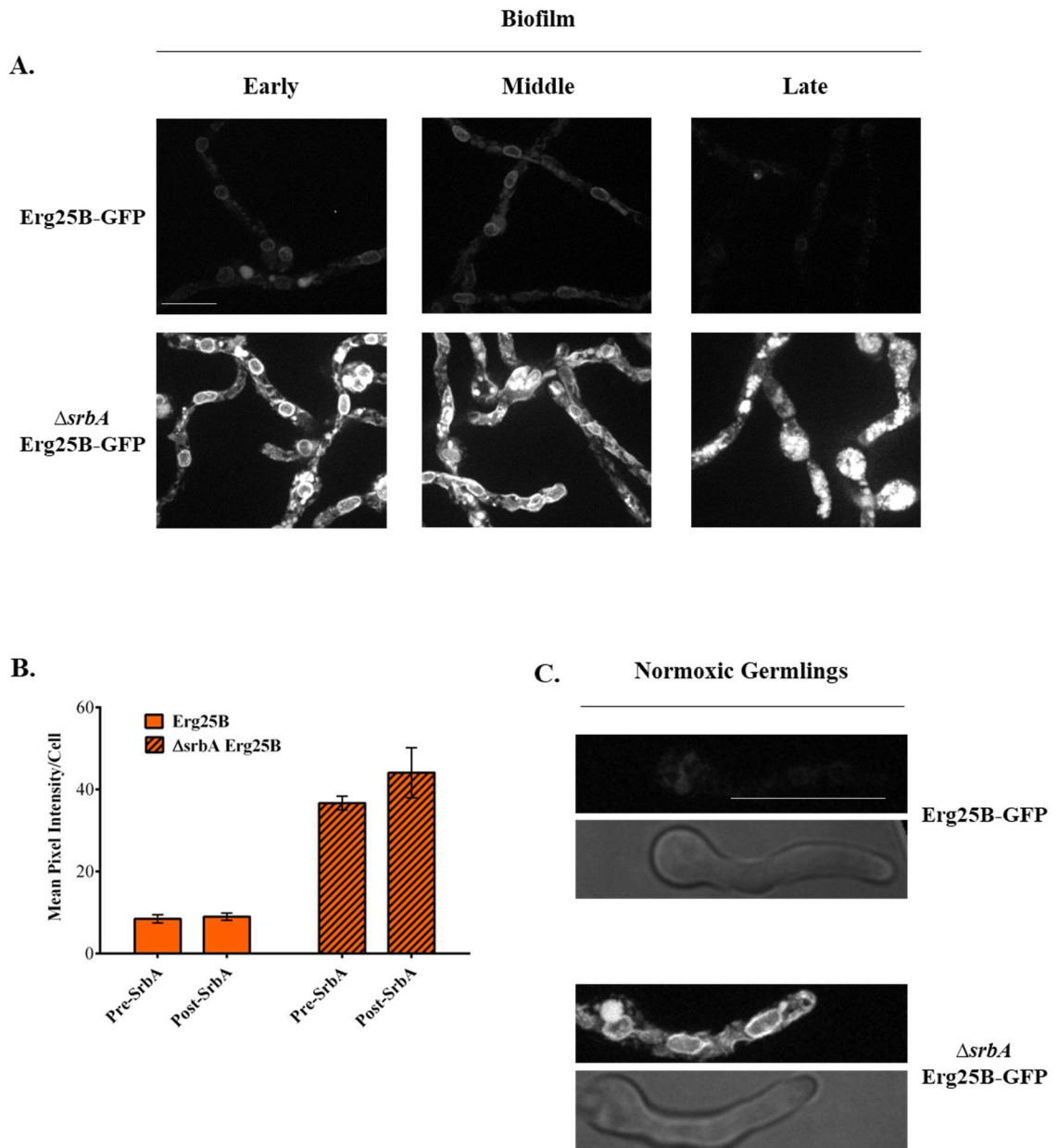


Figure 5. 7 Real-time expression of GFP-tagged Erg25B protein in living *A. nidulans* cells. A. GFP-tagged protein levels in basal cells during early (18-24 hrs), middle (25-32 hrs) and late (32-48 hrs) stage biofilm development. B. Quantification of protein levels by measurement of total GFP intensity within cells (n=3) before Srba activation (Pre-SrbA or Early stage biofilm) and after Srba activation (Post-SrbA or Middle stage biofilm). C. Protein expression in newly germinated cells (germlings) not in a biofilm i.e., under normoxia. Scale bar, 10 μ m.

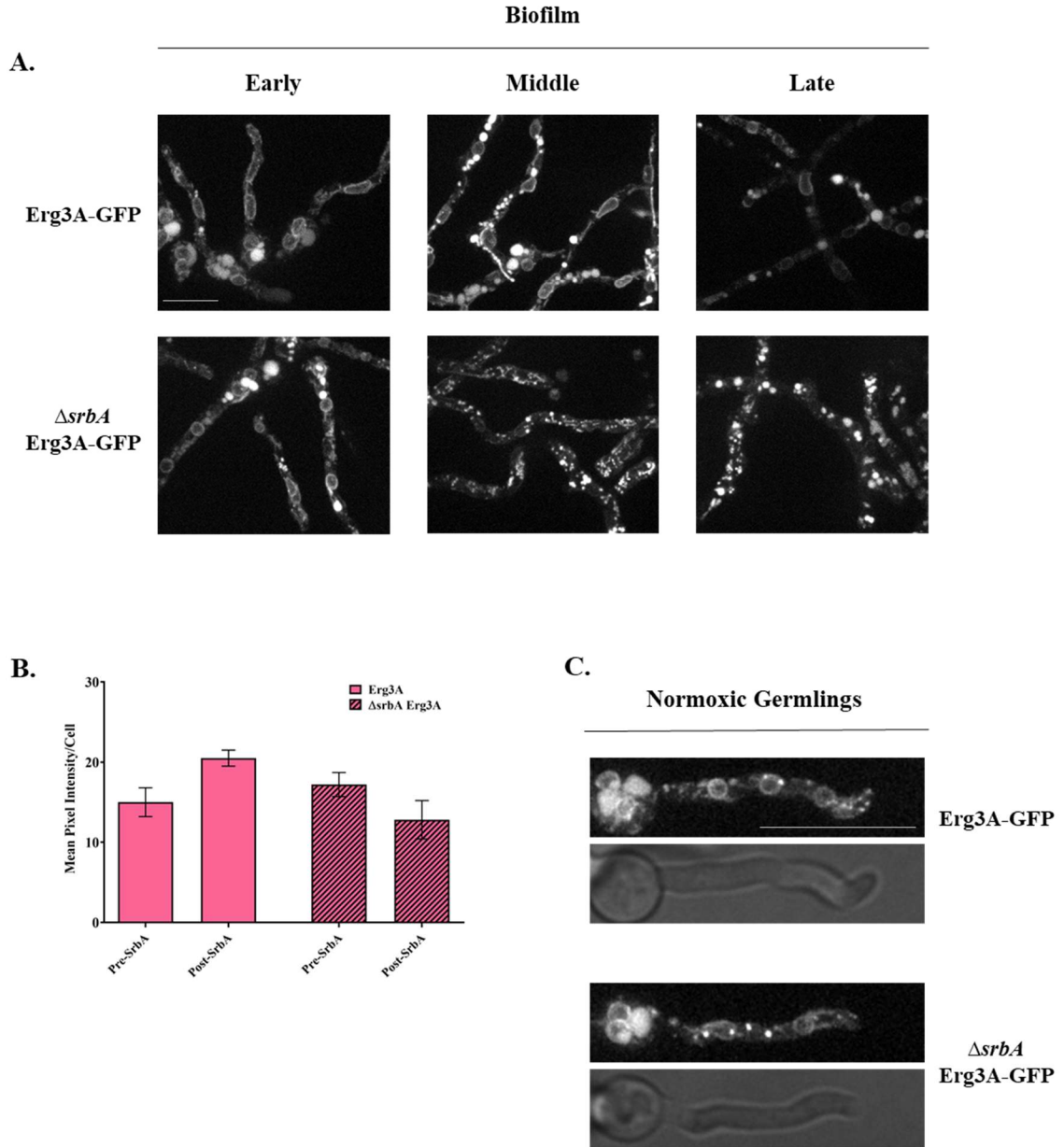


Figure 5. 8 Real-time expression of GFP-tagged Erg3A protein in living *A. nidulans* cells. A. GFP-tagged protein levels in basal cells during early (18-24 hrs), middle (25-32 hrs) and late (32-48 hrs) stage biofilm development. B. Quantification of protein levels by measurement of total GFP intensity within cells (n=3) before SrB activation (Pre-SrB or Early stage biofilm) and after SrB activation (Post-SrB or Middle stage biofilm). C. Protein expression in newly germinated cells (germlings) not in a biofilm i.e., under normoxia. Scale bar, 10 μ m.

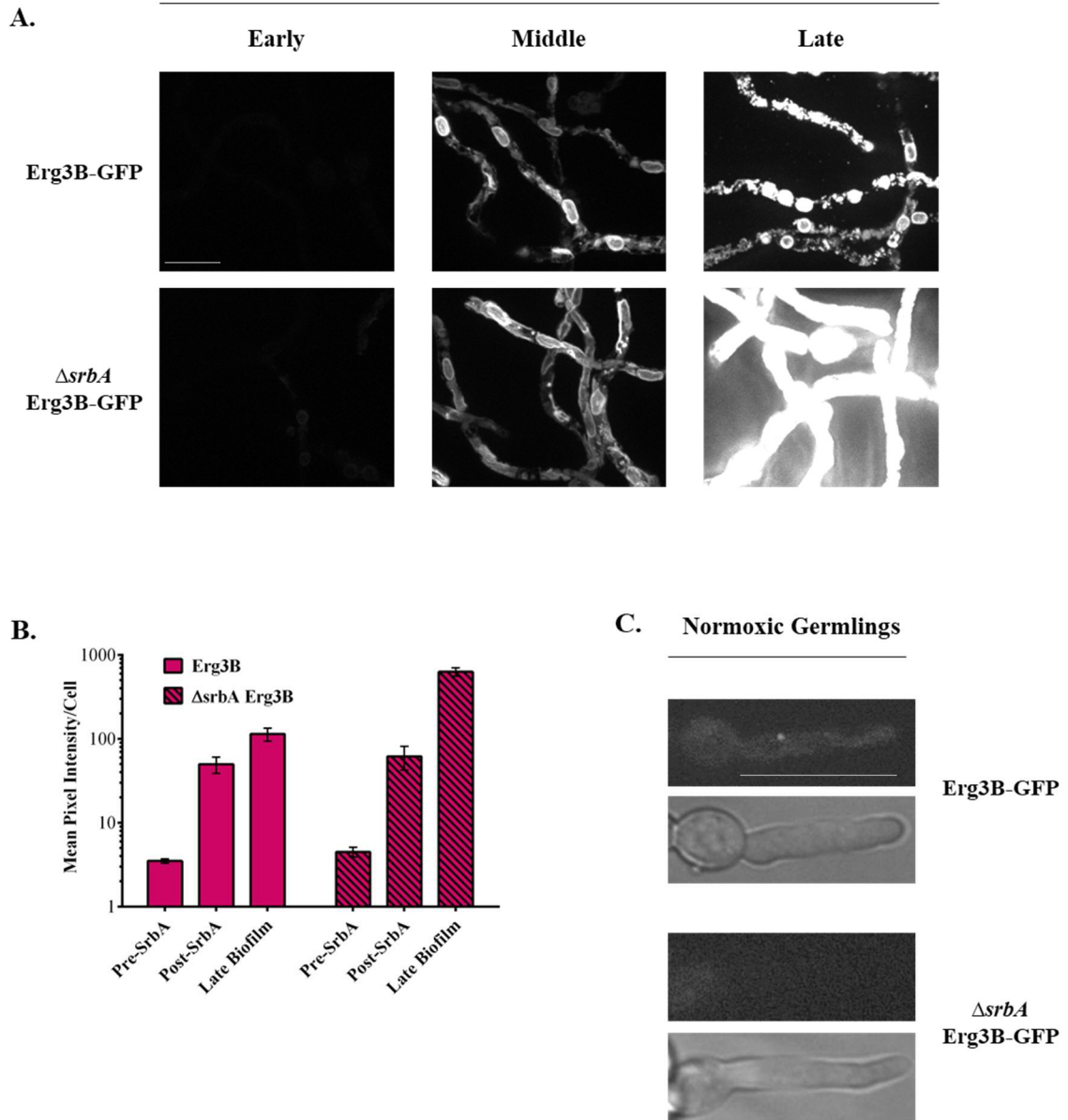


Figure 5.9 Real-time expression of GFP-tagged Erg3B protein in living *A. nidulans* cells A. GFP-tagged protein levels in basal cells during early (18-24 hrs), middle (25-32 hrs) and late (32-48 hrs) stage biofilm development. B. Quantification of protein levels by measurement of total GFP intensity within cells (n=3) before Srba activation (Pre-Srba or Early stage biofilm), after Srba activation (Post-Srba or Middle stage biofilm) and in Late stage biofilm. C. Protein expression in newly germinated cells (germlings) not in a biofilm i.e., under normoxia. Scale bar, 10 μ m.

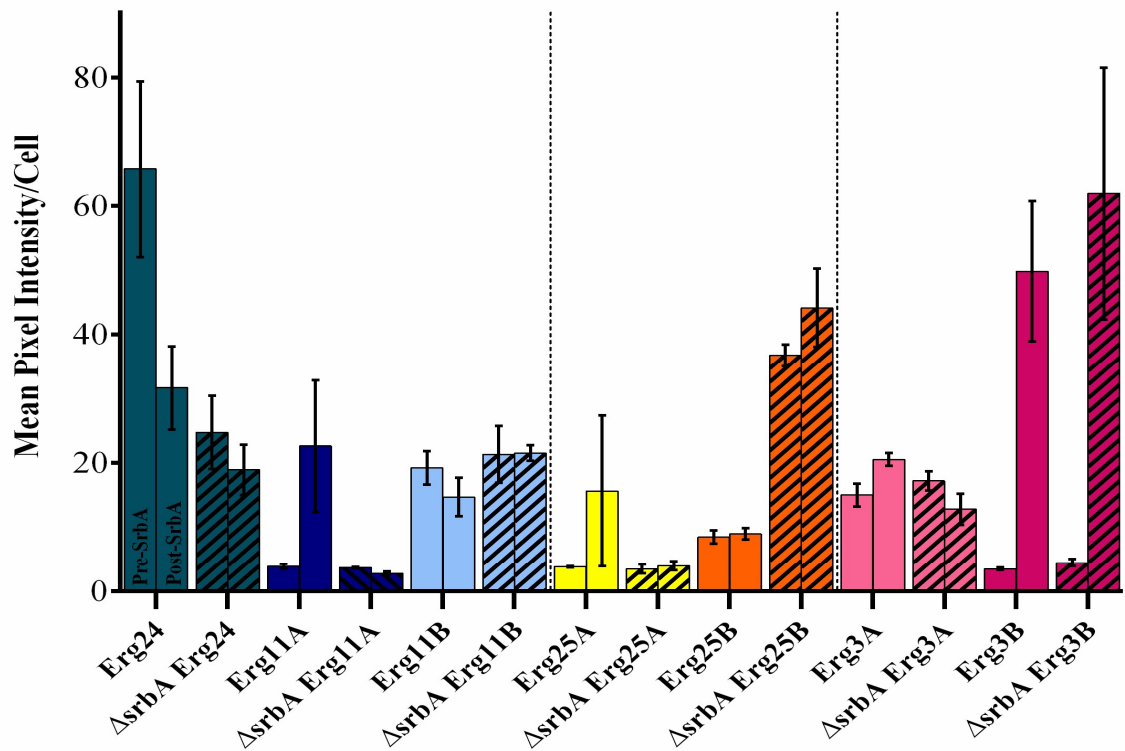


Figure 5. 10 Comparative expression levels of all 7 Erg proteins in the presence or absence of *srbA* during biofilm development. Comparative expression profile of each of the 7 Erg proteins during biofilm development both in the presence (solid bars) and absence (scored bars) of the *srbA* gene. For each protein, expression level was quantified (n=3) at 2 timepoints: one before *SrbA* activation in the biofilm (early stage ~18-24hrs) and one after *SrbA* activation in the biofilm (middle stage ~25-32hrs).

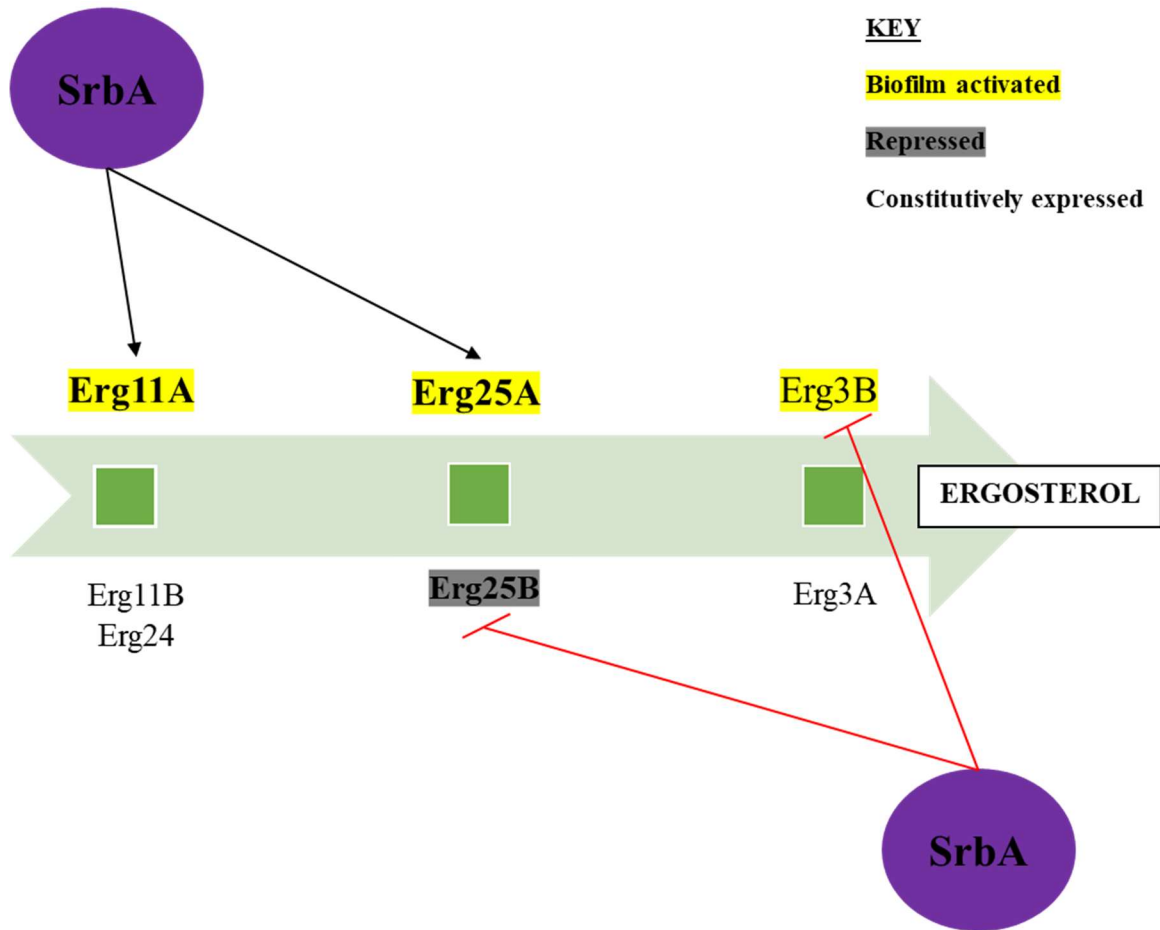


Figure 5. 11 Model of SrbA regulation of ergosterol pathway enzymes during biofilm development. During biofilm maturation the ergosterol biosynthetic pathway is under complex regulation. The sequential steps of the pathway are depicted in the green arrow, with each green square representing a sterol intermediate. The specific erg proteins catalyzing each step are arranged in sequence of their function in the pathway. Paralogs are assumed to catalyze the same chemical reaction. The potential regulatory relationship between SrbA and Erg proteins during biofilm development is depicted with black arrows (activation) or red bars (repression). Erg proteins highlighted yellow undergo biofilm driven activation of protein levels while those highlighted grey are repressed. Erg proteins with no highlights show constant levels during biofilm development and in normoxic germlings.

Chapter 6. Conclusion

This study has demonstrated that SrbA plays a significant role in regulating fungal biofilm cell biology. SrbA protein activation and nuclear translocation responds to the self-generated hypoxia within the developing biofilm and that this activation is reversible in response changes in the gaseous microenvironment through air exchange. Deletion strains inactivating of any one of the three proteolytic pathways required to release the completely processed SrbA transcription factor domain phenocopy the Δ *srbA* strain. This confirms the responsiveness of the SrbA protein to gaseous signaling and supports functional role as a nuclear transcription factor in a relatively natural biofilm context.

In addition to *srbA*, another hypoxia-adaptive transcription factor *atrR* is also required to mediate biofilm-driven changes in cell biology. Although both transcription factors are necessary for hypoxic growth and azole drug resistance, they do not function redundantly. Loss of either *srbA* or *atrR* is sufficient to lose biofilm-driven MT disassembly, while the double deletion is no worse than the single mutants. This suggests that hypoxic adaptation of fungal cells plays a significant role regulating biofilm cell biology and, by extension, biofilm development. Interestingly, when cells are grown under shaking conditions wherein dissolved oxygen concentration is artificially enhanced through agitation, Δ *srbA* and Δ *atrR* are able to trigger MT disassembly just as WT cells. This implies that the role of *srbA* and *atrR* genes is critical only when oxygen is limiting

as in a still culture where the passive diffusion rate of atmospheric oxygen through the liquid culture medium is low. The simplest explanation of this phenomenon is that when dissolved oxygen is high under shaking conditions, cell growth and biomass accumulation can take place unimpeded in WT as well as $\Delta srbA$ and $\Delta atrR$ strains. The accumulated biomass has a sufficiently high oxygen consumption rate that allows for the development of the self-generated gaseous microenvironment (hypoxia) in the basal cells required to trigger MT disassembly. Whereas in the static cultures, the presence of *srbA* and *atrR* genes are needed to adapt to the oxygen limiting conditions to produce sufficient growth. The defective growth in $\Delta srbA$ and $\Delta atrR$ does not produce sufficient biomass to generate the gaseous microenvironment necessary to trigger MT disassembly.

Although both SrbA activation and MT disassembly respond to the naturally developing gaseous microenvironment, they do not occur at the same time in biofilm development. SrbA activation occurs in the early stages ~ 24-27 hrs after inoculation (Fig 3.3, 3.4) while MT disassembly is triggered much later, at ~33-36 hrs post-inoculation (Fig 4.2, 4.3). This means that the gaseous environment that triggers SrbA activation is not the same as the one that triggers MT disassembly. The simplest explanation, involving only oxygen as the signal molecule, would be as follows: In the early-stage biofilm oxygen levels drop to 'Threshold 1' (Fig 6.1) which is sufficient to trigger SrbA activation but not MT disassembly. SrbA activation allows cells to adapt and continue growth under hypoxia, allowing further biomass accumulation and corresponding drop in oxygen concentration. At a later stage when oxygen levels drop to Threshold 2, this serves as the trigger for MT disassembly (Fig 6.1).

srbA and *atrR* are both established as genes necessary for growth under hypoxia (Threshold 1). So, when either of these genes are deleted, once cells reach the hypoxic Threshold 1 (Fig 6.1), cells cannot adapt and continue growth. In order to reach Threshold 2 (Fig 6), fungal cells need to continue growth beyond Threshold 1, which is not possible in Δ *srbA* and Δ *atrR* strains. These cells likely remain stuck at this stage, maintaining active Ebf1 comets and MT polymerization.

A more complex model of biofilm gaseous signaling, involving a combination of multiple gaseous signaling molecules (such as O₂ and NO) each at different concentrations during the course of biofilm maturation, is also possible. Results from chapter 3 show that SrbA activation can be transiently triggered by nitric oxide. The fact that NO-induced activation is transient suggests that additional factors may be involved. Published works have also demonstrated that biofilm driven changes in MTs, ER exit sites, Golgi and actin patches can also be triggered by exogenously supplied gases like nitric oxide³⁵ and, in the case of MTs, hydrogen sulfide³⁴. Gases like NO and H₂S are known to be generated by cells (ranging from yeast to animals) under hypoxia⁹⁷⁻¹⁰¹. Thus, a complex model of biofilm gaseous signaling is certainly possible.

As an example, consider a two-gas model wherein a combination of oxygen and nitric oxide serve as triggers for cell biological processes during biofilm development. In this model, oxygen levels gradually decrease in basal cells during biofilm growth due to the increasing oxygen consumption rate and the decreasing ability of oxygen to penetrate to the biofilm base. These hypoxic cells begin to generate nitric oxide, which gradually accumulates. In the early stage of biofilm growth, at Threshold 1, a somewhat low

oxygen concentration, combined with a very low nitric oxide concentration, may serve as a trigger for *SrbA* activation (Fig 6.1). As biofilm growth continues, O_2 levels continue to drop, while NO level increases further. In a later biofilm stage, at Threshold 2, an extremely low oxygen concentration plus a relatively higher NO concentration may serve as the trigger for MT disassembly. Thus, two different gaseous signals combined at different relative concentrations could produce different gaseous signaling environments that regulate different cell biological processes.

The co-culture experiments reveal a novel and fascinating piece of information concerning cell sensitivity to gaseous signaling. Not only can Δ *srbA* cells respond to the signal produced by WT cells, *ΔsrbA* is more sensitive to the gaseous signal than WT cells. The lid removal and replacement experiments clearly demonstrate that the *ΔsrbA* cells respond to a lower threshold of the MT dispersal signal compared to WT cells. Since *srbA* is a known regulator of ergosterol biosynthetic genes and ergosterol is an important component of the cell membrane influencing membrane permeability, the altered ergosterol content of the *ΔsrbA* cells may be the explanation of the higher sensitivity.

Investigation of ergosterol biosynthetic protein expression in basal cells during biofilm development revealed some new findings. The genes of these Erg proteins are known targets of *srbA* and *atrR* transcriptional regulation.

- i) Erg11A and Erg25A showed the classical *srbA*-dependent upregulation of protein expression in response to biofilm generated hypoxia.

- ii) Erg11B and Erg3A showed constitutive protein expression in the presence or absence of *srbA* and appeared unresponsive to biofilm hypoxia.
- iii) Erg25B and Erg3B showed increased protein expression in the absence of *srbA* suggesting a potential negative regulatory role of *SrbA*. Erg25B maintained constant expression levels throughout biofilm development and under normoxia. Erg3B showed biofilm-driven activation of expression.
- iv) Erg24 showed a drop in protein level in the absence of *srbA* but this drop was evident even under normoxia, a time when *SrbA* protein would not be activated. The rise in Erg25B protein level was also at a time when *SrbA* protein would not be activated (normoxia). This suggests a non-transcriptional regulatory role for *SrbA* protein.

The variation of Erg protein expression during biofilm development, particularly between paralogous genes was unexpected. There is more to be investigated with regards to hypoxic regulation of ergosterol biosynthesis. Why do paralogous Erg proteins show such different expression patterns during biofilm development? Do they perform different functions despite their high sequence similarity (50-70% identity)? Finally, these varied expression patterns in the Δ *srbA* background relative to the WT could result in the production of an altered sterol molecule or a sterol intermediate product instead of ergosterol. The incorporation of such an altered sterol molecule in the cell membrane may alter the permeability of the cell membrane resulting in Δ *srbA* cells having a higher sensitivity to gaseous signaling than the WT.

Overall, these results provide a model of regulation of cell biology in response to the self-generated hypoxia within a biofilm. This hypoxic regulation is mediated by *SrbA* and *AtrR* and allows for cell adaptation to the low oxygen microenvironment of the biofilm. Further changes in cell biology, such as MT disassembly, triggered by gaseous signaling are also dependent on *srbA* and *atrR*. Indeed, *srbA* appears to calibrate the sensitivity of cells to gaseous signaling, possibly through the *SrbA*-dependent regulation of sterol biosynthesis that may result in altered plasma membrane permeability to gaseous molecules.

This thesis also demonstrates the importance of the biofilm microenvironment in regulating cell biology. There is a significant difference in behavior between planktonic cells and cells in the context of a biofilm. Results from experiments carried out on free-living cells are not necessarily representative of biofilm cells found in more natural settings. Consequently, more experimental research on biofilm cells is of great importance.

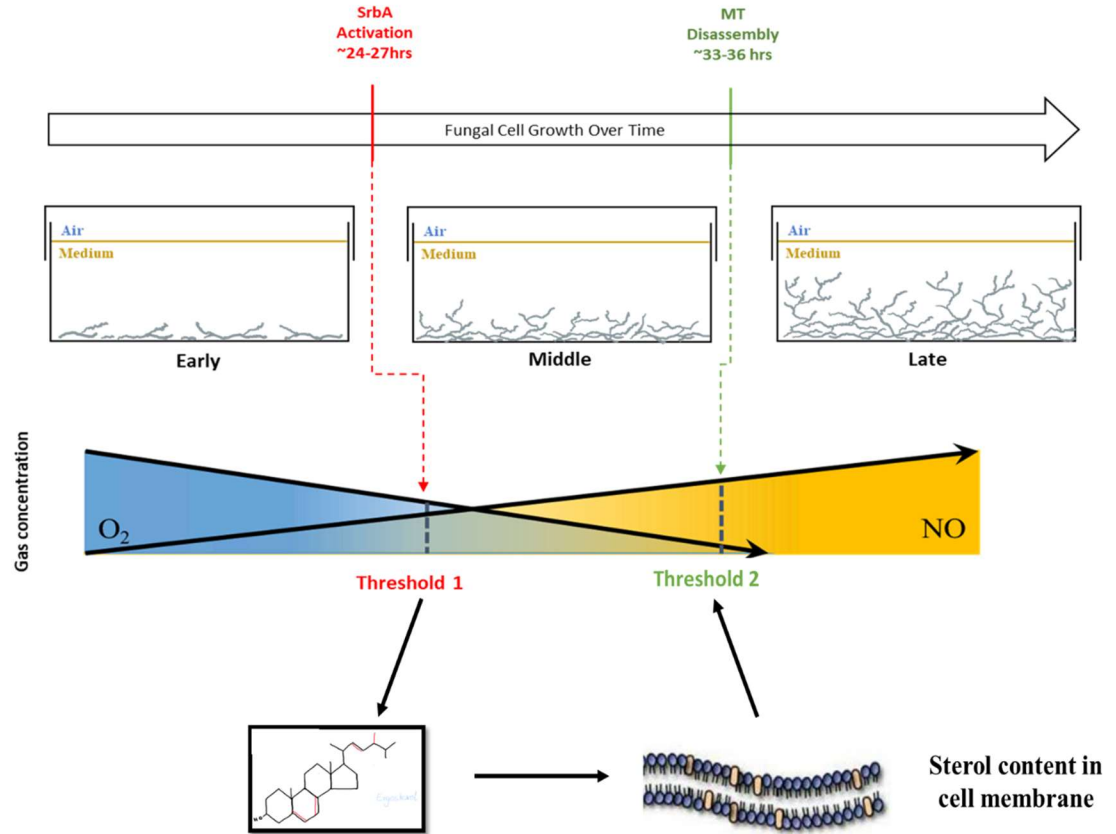


Figure 6. 1 Relative timing of different cell biological changes triggered by gaseous signaling in different stages of biofilm development. Spores inoculated in an imaging culture dish germinate and grow into long, filamentous cells (grey) that adhere to the bottom surface of the dish and continue to grow up through the culture medium. Over time, the basal layer of cells experiences decreasing oxygen levels resulting in a self-generated hypoxia. This may be accompanied by a gradual rise in nitric oxide (NO) produced by hypoxic cells. Threshold 1 is the specific combination of drop in O_2 levels and rise in NO that triggers SrBA proteolytic activation and nuclear translocation. This results in the regulation of the ergosterol biosynthetic proteins which may alter the sterol content of the plasma membrane, allowing for calibration of cell sensitivity to further gaseous signaling. Threshold 2 is a different combination of much lower O_2 and higher NO levels that develops at a later stage of biofilm development and triggers MT disassembly.

Bibliography

1. Costerton, J. W., Geesey, G. G. & Cheng, K.-J. How Bacteria Stick. **238**, 86–95 (1978).
2. Donlan, R. M. & Costerton, J. W. Biofilms: Survival mechanisms of clinically relevant microorganisms. *Clinical Microbiology Reviews* vol. 15 167–193 (2002).
3. Seidler, M. J., Salvenmoser, S. & Müller, F. M. C. *Aspergillus fumigatus* forms biofilms with reduced antifungal drug susceptibility on bronchial epithelial cells. *Antimicrob. Agents Chemother.* **52**, 4130–4136 (2008).
4. Chandra, J. *et al.* Biofilm formation by the fungal pathogen *Candida albicans*: Development, architecture, and drug resistance. *J. Bacteriol.* **183**, 5385–5394 (2001).
5. Bruns, S. *et al.* Functional genomic profiling of *Aspergillus fumigatus* biofilm reveals enhanced production of the mycotoxin gliotoxin. *Proteomics* **10**, 3097–3107 (2010).
6. Nett, J. E., Lepak, A. J., Marchillo, K. & Andes, D. R. Time Course Global Gene Expression Analysis of an in Vivo *Candida* biofilm. *J. Infect. Dis.* **200**, 307–313 (2009).
7. Fanning, S. & Mitchell, A. P. Fungal biofilms. *PLoS Pathog.* **8**, e1002585 (2012).
8. Zarnowski, R. *et al.* Novel entries in a fungal biofilm matrix encyclopedia. *MBio* **5**, 1–13 (2014).
9. Shopova, I. *et al.* Extrinsic extracellular DNA leads to biofilm formation and colocalizes with matrix polysaccharides in the human pathogenic fungus *Aspergillus fumigatus*. *Front. Microbiol.* **4**, (2013).
10. Rajendran, R. *et al.* Extracellular DNA Release Acts as an Antifungal Resistance Mechanism in Mature *Aspergillus fumigatus* Biofilms. (2013) doi:10.1128/EC.00287-12.
11. Mukherjee, P. K. *et al.* Lipidomics of *Candida albicans* biofilms reveals phase-dependent production of phospholipid molecular classes and role for lipid rafts in biofilm formation. *Microbiology* **157**, 3232–3242 (2011).
12. Mukherjee, P. K., Chandra, J., Kuhn, D. M. & Ghannoum, M. A. Mechanism of fluconazole resistance in *Candida albicans* biofilms: Phase-specific role of efflux pumps and membrane sterols. *Infect. Immun.* **71**, 4333–4340 (2003).
13. Tré-Hardy, M., Vanderbist, F., Traore, H. & Devleeschouwer, M. J. In vitro activity of antibiotic combinations against *Pseudomonas aeruginosa* biofilm and planktonic cultures. *Int. J. Antimicrob. Agents* **31**, 329–336 (2008).
14. Ramage, G., Vande Walle, K., Wickes, B. L. & López-Ribot, J. L. Standardized

- method for in vitro antifungal susceptibility testing of *Candida albicans* biofilms. *Antimicrob. Agents Chemother.* **45**, 2475–2479 (2001).
15. Mowat, E. *et al.* Phase-dependent antifungal activity against *Aspergillus fumigatus* developing multicellular filamentous biofilms. doi:10.1093/jac/dkn402.
 16. Lynch, A. S. & Robertson, G. T. Bacterial and fungal biofilm infections. *Annual Review of Medicine* vol. 59 415–428 (2008).
 17. Desai, J. V, Mitchell, A. P. & Andes, D. R. Fungal biofilms, drug resistance, and recurrent infection. *Cold Spring Harb. Perspect. Med.* **4**, (2014).
 18. Mclaughlin-Borlace, L., Stapleton, F., Matheson, M. & Dart, J. K. G. *Bacterial biofilm on contact lenses and lens storage cases in wearers with microbial keratitis.* *Journal of Applied Microbiology* vol. 84 (1998).
 19. Marqué -Calvo, M. In vitro colonization of hydrophilic contact lenses by *Aspergillus niger*. *J. Ind. Microbiol. Biotechnol.* **29**, 6–9 (2002).
 20. Marsh, P. D. & Marsh, D. Dental Plaque as a Microbial Biofilm. *Caries Res* **38**, 204–211 (2004).
 21. Murray, T. S., Egan, M. & Kazmierczak, B. I. *Pseudomonas aeruginosa* chronic colonization in cystic fibrosis patients. *Curr. Opin. Pediatr.* **19**, 83–88 (2007).
 22. Hall-Stoodley, L. *et al.* Direct detection of bacterial biofilms on the middle-ear mucosa of children with chronic otitis media. *J. Am. Med. Assoc.* **296**, 202–211 (2006).
 23. Anderson, G. G. *et al.* Intracellular bacterial biofilm-like pods in urinary tract infections. *Science (80-.)*. **301**, 105–107 (2003).
 24. Cussler, E. L. Diffusion, Mass Transfer in Fluid Systems. *Cambridge Uni. Press* (1997).
 25. Hall, L. A. & Denning, D. W. Oxygen requirements of *Aspergillus* species. *J. Med. Microbiol.* **41**, 311–315 (1994).
 26. Blatzer, M. *et al.* SREBP coordinates iron and ergosterol homeostasis to mediate triazole drug and hypoxia responses in the human fungal pathogen *Aspergillus fumigatus*. *PLoS Genet.* **7**, (2011).
 27. Willger, S. D. *et al.* Dsc orthologs are required for hypoxia adaptation, triazole drug responses, and fungal virulence in *Aspergillus fumigatus*. *Eukaryot. Cell* **11**, 1557–1567 (2012).
 28. Hagiwara, D. *et al.* A Novel Zn²⁺-Cys⁶ Transcription Factor AtrR Plays a Key Role in an Azole Resistance Mechanism of *Aspergillus fumigatus* by Co-regulating *cyp51A* and *cdr1B* Expressions. (2017) doi:10.1371/journal.ppat.1006096.
 29. Paul, S. *et al.* AtrR is an essential determinant of azole resistance in *aspergillus fumigatus*. *MBio* **10**, (2019).
 30. Fox, E. P. *et al.* Anaerobic bacteria grow within *candida albicans* biofilms and induce biofilm formation in suspension cultures. *Curr. Biol.* **24**, 2411–2416 (2014).
 31. Kowalski, C. H., Morelli, K. A., Schultz, D., Nadell, C. D. & Cramer, R. A. Fungal biofilm architecture produces hypoxic microenvironments that drive antifungal resistance. *Proc. Natl. Acad. Sci. U. S. A.* **117**, 22473–22483 (2020).

32. Oostra, J., Le Comte, E. P., Van Den Heuvel, J. C., Tramper, J. & Rinzema, A. Intra-particle oxygen diffusion limitation in solid-state fermentation. *Biotechnol. Bioeng.* **75**, 13–24 (2001).
33. Rahardjo, Y. S. P., Weber, F. J., Paul Le Comte, E., Tramper, J. & Rinzema, A. Contribution of aerial hyphae of *Aspergillus oryzae* to respiration in a model solid-state fermentation system. *Biotechnol. Bioeng.* **78**, 539–544 (2002).
34. Shukla, N., Osmani, A. H. & Osmani, S. A. Microtubules are reversibly depolymerized in response to changing gaseous microenvironments within *Aspergillus nidulans* biofilms. *Mol. Biol. Cell* **28**, 634–644 (2016).
35. Lingo, D. E., Shukla, N., Osmani, A. H. & Osmani, S. A. *Aspergillus nidulans* biofilm formation modifies cellular architecture and enables light-activated autophagy. *Mol. Biol. Cell* **32**, 1181–1192 (2021).
36. Bien, C. M. & Espenshade, P. J. Sterol regulatory element binding proteins in fungi: Hypoxic transcription factors linked to pathogenesis. *Eukaryot. Cell* **9**, 352–359 (2010).
37. Bat-Ochir, C. *et al.* The signal peptide peptidase SppA is involved in sterol regulatory element-binding protein cleavage and hypoxia adaptation in *Aspergillus nidulans*. *Mol. Microbiol.* **100**, 635–655 (2016).
38. Vaknin, Y. *et al.* Identification and Characterization of a Novel *Aspergillus fumigatus* Rhomboid Family Putative Protease, RbdA, Involved in Hypoxia Sensing and Virulence. *Infect. Immun.* **84**, 1866–1878 (2016).
39. Chung, D. *et al.* CHIP-seq and In Vivo Transcriptome Analyses of the *Aspergillus fumigatus* SREBP SrbA Reveals a New Regulator of the Fungal Hypoxia Response and Virulence. *PLoS Pathog.* **10**, (2014).
40. Ramage, G., Rajendran, R., Gutierrez-Correa, M., Jones, B. & Williams, C. *Aspergillus* biofilms: Clinical and industrial significance. *FEMS Microbiology Letters* vol. 324 89–97 (2011).
41. Pontecorvo, G., Roper, J. A., Chemmons, L. M., Macdonald, K. D. & Bufton, A. W. J. The Genetics of *Aspergillus nidulans*. *Adv. Genet.* **5**, 141–238 (1953).
42. Pantazopoulou, A. & Peñ, M. A. Organization and Dynamics of the *Aspergillus nidulans* Golgi during Apical Extension and Mitosis. *Mol. Biol. Cell* **20**, 4335–4347 (2009).
43. Kuwayama, H. *et al.* PCR-mediated generation of a gene disruption construct without the use of DNA ligase and plasmid vectors. *Nucleic Acids Res.* **30**, 2 (2002).
44. Yang, L. *et al.* Rapid production of gene replacement constructs and generation of a green fluorescent protein-tagged centromeric marker in *Aspergillus nidulans*. *Eukaryot. Cell* **3**, 1359–1362 (2004).
45. Szewczyk, E. *et al.* Fusion PCR and gene targeting in *Aspergillus nidulans*. *Nat. Protoc.* **1**, 3111–3120 (2007).
46. Yang, L. *et al.* Rapid production of gene replacement constructs and generation of a green fluorescent protein-tagged centromeric marker in *Aspergillus nidulans*. *Eukaryot. Cell* **3**, 1359–1362 (2004).
47. Nayak, T. *et al.* A versatile and efficient gene-targeting system for *Aspergillus*

- nidulans. *Genetics* **172**, 1557–1566 (2006).
48. Osmani, S. A., May, G. S. & Morris, N. R. Regulation of the mRNA Levels of *nimA*, a Gene Required for the G2-M Transition in *Aspergillus nidulans*.
 49. Schneider, C. A., Rasband, W. S. & Eliceiri, K. W. *NIH Image to ImageJ: 25 years of image analysis. Nature Methods* (2012) doi:10.1038/nmeth.2089.
 50. Schindelin, J. *et al.* Fiji: An open-source platform for biological-image analysis. *Nat. Methods* **9**, 676–682 (2012).
 51. Briggs, M. R., Yokoyama, C., Wang, X., Brown, M. S. & Goldstein, J. L. Nuclear protein that binds sterol regulatory element of low density lipoprotein receptor promoter. I. Identification of the protein and delineation of its target nucleotide sequence. *J. Biol. Chem.* **268**, 14490–14496 (1993).
 52. Goldstein, J. L. & Brown, M. S. Regulation of the mevalonate pathway. (1990).
 53. Smith, J. R., Osborne, T. F., Goldstein, J. L. & Brown, M. S. Identification of nucleotides responsible for enhancer activity of sterol regulatory element in low density lipoprotein receptor gene. *J. Biol. Chem.* **265**, 2306–2310 (1990).
 54. Yokoyama, C. *et al.* SREBP-1, a basic-helix-loop-helix-leucine zipper protein that controls transcription of the low density lipoprotein receptor gene. *Cell* **75**, 187–197 (1993).
 55. Wang, X., Sato, R., Brown, M. S., Hua, X. & Goldstein, J. L. SREBP-1, a membrane-bound transcription factor released by sterol-regulated proteolysis. *Cell* **77**, 53–62 (1994).
 56. Hughes, A. L., Todd, B. L. & Espenshade, P. J. SREBP pathway responds to sterols and functions as an oxygen sensor in fission yeast. *Cell* **120**, 831–842 (2005).
 57. Todd, B. L., Stewart, E. V., Burg, J. S., Hughes, A. L. & Espenshade, P. J. Sterol Regulatory Element Binding Protein Is a Principal Regulator of Anaerobic Gene Expression in Fission Yeast. *Mol. Cell. Biol.* **26**, 2817–2831 (2006).
 58. Willger, S. D. *et al.* A Sterol-Regulatory Element Binding Protein Is Required for Cell Polarity, Hypoxia Adaptation, Azole Drug Resistance, and Virulence in *Aspergillus fumigatus*. *PLoS Pathog.* **4**, e1000200 (2008).
 59. Kim, J. B. *et al.* Dual DNA Binding Specificity of *ADD1/SREBP1* Controlled by a Single Amino Acid in the Basic Helix-Loop-Helix Domain. *MOLECULAR AND CELLULAR BIOLOGY* vol. 15 (1995).
 60. Hrabie, J. A., Klose, J. R., Wink, D. A. & Keefer, L. K. *New Nitric Oxide-Releasing Zwitterions Derived from Polyamines. J. Org. Chem* vol. 58 <https://pubs.acs.org/sharingguidelines> (1993).
 61. Zhou, S. *et al.* Heme-biosynthetic porphobilinogen deaminase protects *Aspergillus nidulans* from nitrosative stress. *Appl. Environ. Microbiol.* **78**, 103–109 (2012).
 62. Ullmann, B. D. *et al.* Inducible defense mechanism against nitric oxide in *Candida albicans*. *Eukaryot. Cell* **3**, 715–723 (2004).
 63. Palmer, L. A., Gaston, B. & Johns, R. A. Normoxic stabilization of hypoxia-inducible factor-1 expression and activity: Redox-dependent effect of nitrogen oxides. *Molecular Pharmacology* vol. 58 1197–1203 (2000).
 64. Kagiya, S., Tsuchihashi, T., Abe, I. & Fujishima, M. Cardiovascular effects of

- nitric oxide in the rostral ventrolateral medulla of rats. *Brain Res.* **757**, 155–158 (1997).
65. Umbrasas, D. *et al.* Nitric oxide donor NOC-18-induced changes of mitochondrial phosphoproteome in rat cardiac ischemia model. *Med.* **55**, (2019).
 66. Arandarcikaite, O., Jokubka, R. & Borutaite, V. Neuroprotective effects of nitric oxide donor NOC-18 against brain ischemia-induced mitochondrial damages: Role of PKG and PKC. *Neuroscience Letters* vol. 586 65–70 (2015).
 67. Inami, K., Sawai, H., Yakushiji, K., Domae, N. & Matsumoto, N. Induction of osteoclast differentiation by NOC-18, a long-acting nitric oxide donor. *Orthod. Waves* **68**, 20–27 (2009).
 68. Noritake, T., Kawakita, K. & Doke, N. Nitric oxide induces phytoalexin accumulation in potato tuber tissues. *Plant Cell Physiol.* **37**, 113–116 (1996).
 69. Shibuta, S., Mashimo, T., Zhang, P., Ohara, A. & Yoshiya, I. A new nitric oxide donor, NOC-18, exhibits a nociceptive effect in the rat formalin model. *J. Neurol. Sci.* **141**, 1–5 (1996).
 70. Kröncke, K. D., Fehsel, K. & Kolb-Bachofen, V. Nitric oxide: Cytotoxicity versus cytoprotection - How, why, when, and where? *Nitric Oxide - Biol. Chem.* **1**, 107–120 (1997).
 71. Stewart, E. V *et al.* Yeast SREBP Cleavage Activation Requires the Golgi Dsc E3 Ligase Complex. *Mol. Cell* **42**, 160–171 (2011).
 72. Hughes, B. T. & Espenshade, P. J. Oxygen-regulated degradation of fission yeast SREBP by Ofd1, a prolyl hydroxylase family member. *EMBO J.* **2783**, 1491–1501 (2008).
 73. Lambooj, J. M., Hoogenkamp, M. A., Brandt, B. W., Janus, M. M. & Krom, B. P. Fungal mitochondrial oxygen consumption induces the growth of strict anaerobic bacteria. *Fungal Genet. Biol.* **109**, 1–6 (2017).
 74. Blosser, S. J. & Cramer, R. A. SREBP-dependent triazole susceptibility in *Aspergillus fumigatus* is mediated through direct transcriptional regulation of *erg11A* (*cyp51A*). *Antimicrob. Agents Chemother.* **56**, 248–257 (2012).
 75. Dhingra, S. *et al.* RbdB, a Rhomboid Protease Critical for SREBP Activation and Virulence in *Aspergillus fumigatus*. *mSphere* **1**, e00035-16 (2016).
 76. Weihofen, A., Binns, K., Lemberg, M. K., Ashman, K. & Martoglio, B. Identification of signal peptide peptidase, a presenilin-type aspartic protease. *Science (80-.)*. **296**, 2215–2218 (2002).
 77. Ramage, G. & Williams, C. The clinical importance of fungal biofilms. in *Advances in Applied Microbiology* vol. 84 27–83 (2013).
 78. Becher, R. & Wirsal, S. G. R. Fungal cytochrome P450 sterol 14 α -demethylase (CYP51) and azole resistance in plant and human pathogens. *Applied Microbiology and Biotechnology* vol. 95 825–840 (2012).
 79. Vanden Bossche, H. Biochemical Targets for Antifungal Azole Derivatives: Hypothesis on the Mode of Action. in *Current Topics in Medical Mycology* (ed. McGinnis, M. R.) 313–351 (Springer New York, 1985). doi:10.1007/978-1-4613-9547-8_12.
 80. Ramage, G., Rajendran, R., Sherry, L. & Williams, C. Fungal biofilm resistance.

- Int. J. Microbiol.* **2012**, (2012).
81. de Mello, T. P., de Souza Ramos, L., Braga-Silva, L. A., Branquinha, M. & dos Santos, A. L. S. Fungal Biofilm – A Real Obstacle Against an Efficient Therapy: Lessons from Candida. *Curr. Top. Med. Chem.* **17**, 1987–2004 (2017).
 82. Brown, A. J. & Galea, A. M. Cholesterol as an evolutionary response to living with oxygen. *Evolution (N. Y.)*. **64**, 2179–2183 (2010).
 83. Galea, A. M. & Brown, A. J. Special relationship between sterols and oxygen: Were sterols an adaptation to aerobic life? *Free Radic. Biol. Med.* **47**, 880–889 (2009).
 84. Bloch, K. E. Sterol, structure and membrane function. *Crit. Rev. Biochem. Mol. Biol.* **14**, 47–92 (1983).
 85. Miersch, S. *et al.* Plasma membrane cholesterol content affects nitric oxide diffusion dynamics and signaling. *J. Biol. Chem.* **283**, 18513–18521 (2008).
 86. Menchaca, H. J., Michalek, V. N., Rohde, T. D., O’Dea, T. J. & Buchwald, H. Decreased blood oxygen diffusion in hypercholesterolemia. *Surgery* **124**, 692–698 (1998).
 87. Buchwald, H. *et al.* Plasma cholesterol: An influencing factor in red blood cell oxygen release and cellular oxygen availability. *J. Am. Coll. Surg.* **191**, 490–497 (2000).
 88. Ukil, L., De Souza, C. P., Liu, H.-L. & Osmani, S. A. Nucleolar Separation from Chromosomes during *Aspergillus nidulans* Mitosis Can Occur Without Spindle Forces. *Mol. Biol. Cell* **20**, 2132–2145 (2009).
 89. Song, J. *et al.* The *Aspergillus fumigatus* damage resistance protein family coordinately regulates ergosterol biosynthesis and azole susceptibility. *MBio* **7**, (2016).
 90. Natter, K. *et al.* The spatial organization of lipid synthesis in the yeast *Saccharomyces cerevisiae* derived from large scale green fluorescent protein tagging and high resolution microscopy. *Mol. Cell. Proteomics* **4**, 662–672 (2005).
 91. Khot, P. D., Suci, P. A., Lance Miller, R., Nelson, R. D. & Tyler, B. J. A Small Subpopulation of Blastospores in *Candida albicans* Biofilms Exhibit Resistance to Amphotericin B Associated with Differential Regulation of Ergosterol and 1,6-Glucan Pathway Genes. *Antimicrob. Agents Chemother.* **50**, 3708–3716 (2006).
 92. Galea, A. M. & Brown, A. J. Special relationship between sterols and oxygen: Were sterols an adaptation to aerobic life? *Free Radic. Biol. Med.* **47**, 880–889 (2009).
 93. Dupont, S. *et al.* Ergosterol Biosynthesis: a fungal pathway for life on land. 2961–2968 (2012) doi:10.5061/dryad.pd28pm7n.
 94. Alcazar-Fuoli, L. *et al.* Ergosterol biosynthesis pathway in *Aspergillus fumigatus*. *Steroids* **73**, 339–347 (2008).
 95. Alcazar-Fuoli, L. & Mellado, E. Ergosterol biosynthesis in *Aspergillus fumigatus*: Its relevance as an antifungal target and role in antifungal drug resistance. *Frontiers in Microbiology* vol. 3 439 (2012).
 96. Dhingra, S. & Cramer, R. A. Regulation of sterol biosynthesis in the human fungal pathogen *Aspergillus fumigatus*: Opportunities for therapeutic development.

- Front. Microbiol.* **8**, 1–14 (2017).
97. Castello, P. R., David, P. S., McClure, T., Crook, Z. & Poyton, R. O. Mitochondrial cytochrome oxidase produces nitric oxide under hypoxic conditions: Implications for oxygen sensing and hypoxic signaling in eukaryotes. *Cell Metab.* **3**, 277–287 (2006).
 98. Taylor, C. T. & Moncada, S. Nitric oxide, cytochrome c oxidase, and the cellular response to hypoxia. *Arteriosclerosis, Thrombosis, and Vascular Biology* vol. 30 643–647 (2010).
 99. Ball, K. A., Nelson, A. W., Foster, D. G. & Poyton, R. O. Nitric oxide produced by cytochrome c oxidase helps stabilize HIF-1 α in hypoxic mammalian cells. *Biochem. Biophys. Res. Commun.* (2012) doi:10.1016/j.bbrc.2012.03.050.
 100. Olson, K. R. Hydrogen Sulfide as an Oxygen Sensor. *Antioxid. Redox Signal.* **00**, 1–21 (2014).
 101. Iranon, N. N., Miller, D. L., Alcedo, J., Powell-Coffman, J. A. & Padilla, P. Interactions between oxygen homeostasis, food availability, and hydrogen sulfide signaling. **1124**, 53–1 (2012).

